Investigating the host determinants of *Listeria monocytogenes* cytosolic infection

Rochelle C. Glover

A dissertation
submitted in partial fulfillment of the
requirements for the degree of

Doctor of Philosophy

University of Washington
2023

Reading Committee:
Michelle Reniere, Chair
Joshua Woodward
Matthew Parsek

Program Authorized to Offer Degree:
Microbiology

University of Washington

Abstract

Investigating the host determinants of *Listeria monocytogenes* cytosolic infection

Rochelle C. Glover

Chair of the Supervisory Committee:
Michelle Reniere
Department of Microbiology

Listeria monocytogenes (*Lm*) is an intracellular foodborne pathogen which causes the severe disease listeriosis in immunocompromised, elderly, and pregnant individuals. *Lm* infects host cells using a well-defined intracellular lifecycle involving invasion, cytosolic replication, and cell-to-cell spread. While the bacterial virulence factors required for this lifecycle have been extensively studied, less is known about the host determinants of intracellular infection. The goal of this dissertation is to identify and characterize host proteins required for two stages of the *Lm* intracellular lifecycle: invasion of phagocytic cells through phagocytosis, and subsequent activation of virulence gene expression in the host cytosol. In this work, I developed and performed unbiased biochemical and genetic screens to identify host factors involved in these processes. First, the role of the host cytosol in activating the master virulence regulator PrfA was investigated using cytosolic cell-free extracts derived from *Xenopus tropicalis* eggs. These studies revealed that a host protein present in eukaryotic cytosol is required for activation of PrfA and expression of virulence factors. Fast protein liquid chromatography was used to separate *Xenopus* extracts and mass spectrometry identified candidate proteins involved in PrfA activation. As a complementary approach, a genome-wide CRISPR/Cas9 screen was performed and mutant macrophages with reduced levels of virulence factor expression were isolated. This screen also identified genes important for phagocytosis of *Lm* by macrophages. The role of one candidate gene, *Pten*, was extensively characterized. I discovered that the tumor suppressor PTEN promotes macrophage phagocytosis of *Lm* and *L. ivanovii*, but not other Gram-positive bacteria. Additionally, I found that PTEN enhances phagocytosis of *Lm* via its lipid phosphatase activity by promoting adherence to macrophages. Using conditional knockout mice lacking *Pten* in myeloid cells, PTEN-dependent phagocytosis was found to be important for host protection during oral *Lm* infection. Overall, this thesis provides a comprehensive identification of macrophage factors involved in regulating *Lm* virulence at the molecular level. In addition, the *in vivo* studies presented here demonstrate for the first time that macrophage phagocytosis is an important immune defense against invasive *Lm* during the foodborne route of infection.

Table of contents

List of Tables and Figures

Chapter 1

Chapter 2

Chapter 3

Chapter 4

Chapter 6

Acknowledgements

I have many people to thank for their guidance and support over the years. First, I'd like to thank my advisor, Michelle Reniere, for her mentorship throughout graduate school. You've helped me grow as a person and scientist and I will always be grateful that you gave me the freedom to explore my scientific interests in your lab. Thank you to my other committee members, Josh Woodward, Michael Lagunoff, Matt Parsek, and Kevin Hybiske for your advice and support throughout my PhD.

I would also like to thank all members of the Reniere Lab, past and present, for their companionship and unwavering support. In particular, I'd like to acknowledge Brittany Ruhland, Cortney Halsey, Monica Cesinger, Nikki Schwardt, Maddy Sanchez, Lauren Shull, and Shania Leano. Special shout out to Shania and Nikki for their instrumental help with many mouse experiments. Nikki and Maddy, it was such a joy to mentor both of you and I am so proud of the scientists that you are today. I truly could not imagine a better group of people to spend graduate school with!

Thank you to Josh Woodward and past and present members of the Woodward Lab for being an excellent sister lab to us. I'd especially like to thank Josh and Adelle McFarland for their mentorship during my rotation in the lab. I learned so much from both of you that I still carry with me today. I'd also like to specifically acknowledge Qing Tang, Melissa Locke, Chelsea Stamm, and Susan Brewer for always being willing to answer my many questions about everything tissue culture and mice. You all have been very generous and supportive and it does not go unnoticed. Huge thank you to Maureen Thomason for supporting me through everything and always being there for me when times were tough. You are an incredible person and scientist and you inspire me every day. Thank you to Alex Pollock and Hannah Tabakh for being so welcoming to me as a first year student and for your continued friendship.

The UW Microbiology graduate student community is something that I will cherish always and miss dearly. Thank you all for so many unforgettable memories and keeping me sane over the years. Outside of the graduate students I've already mentioned, special thank you to Neel Salukhe, Lyndsey Moore, and Carley Gray for your incredible friendship. I will also thank Monica again for being one of the greatest friends I could ever ask for. We've been through all the ups and downs together and I could not have done it without you! Thank you to our amazing advisors Amy Gundlach-Ritter and Andrea Pardo for your dedication and support of us grad students. I also need to thank my amazing friends outside of graduate school for their support, specifically Kat and Steve Kothen-Hill, Sumedha Ravishankar, and Cara Mitchell. I am very thankful that I've been able to spend time with all of you during my grad school years despite the distance.

Thank you so much to my parents, Don and Mary Glover, and my sister, Nicole Glover. You have been there for me literally since the beginning and have always supported me in my endeavors. I will always be thankful to my parents for giving me the freedom to pursue my passions in life and for being proud of the path that I've carved out. Nicole, it's been amazing to watch you become a world-class musician and I am very proud to be your sister.

Finally, thank you to my partner, Shivam Zaver, for being there for me always. Thank you for cooking for me when I was stressed, picking me up when I had late nights in lab, helping me

with biochemistry, listening to my practice talks, and generally supporting me in all facets of my life during grad school. You are an incredible scientist and will be an attentive and compassionate doctor. You inspire me with everything that you do and I am so lucky to have you in my life. Thank you for everything!

In loving memory of Harriet Boblak and Dr. Edwin Glover

Chapter 1: Introduction

Listeria monocytogenes as a model human pathogen

The genus *Listeria* consists of 21 species of Gram-positive bacteria which are ubiquitous in the environment[1]. Two of these species, *Listeria monocytogenes* (*Lm*) and *Listeria ivanovii*, are mammalian pathogens, although only *Lm* is considered pathogenic to humans. Contamination of fruit, vegetables, and livestock through contact with soil introduces *Lm* to the food supply, where it can be ingested and cause the severe foodborne disease listeriosis. *Lm* is difficult to eradicate from food processing environments as it readily forms biofilms on surfaces, equipment, and utensils[2]. In addition, *Lm* can grow at refrigeration temperatures and under high salt and acidic conditions, which allow it to persist in many ready-to-eat foods. Despite rigorous disinfection of food processing equipment and surveillance of food supplies, *Lm* causes multiple outbreaks in the United States each year; in 2022 alone, there were five listeriosis outbreaks with a 91% hospitalization rate[3].

While case numbers during listeriosis outbreaks are generally relatively small, the high mortality rate of listeriosis (~20%) makes it the third leading cause of foodborne illness deaths in the United States[4]. Otherwise healthy patients experience a mild, self-limiting gastritis that resolves without antibiotic treatment. In patients with risk-factors such as old age, immunocompromised status, and pregnancy, infection spreads beyond the gastrointestinal (GI) tract to cause invasive listeriosis, which may present as septicemia, meningitis, encephalitis, or pregnancy complications such as pre-term labor or miscarriage. Antibiotic therapy is the only treatment for listeriosis and is not always successful in eliminating invasive *Lm* infections.

Lm can replicate both extracellularly and within the cytosol of eukaryotic cells. Intracellular growth requires the expression of virulence factors found on the *Listeria* pathogenicity island LIPI-1. To initiate the intracellular lifecycle, *Lm* is phagocytosed by professional phagocytes or induces uptake into non-phagocytic cells using surface proteins called internalins[5]. Once inside the cell, the bacteria briefly reside in the phagosomal/endosomal vacuole where secretion of phospholipases (PlcA and PlcB) and the pore-forming toxin listeriolysin O (LLO) ruptures the vacuolar membrane and allows escape into the host cell cytosol[6,7]. *Lm* undergoes transcriptional reprogramming in the cytosol compartment, including expression of metabolic genes which allows scavenging of glucose-6-phosphate, glycerol, and amino acids to fuel cytosolic growth[8]. In addition, the actin assembly-inducing protein ActA is specifically expressed in host cytosol, which initiates polymerization of host actin to propel the bacteria throughout the cell and directly into neighboring cells without leaving the intracellular niche[9]. Intracellular growth and cell-to-cell spread occurs in intestinal epithelial cells, endothelial cells, splenocytes, hepatocytes, and immune cells and is critical for egress from the GI tract, replication in peripheral organs, and crossing the blood-brain barrier[10–12].

Since its discovery in the 1920s, *Lm* has become a hallmark model organism for cell biology, immunology, and bacteriology. As an intracellular pathogen, *Lm* elicits a robust $CD8^+$ T-cell response and was used to make fundamental discoveries in cell-mediated immunity[13,14]. The bacterium's close association with and manipulation of host cellular machinery has led to its use as a tool to study biological processes in eukaryotic cells such as signal transduction, actin

polymerization, and endosomal trafficking[15,16]. *Lm* has a broad ecological niche and adapts to constantly changing environments both in nature and within an animal host, making it an excellent model for investigating stress responses and genetic regulation in bacteria[17,18]. In particular, understanding how *Lm* senses the host environment and interacts with mammalian cells to cause disease may reveal conserved strategies used by facultative pathogens to thrive both within and outside their hosts.

Regulation of *Lm* virulence factor expression by PrfA

In the environment, *Lm* lives as a saprophyte and grows on decaying organic material. Once ingested by a susceptible host, however, *Lm* must undergo transcriptional reprogramming to adjust to this vastly different environment. The transition to a pathogenic lifestyle involves the upregulation of virulence factors required for successful infection. Transcriptional control of *Lm* virulence factors is complex and involves several cues from both the bacterium and host to ensure that virulence gene expression is robustly and specifically induced upon infection.

At the center of this regulatory network is the master transcriptional regulator PrfA. PrfA directly activates transcription of the virulence gene cluster found in LIPI-1 (*prfA*, *plcA*, *hly*, *mpl*, *actA*, and *plcB*) as well as virulence genes found elsewhere on the chromosome (*inlA*, *inlB*, *inlC*, and *hpt*)[19]. Directly-regulated genes contain a consensus sequence in their promoters called a PrfA box which binds the helix-turn-helix (HTH) domain of PrfA to activate transcription. In addition, over 140 genes are differentially expressed in the absence of PrfA, likely through indirect regulation[19–21]. Mutants lacking *prfA* are avirulent while strains with constitutively activated PrfA exhibit attenuated growth and motility in broth culture[22–24], highlighting the importance of proper PrfA regulation for fitness both in the environment and during infection. Induction of PrfA-regulated genes requires multiple stages of PrfA activation, including PrfA expression, amino acid modification, and allosteric activation.

PrfA protein abundance is regulated through both transcriptional and translational control. Transcription of *prfA* is driven by three promoters: monocistronic P1*prfA* and P2*prfA* directly upstream of *prfA*, and P*plcA* which drives bicistronic expression of the prfA-plcA transcript[24,25]. Transcription from P1*prfA* occurs constitutively at a low level, allowing prfA transcript to be present in the cell at steady state. Activation of the P2*prfA* promoter is partially dependent on the alternative sigma factor σ_B, which connects virulence factor regulation to the σ_B stress response[26]. Once transcribed, secondary structure in the 5' untranslated region (UTR) of the P1-driven prfA transcript blocks the ribosome binding site to prevent translation at temperatures ≤30ºC. At higher temperatures, such as human body temperature (37ºC), this structure denatures to allow translation of PrfA protein[27]. This RNA thermosensing mechanism ensures that transcription of virulence factors remains off in the cooler temperatures of the environment and allows rapid production of PrfA upon the transition to a mammalian host. Once translated, PrfA activates transcription of PrfA-dependent promoters, including P*plcA* which creates a positive feedback loop to produce a high abundance of PrfA protein[28].

Transcriptional activation of PrfA-dependent promoters is further regulated by affinity of PrfA to the PrfA box in the promoter of target genes, which is affected by post-translation modifications of PrfA that occur upon entry of *Lm* to the host cytosol. Unmodified PrfA weakly binds and activates promoters with high-affinity PrfA boxes, which includes genes such as *hly* and

plcA-prfA. Exposure of *Lm* to the highly reducing environment of the host cell cytosol reduces cysteine residues on PrfA to increase affinity for DNA-binding[29]. In addition, PrfA becomes allosterically activated by reduced glutathione (GSH) which locks it into a DNA-binding conformation[29,30]. Together, these post-translational modifications fully activate PrfA and allow for binding to low-affinity PrfA boxes, such as in the *actA* promoter, when *Lm* contacts the host cytosol. Importantly, PrfA is activated by bacterially-derived GSH, as deletion of the *Lm* glutathione synthase *gshF* abrogates *actA* expression, while inhibition of host glutathione synthesis has no effect[29]. Transcription of *gshF* is upregulated ~10-fold during cytosolic infection, which increases intracellular GSH concentrations above a threshold to allow PrfA activation. Allosteric activation of PrfA by GSH is critical for full virulence by highly inducing virulence gene expression in the cytosolic compartment; indeed, *actA* transcription increases over 200-fold in the host cytosol compared to extracellular growth[31].

The mechanism by which *Lm* senses its position in the host cytosol to induce GSH production and allosterically activate PrfA remains unknown. Addition of reducing agents during growth in minimal medium fully activates PrfA *in vitro*[32]. Importantly, this was dependent on bacterial glutathione production, as a mutant lacking *gshF* was unable activate PrfA using reducing agents alone. Correspondingly, the presence of reducing agents increased intracellular concentrations of GSH[32]. While these data suggest a model in which the reducing environment of the host cytosol triggers increased production of GSH to activate PrfA, this has only been observed during *in vitro* growth and has not been empirically tested during infection. Whether reducing conditions alone are sufficient for PrfA activation *in vivo* remains to be determined.

While exposure to activating factors in the host cytosol is critical for robust induction of virulence genes, there is evidence that nutrient availability acts to fine-tune virulence factor expression during extracellular growth. Growth in the presence of simple sugars which are imported through phosphotransferase systems (PTS), such as cellobiose and glucose, represses expression of virulence factors[33,34]. Non-PTS carbon sources such as hexose phosphates and glycerol do not repress virulence factor expression, suggesting that carbon source-dependent regulation requires PTS-mediated transport of sugars[35,36]. Indeed, mutants lacking *hprK* and *ptsH*, components of the phosphorelay signaling pathway that occurs downstream of PTS sugar import, have high expression of PrfA-regulated genes when grown in rich medium[37]. Notably, expression of a constitutively active PrfA variant (PrfA*), which no longer requires GSH for allosteric activation, rescues inhibition of virulence gene expression by PTS sugars[36]. Together, these data suggest that uptake of sugars through PTS-dependent transport initiates signaling cascades which repress PrfA activation. This may be an additional mechanism to prevent expression of virulence factors in the environment, where plant-derived mono and disaccharides are abundant.

Sensing of amino acid availability comprises an additional link between metabolic state and virulence gene expression. Activation of the stringent response by amino acid starvation appears to be required for full PrfA activity, and mutants unable to mount a stringent response are nearly attenuated in mice[32,38]. The connection between the stringent response and virulence may be mediated by CodY, a transcriptional regulator in low G+C Gram-positive bacteria which represses transcription of its regulon while bound to branched-chain amino acids (BCAAs) or GTP[39]. Activation of the stringent response during BCAA starvation and subsequent depletion of GTP pools by pp(G)pp synthesis relieves CodY repression to activate target genes[40]. While CodY canonically acts as a repressor of transcription, it has been demonstrated that CodY activates

transcription of *prfA* during BCAA starvation[41,42]. Accordingly, growth of *Lm* in minimal media leads to modest PrfA activation *in vitro* while growth in the presence of amino acids, particularly those containing BCAAs, abrogates this activation[32,43]. Overall, BCAA availability may serve as an additional cue to *Lm* to accurately sense its localization in different niches and link metabolic rewiring during infection to virulence gene expression.

A model for regulation of *Lm* virulence genes by PrfA in extracellular and intracellular niches is summarized in Figure 1. Transcription of *prfA* is present but limited in the environment due to absence of transcriptional activators such as σ_B, CodY, and PrfA itself. Translation of prfA transcripts is repressed due to low temperature, and activation of any PrfA protein is blocked by signaling through PTS-mediated sugar transport. Upon entering a mammalian host, prfA transcripts are translated due to increased temperature, and limited transcription of factors required early during infection such as LLO is initiated at high-affinity PrfA boxes. Stressors encountered during infection, including oxidative stress or activation of the stringent response, increase *prfA* transcription through activation of σ_B and CodY. After invasion into host cells and escape from the vacuole, a reducing environment and potentially additional host-derived cues present in the cytosol trigger upregulation of *gshF* and increased production of GSH to allosterically activate PrfA. Active PrfA initiates transcription of its entire regulon to induce expression of virulence factors in the host cytosolic compartment.

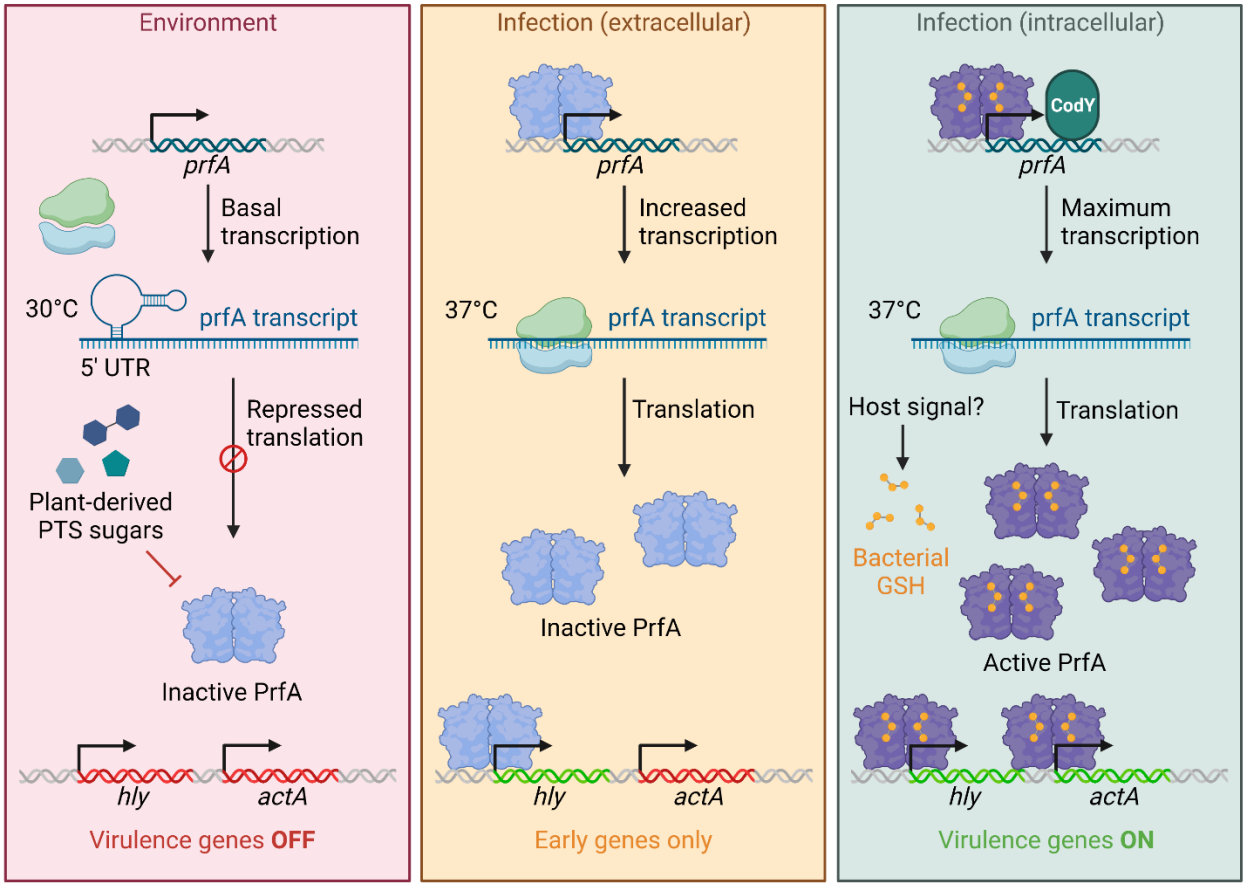

Figure 1. Model of *Lm* virulence factor regulation by PrfA. prfA transcripts are kept low in the environment, and translation and activation of PrfA is repressed. Transition to a mammalian host allows rapid translation of prfA transcripts. PrfA can then activate early genes, such as *hly*, as well as increase

transcription of its own promoter. Once *Lm* becomes intracellular, GSH is synthesized to allosterically activate PrfA, allowing transcription of late genes such as *actA*. Transcription of *prfA* is maximized intracellularly by activated PrfA and CodY.

Phagocytosis of *Lm* by macrophages

In order to enter the intracellular niche and fully activate PrfA, *Lm* must first invade host cells to initiate the intracellular lifecycle. *Lm* is capable of infecting a wide variety of cell types in mammals, including both phagocytes and non-phagocytic cells. Invasion of non-phagocytes requires both *Lm* virulence factors and host cell machinery and has been well-studied over the last 30 years[5]. Briefly, the internalins InlA and InlB present on the *Lm* surface bind to the host receptors E-cadherin and c-Met, respectively[44,45]. This triggers activation of a complex signaling cascade in the host cell which involves activation of phosphoinositide-3-kinase (PI3K) and small GTPases to trigger actin polymerization at the host cell membrane and subsequent engulfment of *Lm*[46–50]. While InlA and InlB are known to mediate entry into many non-phagocytic cell types such as enterocytes, hepatocytes, and endothelial cells[51], additional internalins such as InlF and InlP have recently been described and may be important for invasion of the central nervous system (CNS) and placenta[52–54].

Lm invasion of professional phagocytes such as macrophages, monocytes, and dendritic cells has been relatively understudied. Phagocytes are named for their ability to engulf a diverse array of extracellular particles, known as phagocytosis. Phagocytosis acts to both capture invading pathogens and clear apoptotic cells and debris, making it a critical process for immune function and homeostasis[55,56]. Phagocytes are equipped with several phagocytic receptors to recognize and engulf various substrates, including bacteria. Opsonin-dependent receptors, such as Fc receptors and complement receptors, mediate phagocytosis of bacteria which have been opsonized with antibodies and components of the complement system, respectively[56]. Non-opsonic receptors bind bacteria directly through recognition of pathogen-associated molecular patterns (PAMPs). These include C-type lectin receptors, which recognize specific polysaccharide signatures on microbial cell surfaces, and scavenger receptors, which bind polyanionic ligands such as lipopolysaccharides (LPS) or lipoteichoic acids (LTA) on bacteria[56]. Binding of a phagocytic receptor to its ligand triggers intracellular signaling which activates cellular machinery to facilitate internalization of the particle as well as regulates the fate of the particle once engulfed. Phagocytic receptors often cooperate with pattern recognition receptors (PRRs) to modulate intracellular signaling and provide crosstalk between phagocytosis and the innate immune response[57]. Toll-like receptors (TLRs) are a canonical example of PRRs involved in phagocytosis, as impaired TLR signaling has been shown to restrict phagocytosis of several bacterial pathogens[58–61].

While *Lm* is engulfed by all professional phagocytes, only macrophages support robust intracellular replication of *Lm*[62,63]. Because phagocytosis of *Lm* is generally more efficient than internalin-mediated uptake, macrophages are a widely used model cell type to study cytosolic infection by *Lm*. Indeed, the famous illustration of the *Lm* intracellular lifecycle by Tilney and Portnoy is based off of electron micrographs of infected macrophages[9]. Despite the prevalent use of macrophages to investigate *Lm*-host interactions and the relevance of macrophages to disease progression, the mechanism by which *Lm* initially invades these cells has not been thoroughly characterized. It has long been assumed that entry of *Lm* into macrophages is through “passive”

phagocytosis. However, phagocytosis is a diverse and dynamic process which involves specific macrophage receptors, complex intracellular signaling networks, and bacterial factors[56]. The molecular details of each of these components of the phagocytic process remain to be determined for phagocytosis of *Lm*.

The few existing studies on phagocytosis of *Lm* have primarily focused on opsonin-mediated phagocytosis. Following opsonization by serum, *Lm* becomes coated with C3b which mediates uptake into macrophages through complement receptor 3 (CR3)[64]. However, phagocytosis through CR3 restricts *Lm* to the phagosome and results in bacterial killing[65,66], indicating that entry into the cytosol of macrophages and subsequent intracellular replication occurs through a distinct uptake pathway. Indeed, early *in vitro* work demonstrated that phagocytosis of non-opsonized *Lm* is independent of CR3 and results in cytosolic infection[65,67] (Figure 2). Few non-opsonic phagocytosis receptors for *Lm* have been described. Fcγ-receptor 1A (FcγR1a or CD64) was recently shown to mediate antibody-independent uptake of *Lm* by human macrophages in serum-free conditions[68]. However, deletion of *FCGR1A* had a rather small effect on phagocytosis (~14% reduction), and this was species-specific as murine FcγR1a did not promote *Lm* phagocytosis. The macrophage scavenger receptor SR-A I/II (*Msr1*) reportedly promotes phagocytosis of *Lm* by peritoneal macrophages and Kupffer cells during intravenous (i.v.) infection of mice, however internalization via this pathway is listericidal[69] (Figure 2). Receptors which mediate phagocytosis and subsequent cytosolic replication of *Lm* remain unknown. Even less is known about downstream signaling involved in mediating phagocytosis of *Lm*. A single report found that activation of PI3K and the small GTPase Rac1 downstream of TLR2 is important for proper phagocytosis of *Lm*[70]. A comprehensive understanding of the host and bacterial factors involved in mediating phagocytosis of *Lm* by macrophages would allow more thorough investigations into the role that *Lm*-phagocyte interactions play during listeriosis.

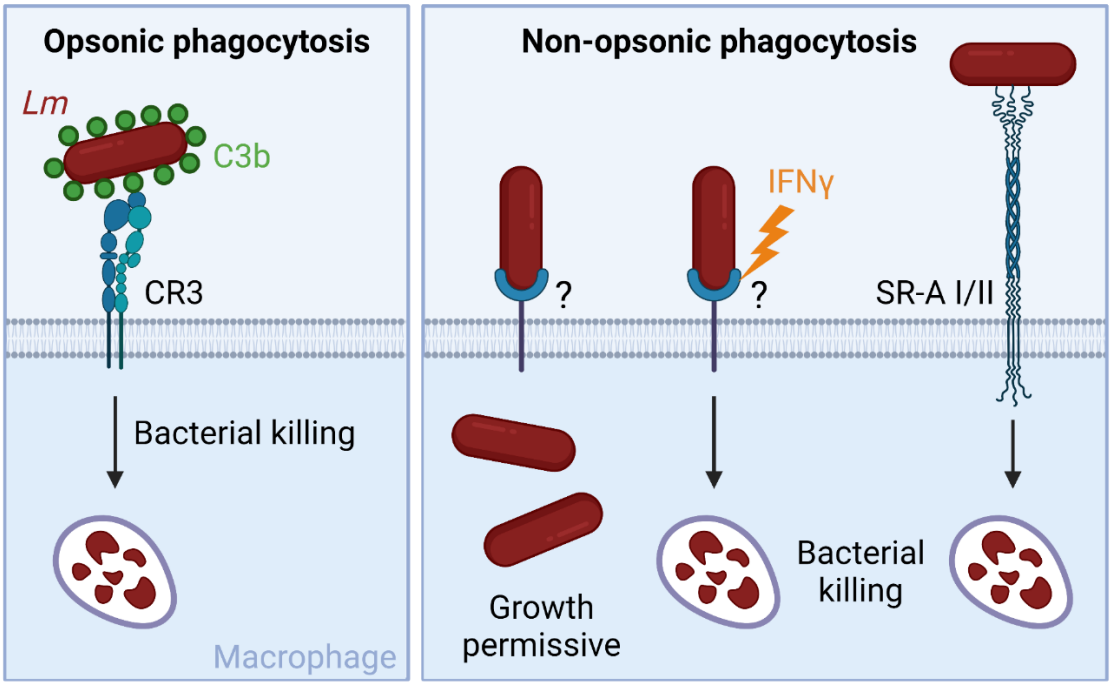

Figure 2. Phagocytosis of *Lm* by macrophages. *Lm* opsonized by C3b is taken up through CR3, resulting in bacterial killing. In the absence of opsonins, *Lm* is taken up through an uncharacterized pathway which

leads to cytosolic growth. In the presence of IFNγ, growth-permissive uptake pathways become bactericidal. In addition, *Lm* can be internalized through the scavenger receptor SR-A I/II, resulting in bacterial killing.

The dual roles of macrophages during *Lm* infection

Lm undergoes a multi-organ trafficking circuit to cause invasive listeriosis[10,71]. Following the consumption of *Lm*-contaminated food, the bacteria cross the intestinal barrier through InlA-mediated invasion of enterocytes at the tips of intestinal villi or InlA-dependent transcytosis through goblet cells[72–74]. The bacteria can also cross the intestinal epithelium in an InlA-independent manner via transcytosis through antigen-sampling microfold (M) cells into intestinal Peyer's Patches[75–77]. Invasion through either route results in bacterial entry into the lamina propria and transit to the draining mesenteric lymph nodes (MLN). From there, *Lm* enters the systemic circulation and disseminates through the bloodstream to the spleen and liver. After replicating to high numbers in these organs, the bacteria re-enter systemic circulation and cross the blood-brain barrier or placental barrier to initiate CNS infection or fetal infection, respectively[5]. While the route of *Lm* dissemination has been characterized, the precise mechanisms underlying the method of dissemination from the GI tract are a current area of study.

A growing body of literature supports a model in which phagocytic monocytes and macrophages promote dissemination of *Lm* to internal organs. In the intestinal lamina propria, *Lm* encounters resident immune cells and is thought to replicate intracellularly in phagocytes such as macrophages[78,79]. Development of an oral infection model of listeriosis in recent years has allowed for closer examination of *Lm* dissemination from the lamina propria, with emerging hypotheses suggesting transit of bacteria from the lamina propria to the MLN occurs within phagocytes[71,78]. In support of this model, intracellular replication in growth-permissive lamina propria cells, which may include resident macrophages, is important for initial dissemination to the MLN[79]. In addition, several studies have demonstrated the importance of *Lm*-infected monocytes in establishing CNS infection in both i.v. and oral models of infection[11,80–83].

In contrast to the role macrophages and monocytes play in systemic dissemination of *Lm*, these inflammatory phagocytes are also critical for bacterial clearance and host protection[84,85]. Growth-permissive macrophages become listericidal upon activation by interferon gamma (IFNγ), which is crucial for limiting bacterial replication *in vivo*[86–88] (Figure 2). Importantly, studies demonstrating the role of macrophages in host protection against *Lm* were performed using i.v. or intraperitoneal inoculation, which models systemic infection but bypasses the intestinal phase. Thus, the relative contributions of macrophages to pathogen dissemination versus bacterial restriction during foodborne listeriosis remain unclear, particularly in the case of lamina propria macrophages during the GI phase of infection (Figure 3).

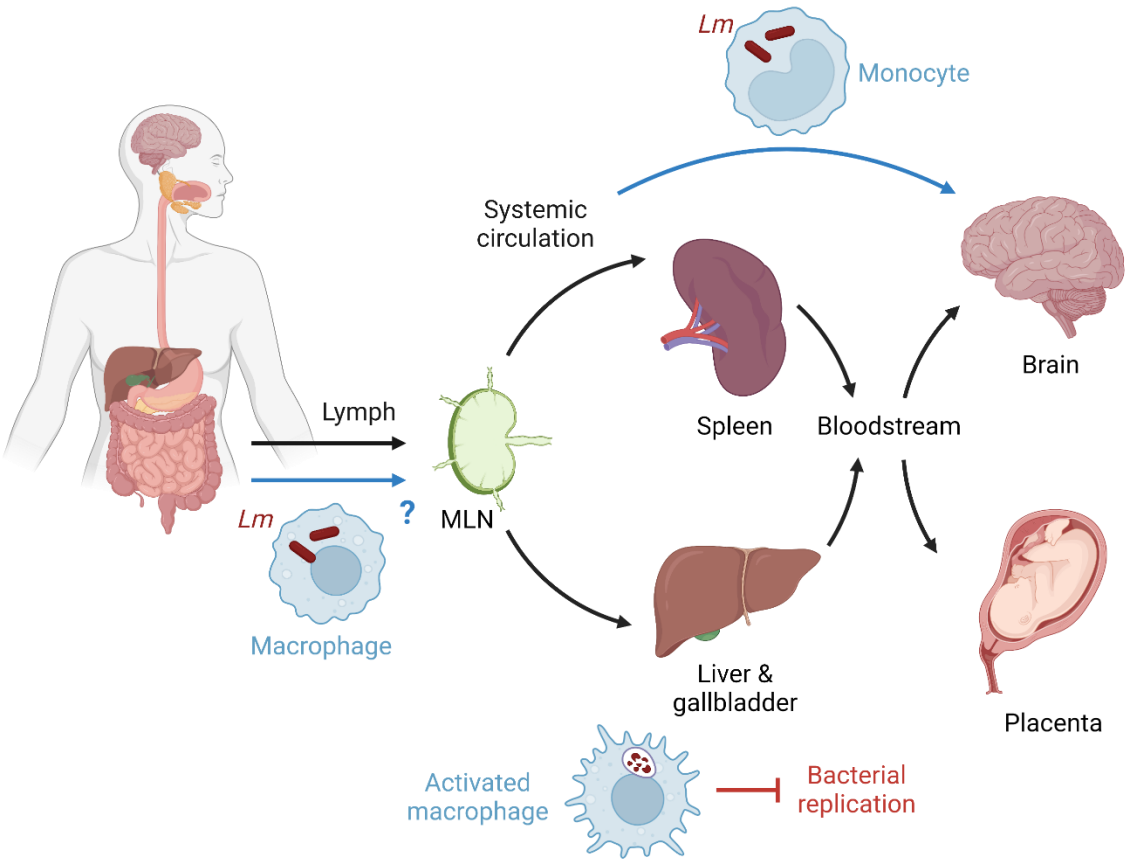

Figure 3. Potential roles of macrophages during foodborne listeriosis. *Lm* disseminates from the GI tract through the lymphatics and enters systemic circulation via the mesenteric lymph nodes (MLN). Macrophages in the intestinal lamina propria are hypothesized to serve as a replicative niche for *Lm* and promote dissemination of *Lm* from the GI tract to peripheral organs. Monocytes harboring intracellular *Lm* are known to promote invasion of the CNS. Macrophages activated by IFNγ are critical for restricting bacterial replication during the systemic phase of infection.

State of the field and open questions

While *Lm* virulence factors have been extensively studied over the last 40 years, host determinants of infection are less understood. Regulation of virulence factor expression by PrfA is tightly controlled by both bacterial and host factors. In particular, transcription of *actA* is strikingly restricted to the cytosolic compartment of host cells; because of this, it has long been hypothesized that a specific chemical signature of host cell cytosol acts as a cue to trigger *actA* expression. While several studies have identified various exogenous molecules that impact PrfA activation, most of these experiments have been performed using *in vitro* systems. Identification and characterization of host cell-derived factors responsible for triggering PrfA activation *in vivo* will not only unify decades of studies on this *Lm* transcriptional regulator but may also reveal properties of the cytosolic environment which impact virulence of other intracellular pathogens.

Additionally, the mechanism of *Lm* entry into phagocytic cells such as macrophages is a severely understudied area of *Lm* pathogenesis. Bacterial surface molecules, macrophage receptors, and intracellular signaling components involved in mediating opsonin-independent

phagocytosis and subsequent cytosolic infection are currently unknown. A handful of studies have begun to identify pieces of this puzzle, however a complete understanding of this pathway will be critical for investigations of *Lm*-macrophage interactions *in vivo*. The contribution of opsonin-independent phagocytosis to *Lm* disease progression remains to be determined. The vast majority of studies focused on phagocytosis of *Lm* during murine infection have been performed using i.v. inoculation in which *Lm* becomes opsonized in the bloodstream. Recent studies using a foodborne listeriosis model have begun to study whether invasion and replication within phagocytes contributes to dissemination of *Lm* from the GI tract. Identification and perturbation of factors involved in opsonin-independent phagocytosis will provide an important tool to dissect the relevance of this pathway *in vivo*.

Overall, the goal of my thesis is to identify and characterize host factors impacting pathogenesis of *Lm*. The work presented here investigates two major questions in the field regarding host-*Lm* interactions: 1) What properties of the host cytosol lead to activation of PrfA specifically in this compartment? 2) What host proteins (receptors, signaling pathways, or cellular machinery) are involved in phagocytosis of *Lm*? First, experiments using a cell-free extract system revealed that one or more proteins contained within the cytosolic fraction of eukaryotic cells is sufficient to activate PrfA *in vitro* (Chapter 2). To investigate the identity of this protein or proteins, a genome-wide CRISPR/Cas9 was performed to isolate mutant macrophages which no longer activate transcription of *actA* in *Lm* (Chapter 3). During this screen, we also isolated macrophages which were no longer able to phagocytose *Lm* to identify host genes important for phagocytosis. Finally, follow up studies characterized the role of the host gene *Pten* in promoting phagocytosis of *Lm* both *in vitro* and *in vivo* (Chapter 4). Together, these studies have identified properties of the host cell which influence *Lm* gene expression and uptake, revealed complexity in the host and bacterial determinants of phagocytosis, and demonstrated the role of macrophages in *Lm* pathogenesis during foodborne listeriosis.

Chapter 2: Investigating the role of the host cell cytosol in activating *Lm* virulence using *Xenopus* cell-free extracts

Introduction

The master transcriptional regulator PrfA specifically and robustly induces the expression of the virulence gene *actA* in the host cell cytosol. After invasion of *Lm* into the host cytosol, the *Lm* glutathione synthase *gshF* is upregulated and GSH is synthesized to high concentrations, allosterically activating PrfA[29] (Figure 1). The external cue present in the host cytosol which triggers upregulation of *gshF* is unknown. Addition of reducing agents during growth in minimal medium increases *gshF* transcription and activates PrfA *in vitro*. However, these experiments were only performed during broth growth; whether or not a reducing environment alone activates PrfA during cytosolic growth remains to be determined. In addition, overexpression of *gshF* during broth growth is not sufficient to activate PrfA *in vitro* (data not shown), indicating the presence of additional host-derived regulatory factors required for full PrfA activation.

Manipulating the cytosol of intact eukaryotic cells is a difficult challenge. While the use of small molecules and enzymatic inhibitors can target specific cellular processes, changing the biochemical properties of the cytosol are likely to have detrimental effects on the host cell and lead to cell death. Genetic studies in eukaryotes have become feasible in recent years due to development of CRISPR-mediated gene editing, however this is still a laborious process and can only be used to target a small number of genes at one time. To overcome these challenges, we utilized a *Xenopus* cell-free extract system to study activation of *Lm* virulence factors in eukaryotic cytosol.

Xenopus cell-free extracts are a biochemically tractable cytosol derived from the eggs of *Xenopus laevis* or *Xenopus tropicalis* frogs and have been used to make fundamental discoveries in DNA replication, cell cycle progression, and developmental biology over the last 50 years[89]. *Xenopus* eggs are single cells measuring ~1 mm, allowing extraction of a relatively large amount of biofluid per cell compared to cultured cells. In addition, a purified cytosolic fraction can be easily separated from membranes and cell debris through high-speed centrifugation, eliminating the need for dilution and contamination by lysis agents[89]. *Xenopus* cell-free extracts contain physiological levels of enzymes, cytoskeletal components, organelles, and small biomolecules such as nucleotides and amino acids. In addition, molecular pathways and processes are biochemically active in cell-free extracts; indeed, exogenous mRNAs are fully translated to high levels when added to *Xenopus* egg extract[90]. Importantly, cytosolic extracts are highly manipulable using standard biochemical approaches, making them an excellent *in vitro* model for eukaryotic cytosol.

While *Lm* is mainly thought of as a mammalian pathogen it is capable of infecting other animals such as insects (*Drosophila*)[91] and fish (*Danio rerio*)[92], suggesting that host determinants of *Lm* virulence factor expression are conserved among metazoans. In support of this, *Lm* grown in *Xenopus* cell-free extracts undergo ActA-mediated actin-based motility, and this system was successfully used to study the dynamics of actin-based motility in *Lm* and identify host cytosolic proteins involved in the process[93–95]. Notably, these studies used a strain of *Lm* harboring a PrfA* mutation causing aberrant virulence gene expression[96]. Whether or not host cytosolic factors

capable of activating the *Lm* virulence regulon are conserved in *Xenopus* cell-free extracts remains to be determined.

The goal of the experiments presented in this chapter is to identify host factors required for PrfA activation using *Xenopus* cell-free extracts. First, we validated a method for investigating PrfA activation in cell-free extracts. Subsequent biochemical manipulation of cytosolic extracts revealed that a host factor of proteinaceous nature is responsible for activating virulence gene expression in *Lm*. To identify this host protein(s), we fractionated *Xenopus* egg extracts using fast protein liquid chromatography (FPLC). Anion-exchange chromatography was capable of reproducibly isolating a protein fraction which retained PrfA-activating activity. Mass spectrometry of active and non-active fractions identified candidate proteins which may be involved in activating *Lm* virulence genes. Overall, these studies established a system for recapitulating cytosolic *Lm* virulence gene expression *in vitro* and revealed properties of the host cytosol which are required for activating PrfA. While I performed the vast majority of the experiments presented here, Dr. Michelle Reniere, Dr. Aaron Whiteley, and Dr. Alex Pollock were instrumental in the design and optimization of this system. Handling of *X. tropicalis* frogs and procedures performed on these animals were carried out by Dr. Andrea Wills and Dr. Hannah Arbach.

Results

Xenopus cell-free extracts activate PrfA and expression of *actA*

To investigate activity of PrfA in *Xenopus* cell-free extracts, we used transcriptional activation of *actA* as a readout for PrfA activation. Transcription of *actA* is off during growth in broth and is specifically induced over 200-fold in the host cell cytosol after PrfA becomes allosterically activated by GSH[29]. We took advantage of a strain of *Lm* which was originally designed for use as a vaccine vector and dies upon entry to the host cytosol. This strain, named the “suicide strain”, contains *loxP* sites flanking the origin of replication on the *Lm* chromosome as well as expression of Cre recombinase driven by the *actA* promoter[29,97]. When grown under conditions which activate PrfA, such as cytosolic replication, transcriptional activation of the *actA* promoter leads to production of Cre, excision of the origin of replication, and bacterial death. The suicide strain grows identically to wildtype (wt) *Lm* in broth, however is almost completely eliminated after 8 hours of growth within macrophages[29]. Thus, the suicide strain can be used to measure induction of *actA* transcription using simple growth-based assays and CFU readouts.

We first wanted to establish whether cell-free extracts from *Xenopus tropicalis* eggs are capable of activating *actA* transcription *in vitro*. Both wt *Lm* and the suicide strain were grown in cell-free extracts for 4 hours, and both input and output CFU were enumerated to calculate the percent survival of each strain. To encourage robust replication in the extracts, which is necessary for cell death via excision of the origin of replication, extracts were mixed 1:1 with 2X BHI just prior to the experiment. During cytosolic growth in macrophages, the suicide strain exhibits a ~3-log survival defect compared to wt at 4 hours post-infection, therefore we reasoned that the maximum survival defect we could observe in *Xenopus* extracts would be 3-logs. Excitingly, we found that the suicide strain had a 3-log survival defect in cell-free extracts, similarly to growth in the cytosol of live cells (Figure 4A). These data demonstrate that a component or property of host cytosol activates PrfA and is conserved in *Xenopus*.

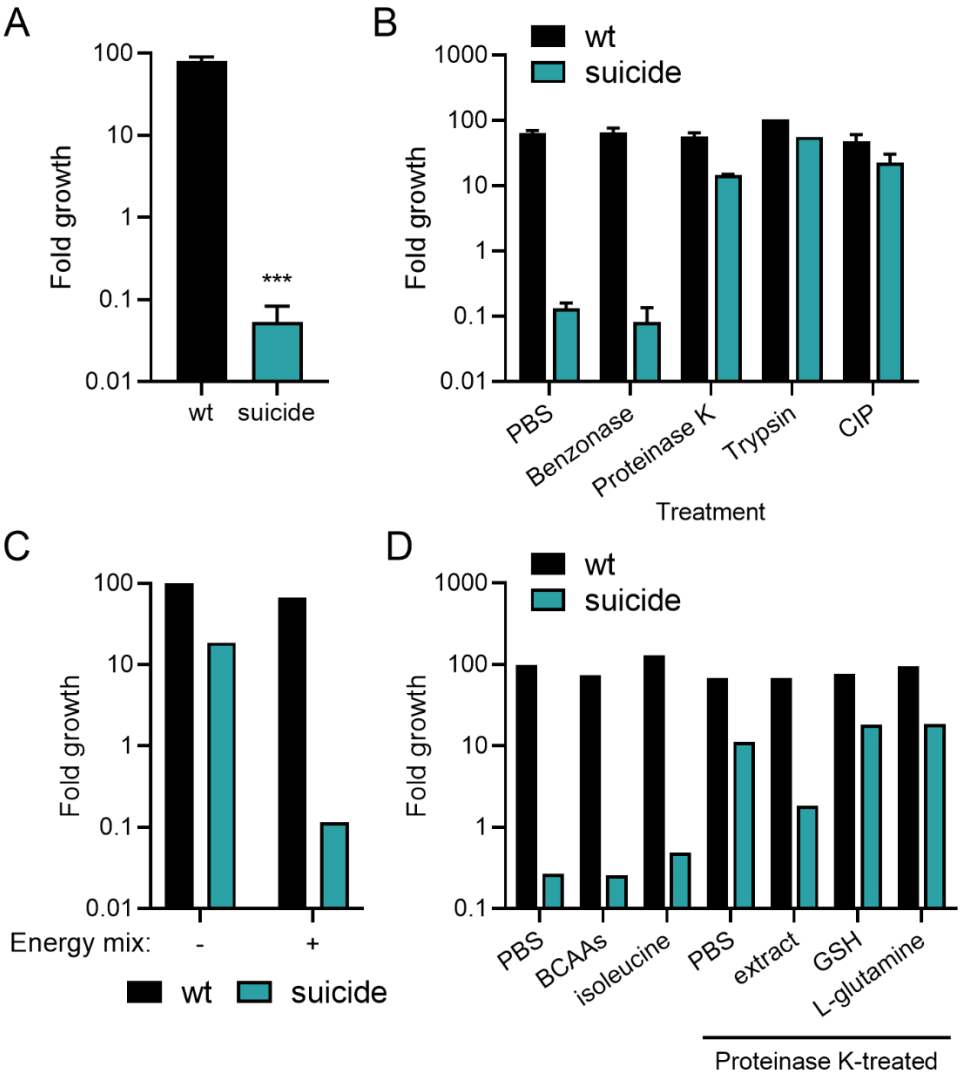

Figure 4. *Xenopus* cell-free extracts activate PrfA *in vitro*. (A) Cell-free extracts were isolated from *X. tropicalis* eggs, diluted 1:5 with PBS and 2X BHI (final concentration of 1X BHI), and supplemented with energy mix. Mixtures were inoculated with wt *Lm* or the suicide strain and CFU were enumerated at the time of inoculation and 4 hours post-inoculation. Data are reported as fold growth at 4 hours compared to the inoculum and are means and SEM of 3 independent experiments. ***$p<0.001$ as determined by unpaired *t* tests. (B) Extract mixtures were prepared as in (A) and supplemented with 0.156 U/µL Benzonase, 8 U/µL Proteinase K, 12.5 ng/µL Trypsin, 50 ng/µL biotinylated-CIP, or PBS as a control. Extracts were incubated for 1 hour at 37ºC and subsequently assayed for suicide strain survival. Data are means and SEM of 3 independent experiments except Trypsin treatment which represents a single experiment. (C) Extracts were supplemented with or without energy mix and assayed for suicide strain survival. Data represent a single experiment. (D) Untreated extracts were supplemented with PBS, 1 mM BCAAs (leucine, isoleucine, and valine), or 1 mM isoleucine. Proteinase K-inactivated extracts were treated with 2 mM PMSF for 20 minutes to quench the reaction. Inactivated extracts were supplemented with PBS, untreated extract, 10 mM GSH, or 4 mM L-glutamine. Extracts were assayed for suicide strain survival. Data represent a single experiment.

A protein component of *Xenopus* extracts activates PrfA and requires phosphorylation and energy regeneration

To determine the nature of this host-derived signal, we next pre-treated *Xenopus* extracts with various enzymes to deplete specific biomolecules. Benzonase was used to degrade DNA and RNA, Proteinase K (low-specificity) and Trypsin (higher specificity) to degrade proteins, and calf intestinal alkaline phosphatase (CIP) which dephosphorylates nucleic acids and proteins. Pre-treatment with Benzonase had no effect on extract activity, indicating that nucleic acids are not required to activate PrfA (Figure 4B). Interestingly, both Proteinase K and Trypsin treatment eliminated activity of *Xenopus* extracts, demonstrating that one or more proteins present in cell-free extracts is required to induce *actA* expression (Figure 4B). Treatment with CIP also completely abrogated extract activity, suggesting that phosphorylation of a nucleic acid or protein is also required for activity (Figure 4B). Since DNA or RNA does not appear to be important for activity, we hypothesize that one or more phosphorylated proteins are involved in mediating PrfA-activating activity of *Xenopus* extracts.

In order to maintain high biological activity, *Xenopus* cell-free extracts are routinely supplemented with an "energy mix" consisting of creatine phosphate, ATP, and $MgCl_2$. The experiments performed above used extracts supplemented with energy mix. To determine whether energy mix is required for PrfA activation in this system, extracts were prepared with or without addition of energy mix, and survival of the suicide strain was assessed. Extracts lacking energy mix no longer induced death of the suicide strain, indicating that energy regeneration in *Xenopus* extracts is required for induction of *actA* expression (Figure 4C). Based on our findings that a protein present in cell-free extracts is involved in PrfA activation, we hypothesize that this protein is an enzyme requiring a component of energy mix.

Various biomolecules have been previously implicated in inhibiting or promoting PrfA activation (Figure 1). High concentrations of BCAAs, particularly isoleucine, have been shown to inhibit PrfA activity during growth in minimal medium[32,41], however this has not been tested in the native cytosolic environment. We supplemented cell-free extracts with high concentrations of BCAAs or isoleucine alone and measured survival of wt *Lm* and the suicide strain. Neither BCAAs or isoleucine inhibited activity of *Xenopus* extracts, suggesting that these amino acids do not repress PrfA activation during infection (Figure 4D). During growth in minimal medium, both L-glutamine and exogenous GSH have been reported to activate PrfA[32,98]. To test whether treatment with Proteinase K eliminates extract activity through modulation of L-glutamine or GSH, extracts were pre-treated with Proteinase K and subsequently supplemented with the protease inhibitor PMSF to inactivate Proteinase K. PMSF treatment had no effect on growth of *Lm* or extract activity (data not shown). Exogenous L-glutamine or GSH were then added to inactivated extracts to test whether these compounds could restore activity of Proteinase K-treated extracts. The addition of untreated extracts to inactivated extracts restored ~1-log of suicide strain survival, however addition of L-glutamine or GSH had no effect on growth of the suicide strain (Figure 4D). These data suggest that exogenous L-glutamine or GSH are not sufficient to activate PrfA in eukaryotic cytosol.

PrfA-activating proteins can be isolated using FPLC

To identify proteins present in *Xenopus* extracts which are involved in activating PrfA, we used FPLC to isolate protein fractions from extracts. To begin, we fractionated cell-free extracts using anion-exchange chromatography, which separates proteins based on negative charge. Fractions were tested for activity by growing wt *Lm* or the suicide strain in each fraction similarly to growth in extracts, and measuring suicide strain survival. Excitingly, growth of the suicide strain in a single fraction (fraction 12) displayed a 2-log defect compared to wt *Lm* (Figure 5A). We repeated this experiment but pre-treated the extracts with Benzonase before running on the column to reduce viscosity. Isolation of a single active fraction was reproducible, and this fraction had similar activity to the previous experiment (~2-logs) (Figure 5A). Interestingly, Benzonase treatment shifted the retention time of the active fraction to elute much earlier than previously (Figure 5A). These data suggest that PrfA-activating proteins have higher negative charge in the presence of nucleic acids.

The active fraction from the Benzonase-treated extracts (fraction 4) was re-tested for activity with or without Proteinase K treatment. Proteinase K eliminated activity of fraction 4, indicating that this fraction contains PrfA-activating proteins. To visualize the protein content of the active fraction, the column input (whole extract) as well as fractions 1-6 were separated by SDS-PAGE and stained with Coomassie. The first fractions to elute off of the column, particularly fractions 2 and 3, displayed very similar protein composition to the column input and likely represent the majority of proteins which did not interact with the column (Figure 5C). While still rather complex, fraction 4 had a distinct banding pattern from the column input or fractions 2 and 3. In addition, fractions 5 and 6, which did not have PrfA-activating activity, had a reduced number of protein bands compared to fraction 4. These data suggest that fraction 4 contains a distinct protein composition compared to the surrounding non-active fractions.

To identify unique proteins present in fraction 4, we used mass spectrometry analysis on fraction 4 and fraction 5. In addition, we performed an additional round of anion-exchange chromatography on Benzonase-treated extracts and isolated a second active fraction. This fraction eluted from the column similarly to the first experiment (fraction 6) and displayed activity similar to whole extracts (data not shown). Fraction 6 from the second experiment, as well as an adjacent non-active fraction, was also analyzed by mass spectrometry. Overall, we identified 62 proteins which were enriched at least 1.5-fold in both active fractions compared to their corresponding non-active fractions (Table 1).

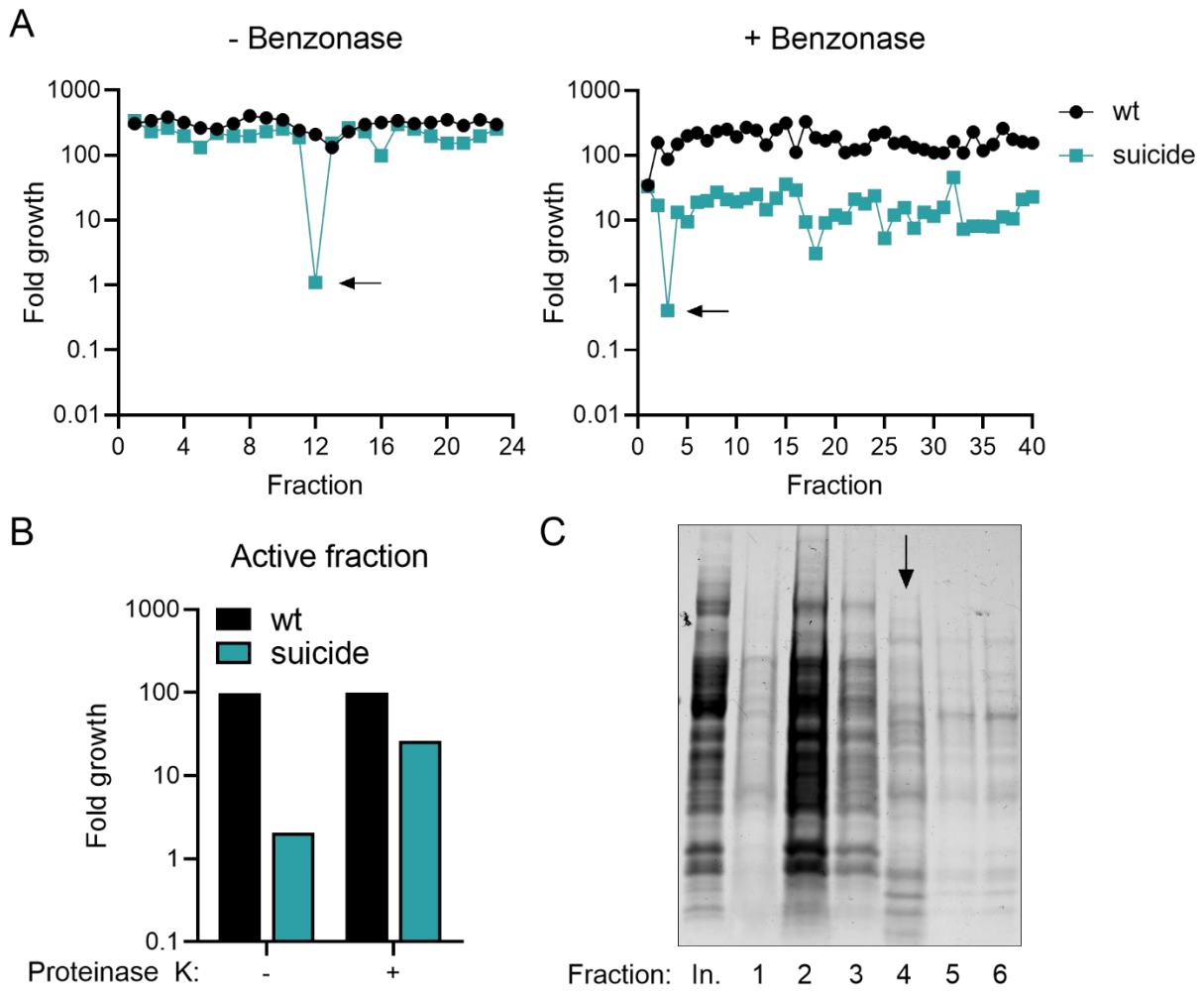

Figure 5. Isolation of PrfA-activating proteins using anion-exchange chromatography. (A) 1-2 mL of *X. tropicalis* cell-free extracts with and without Benzonase pre-treatment were separated using anion-exchange FPLC. Fractions were combined 1:1 with 2X BHI, supplemented with energy mix, and assayed for suicide strain survival. Active fractions are indicated with an arrow. (B) The active fraction from panel A (+ Benzonase) was stored at 4ºC overnight, treated with 8 U/µL Proteinase K, and assayed for suicide strain survival. Data represent a single experiment. (C) Column input (In.) or fractions 1-6 from panel A (+ Benzonase) were separated by SDS-PAGE and visualized with Coomassie. The active fraction is indicated with an arrow.

Table 1. Proteins enriched in the active fractions of extracts separated by anion-exchange chromatography.

		Column 1 (Exclusive spectrum count)		Fold change (active/non-active)		Column 2 (Exclusive spectrum count)	
Protein	**Name**	**Active**	**Non-active**	**Column 1**	**Column 2**	**Active**	**Non-active**
Psma4	Proteasome subunit alpha 4	17	0	-	-	2	0
Dynll2	Dynein light chain LC8-type 2	4	0	-	-	4	0

Ddt	D-dopachrome decarboxylase	3	0	-	5.33	32	6
Eci1	Dodecenoyl-Coenzyme A delta isomerase	6	0	-	2.50	5	2
Tmsb4x	Thymosin beta 4, X-linked	5	0	-	2.25	18	8
Fabp4	Fatty acid-binding protein 4, adipocyte	3	0	-	2.25	63	28
Psma7	Proteasome subunit alpha 7	12	1	12.00	-	1	0
Gamt	Guanidinoacetate N-methyltransferase	50	5	10.00	-	2	0
Hadh	**Hydroxyacyl-CoA dehydrogenase**	**8**	**1**	**8.00**	**-**	**2**	**0**
Akr1c	Novel Aldo-keto reductase family 1 C protein	16	3	5.33	-	3	0
Acat2	Acetyl-CoA acetyltransferase 2	5	1	5.00	-	3	0
Got2	Aspartate aminotransferase	43	9	4.78	2.75	11	4
Gpx4	**Glutathione peroxidase 4**	**14**	**3**	**4.67**	**5.86**	**41**	**7**
Nit2	Nitrilase family member 2	14	3	4.67	4.75	19	4
Aldh7a1	Aldehyde dehydrogenase 7 family, member A1	14	3	4.67	1.59	35	22
Apex1	DNA-(apurinic or apyrimidinic site) lyase	8	2	4.00	-	5	0
Dynll1	Dynein light chain 2	8	2	4.00	2.00	16	8
Paics.1	Phosphoribosylaminoimidazole carboxylase	22	6	3.67	3.67	22	6
Qdpr	**Quinoid dihydropteridine reductase**	**14**	**4**	**3.50**	**14.00**	**14**	**1**
Tars	Threonyl-tRNA synthetase-like 2	7	2	3.50	3.00	3	1
Msn	Moesin	36	11	3.27	-	1	0
Eno3	Enolase 3	91	30	3.03	2.00	8	4
Bdh2	**3-hydroxybutyrate dehydrogenase 2**	**6**	**2**	**3.00**	**5.00**	**5**	**1**
Vcl	Vinculin	27	9	3.00	2.64	58	22
Mpi	Mannose-6-phosphate isomerase	3	1	3.00	1.83	11	6
Dhrs11	Dehydrogenase/reductase (SDR family) member 11	21	7	3.00	1.80	9	5
Akr1b1	Aldo-keto reductase family 1, member B1	41	14	2.93	1.74	33	19
Ppa2	Pyrophosphatase (inorganic) 2	23	8	2.88	-	4	0
Cyria	CYFIP related Rac1 interactor A	14	5	2.80	2.25	9	4
Sod2	Superoxide dismutase 2	25	9	2.78	3.00	3	1
Mmp9.2	14 kDa phosphohistidine phosphatase	8	3	2.67	4.14	29	7
Pgm1	Phosphoglucomutase 1	124	47	2.64	1.76	67	38
Stard15	StAR-related lipid transfer (START) domain containing 15	13	5	2.60	4.25	17	4

Ddah1	Dimethylarginine dimethylaminohydrolase 1	23	9	2.56	7.00	7	1
Rpia	Ribose 5-phosphate isomerase A	33	13	2.54	-	6	0
XB5909790	Thioredoxin	15	6	2.50	-	1	0
Hint1	Histidine triad nucleotide-binding protein 1	5	2	2.50	2.00	8	4
Abracl	ABRA C-terminal like	22	9	2.44	10.00	10	1
Hspa9	Heat shock protein family A (Hsp70) member 9	27	12	2.25	-	3	0
Acp1	Acid phosphatase 1, soluble	11	5	2.20	1.63	13	8
Ak2	Adenylate kinase 2, mitochondrial	24	11	2.18	4.17	25	6
Rida	Reactive intermediate imine deaminase A homolog	15	7	2.14	1.67	5	3
Hbz	Hemoglobin subunit zeta	31	15	2.07	-	1	0
Ldhb	L-lactate dehydrogenase	81	40	2.03	2.38	88	37
Atox1	ATX1 antioxidant protein 1 homolog	6	3	2.00	7.00	7	1
Pitpna	Phosphatidylinositol transfer protein alpha	2	1	2.00	6.00	6	1
Mtap	S-methyl-5'-thioadenosine phosphorylase	8	4	2.00	5.00	5	1
Arl3	ADP ribosylation factor-like GTPase 3	8	4	2.00	3.67	22	6
Tes	Testin	2	1	2.00	2.40	12	5
Ppib	Peptidylprolyl isomerase B	6	3	2.00	2.25	9	4
Akr1a1	Aldo-keto reductase family 1, member A1	8	4	2.00	1.50	36	24
Ckb	Creatine kinase, brain	313	158	1.98	4.57	32	7
Gstm1	Glutathione S-transferase M1	21	11	1.91	2.23	89	40
Cpne1	Copine I	18	10	1.80	3.86	27	7
Serpinb6	Serpin family B member 6	59	33	1.79	-	6	0
Cgl.2	Egg cortical granule lectin	7	4	1.75	1.50	3	2
Mdh1	Malate dehydrogenase, cytoplasmic	59	34	1.74	1.65	124	75
Taldo1	Transaldolase	66	39	1.69	11.00	11	1
Anxa5	Annexin A5	41	25	1.64	-	1	0
Sri	Sorcin	29	18	1.61	5.50	11	2
Anxa3	Annexin A3	31	20	1.55	2.23	29	13
Gdi2	Rab GDP dissociation inhibitor	122	79	1.54	-	3	0

Our previous results suggested that the PrfA-activating protein present in *Xenopus* extracts is an enzyme which requires phosphorylation (Figure 4). Therefore, we focused our efforts on investigating enzymes identified by our mass spectrometry analysis. Two of the enzymes in the top 25 hits (ranked by fold enrichment in the active fraction from column 1) produce a single enzymatic product that may serve as specific chemical signatures of the intracellular environment: Quinoid dihydropteridine reductase (Qdpr) produces the compound

tetrahydrobiopterin (BH4), a cofactor required for phenylalanine biosynthesis, and 3-hydroxybutyrate dehydrogenase 2 (Bdh2) produces acetoacetate during β-oxidation of fatty acids. To determine whether either of these enzymatic products mediate PrfA activation, Proteinase K-inactivated extracts were supplemented with untreated extract, BH4, or acetoacetate. While addition of untreated extract restored PrfA activation, exogenous BH4 and acetoacetate did not restore activity, indicating that these compounds are not involved in PrfA activation (Figure 6A).

To assess the contribution of other identified enzymes to PrfA activation, we used CRISPR/Cas9-mediated genome editing to make genetic deletions in macrophages. Single guide RNAs (sgRNAs) targeting hydroxyacyl-CoA dehydrogenase (*hadh*), Aldehyde dehydrogenase 7 family, member A1 (*aldh7a1*), or glutathione peroxidase 4 (*gpx4*) were introduced into immortalized bone marrow-derived macrophages expressing Cas9 (iBMMs) via lentiviral transduction. Antibiotics were used to select for iBMMs which were successfully transduced with sgRNA-containing lentivirus. Cells transduced with either sgRNA targeting *aldh7a1* or sgRNA 2 targeting *gpx4* did not survive antibiotic selection, so only cells transduced with sgRNAs targeting *hadh* or *gpx4* were used for subsequent experiments. To test whether deletion of *hadh* or *gpx4* impacted PrfA activation, wildtype (WT) and knockout iBMMs were infected with wt *Lm* or the suicide strain, and intracellular growth was measured over 8 hours. Death of the suicide strain was not rescued in any of the cell lines tested, suggesting that Hadh and Gpx4 are not required for PrfA activation during infection (Figure 6B).

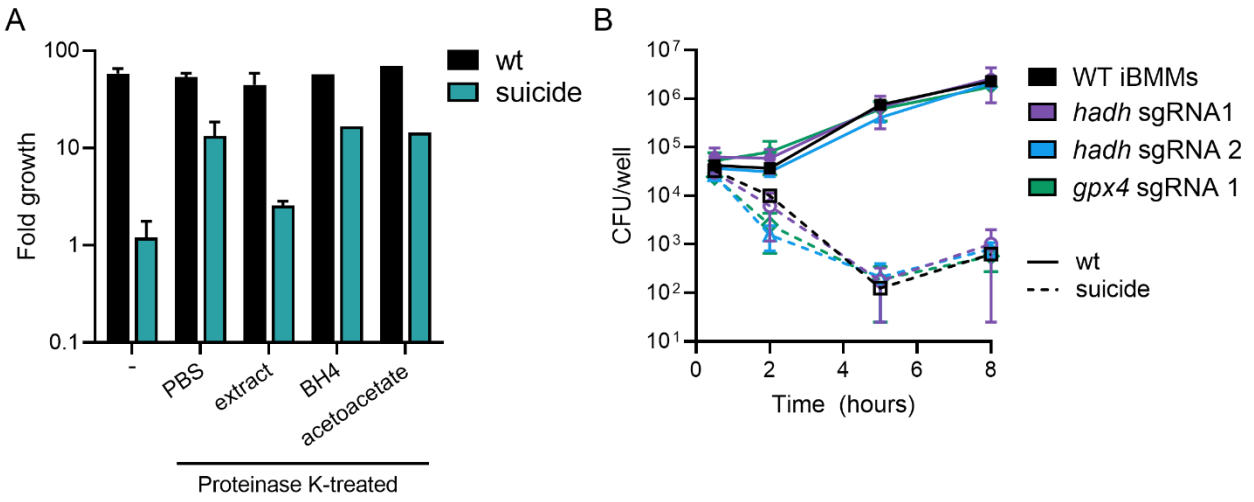

Figure 6. Role of Qdpr, Bdh2, Hadh, and Gpx4 in activating PrfA. (A) Extracts were treated with 8 U/μL Proteinase K and 2 mM PMSF was added to stop the reaction. Treated extracts were supplemented with PBS, untreated extract, 1 mM BH4, or 1 mM acetoacetate and assayed for suicide strain survival. Growth in untreated extracts alone was measured as a control. Data are means and SEM of two independent experiments (control, PBS, and extract) or represent a single experiment (BH4 and acetoacetate). (B) WT iBMMs or iBMMs expressing sgRNAs targeting *hadh* or *gpx4* were infected with wt *Lm* or the suicide strain at a multiplicity of infection (MOI) of 1. Gentamicin was added 30 minutes post-infection and intracellular CFU were enumerated at 0.5, 2, 5, and 8 hours post-infection. Data are means and SEM of two independent experiments except for WT iBMMs which represent a single experiment.

Discussion

The regulation of *Lm* virulence genes by PrfA has been extensively studied over the last 20 years, however the identity of signals present in the host cytosol which trigger full activation of PrfA is unknown. Several studies have found various biomolecules to activate PrfA *in vitro*, however these experiments were all performed in an artificial minimal medium system which does not closely mimic the host cell environment. We developed a biologically relevant system to study PrfA activation *in vitro* using *Xenopus* cell-free cytosolic extracts. Using survival of the *Lm* suicide strain as a readout of PrfA activation, we found that *Xenopus* extracts potently activate PrfA *in vitro* to similar levels as seen during infection of macrophages. Biochemical manipulation of cell-free extracts revealed that the PrfA-activating component of the extracts was proteinaceous in nature, sensitive to phosphatase treatment, and required addition of an energy regeneration supplement. Using anion-exchange chromatography, we were able to reproducibly isolate a single fraction which retained the ability to activate PrfA. Mass spectrometry identified a set of proteins which were enriched in the active fractions and may be involved in maintaining the PrfA-activating property of eukaryotic cytosol.

A major benefit of using *Xenopus* extracts over other experimental systems is the ease with which these extracts can be biochemically manipulated. Using simple enzymatic treatments, we were able to identify the biochemical nature of the PrfA-activating component of eukaryotic cytosol. Based on these studies, we hypothesize that an enzyme present in cytosol produces a small molecule or other specific product which acts as a cue to *Lm* to activate virulence gene expression. It is also possible that enzymatic modification of a molecule on the *Lm* cell surface initiates a signaling cascade leading to PrfA activation. Further biochemical modulation of cell-free extracts would reveal additional properties of proteins of interest which may aid in their identification. In addition, *Xenopus* cell free extracts may be an ideal system to investigate *Lm* gene expression in the cytosolic environment. Extraction of *Lm* RNA from infected cells is laborious and requires a large number of cells. The experiments described here in cell-free extracts were performed with as little as 4 uL of extract per condition, which can easily be scaled up to accommodate an appropriate number of bacteria for RNA extraction. In particular, determining whether the proteinaceous component of *Xenopus* extracts activates PrfA through upregulation of *gshF* would be intriguing. Overexpression of *gshF* alone is not sufficient to activate PrfA *in vitro*, suggesting that host factors present in eukaryotic cytosol may activate PrfA through a different mechanism.

Exogenous GSH and L-glutamine have previously been shown to activate PrfA *in vitro*. However, when added to inactivated *Xenopus* extracts at the same concentrations, none of the tested compounds had any effect on PrfA activation. Considering that *Xenopus* extracts closely mimic the cytosolic compartment of eukaryotic cells, it is possible that the effects of these modulators are artifacts of using a minimal medium system. In addition, it is well documented that rich broth, such as BHI, inhibits activation of PrfA and contributes to keeping virulence factor expression off during extracellular growth. However, we observed potent activation of PrfA by *Xenopus* extracts even in the presence of 1X BHI, suggesting that the activating components of eukaryotic cytosol override the inhibitory effects of BHI. This may also be the case for BCAAs, which also could not repress PrfA activation by cytosolic extracts even at a high concentration.

Collectively, these results highlight the importance of using biologically relevant models to study PrfA activation.

To identify specific proteins present in *Xenopus* extracts involved in activating PrfA, we took an unbiased approach and screened for PrfA activity in fractions generated by anion-exchange chromatography. In three independent experiments, we were able to isolate a single fraction which retained the ability to kill the suicide strain and was sensitive to Proteinase K treatment. Interestingly, the retention of the PrfA-activating protein(s) was changed after Benzonase treatment. Anion-exchange columns bind negatively-charged molecules, therefore longer retention times indicate stronger negative charge. Without Benzonase treatment, PrfA-activating compounds bound to the column tighter than with nucleic acid depletion. These results suggest that PrfA-activating proteins associate with negatively-charged DNA or RNA in *Xenopus* extracts. Whether or not association with nucleic acids is non-specific or a dedicated function of PrfA-activating proteins remains to be determined. Because the active fractions in Benzonase-treated extracts did not associate strongly with the anion-exchange column, our proteins of interest may be positively-charged or have neutral charge. Other methods of chromatography, such as cation-exchange or size-exclusion chromatography, may be better suited to isolating active fractions which have a lower protein complexity.

We identified 62 proteins which were enriched at least 1.5-fold in two independent active fractions. Unfortunately, we were not able to validate the involvement of any candidate proteins in PrfA activation, however only a small number of proteins were tested. While the iBMM CRISPR knockouts were subjected to antibiotic selection before testing, the efficiency of genome-editing was not determined so it is possible that one or more of the cell lines were not true knockouts. In addition, despite the large dynamic range of measuring PrfA activation via suicide strain survival, this method may not be sensitive enough to detect smaller changes in *actA* expression. Another method of detecting *actA* expression, such as use of a fluorescent reporter, may be more appropriate to quantify PrfA activation in knockout cells.

Overall, this work constitutes a major step towards a complete picture of PrfA regulation in *Lm*. The transition of *Lm* from a saprophyte to intracellular pathogen requires tremendous coordination of gene regulation and proper sensing of the host environment, the latter of which is a current area of study. We propose *Xenopus* cell-free extracts as a biologically relevant model to study interaction of *Lm* with host cytosol, and have begun to elucidate cytosolic signals that *Lm* uses to activate virulence gene expression.

Chapter 3: Genome-wide CRISPR/Cas9 screen to identify host factors required for *Lm* virulence

Introduction

The experiments in Chapter 2 revealed that one or more host proteins is required for PrfA activation in eukaryotic cytosol. As an alternative to the *in vitro* biochemical approaches used in Chapter 2, we turned to a genetic system in live cells to identify host proteins involved in PrfA activation. CRISPR/Cas9 screening is a powerful tool to dissect gene essentiality in mammalian cells (Figure 7). Briefly, a pooled sgRNA library is introduced into cells using lentiviral transduction, which allows for single integration events in each cell and results in a pooled library of knockout cells. The CRISPR/Cas9 knockout cell library is then subjected to challenge conditions and cells are sequenced to identify the mutants present in the population after selection. CRISPR screening technology has not yet been used to study *Lm* pathogenesis despite the potential to uncover novel host determinants of *Lm* infection.

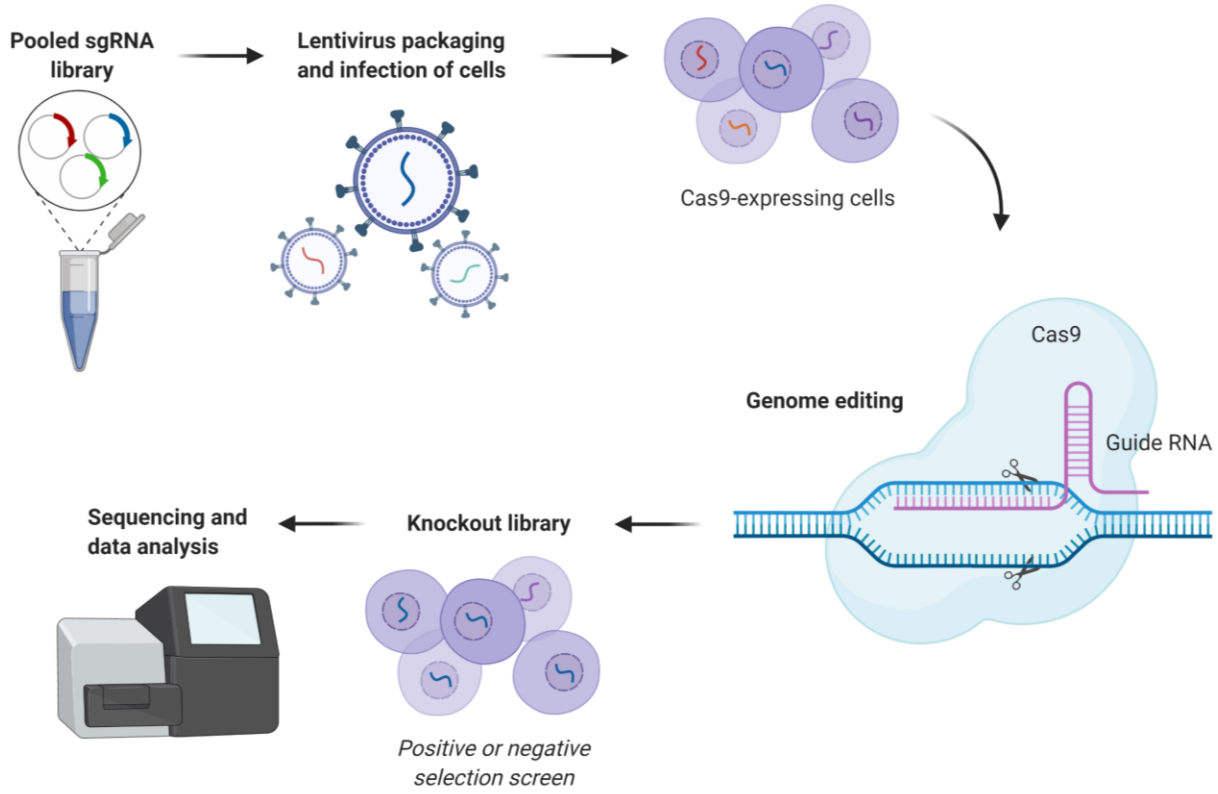

Figure 7. Genetic screening using CRISPR/Cas9-mediated genome editing. A pooled library of sgRNAs is introduced into Cas9-expressing cells using lentiviral transduction. Expression of Cas9 and the introduced sgRNA allows for creation of insertions or deletions at target genes to knockout functional protein production. The resulting population of mutant cells is subjected to positive or negative selection strategies and sequenced to identify essential genes for a phenotype of interest.

We aimed to apply the versatility of CRISPR screening to investigate host factors involved in multiple phenotypes critical to *Lm* pathogenesis. In addition to characterizing host genes required for PrfA activation by the host cytosol, we took the opportunity to study involvement of host factors in mediating phagocytosis of *Lm.* As outlined in Chapter 1, the macrophage receptors and downstream signaling components required for non-opsonic phagocytosis of *Lm* have not been characterized. To simultaneously identify host genes involved in macrophage phagocytosis of *Lm* and PrfA activation in the cytosol, we designed a genome-wide CRISPR screening approach using bacterial fluorescent reporters and flow-associated cell sorting (FACS). Our screen identified hundreds of candidate genes potentially involved in mediating macrophage infection by *Lm*. In particular, we found that host cell transcription is required for proper phagocytosis of *Lm* by macrophages. This was specific to *Lm*, as transcription was dispensable for phagocytosis of other bacteria. *Lm* exhibited enhanced internalization into macrophages compared to other bacterial species, suggesting that *Lm* is phagocytosed using a distinct pathway which involves host cell transcription. Overall, this screen was the first application of CRISPR screening technology to studies of *Lm* virulence and identified hundreds of novel genes impacting *Lm* pathogenesis.

Some of the work presented in this chapter is published in: Glover RC, Schwardt NH, Leano SE, Sanchez ME, Thomason MK, Olive AJ, Reniere ML. 2023. A genome-wide screen in macrophages identifies PTEN as required for myeloid restriction of *Listeria monocytogenes* infection. *PLoS Pathogens*. 19(5): e1011058. 10.1371/journal.ppat.1011058.

Results

Genome-wide CRISPR/Cas9 screen

To simultaneously measure uptake of *Lm* and PrfA activation in macrophages, we designed a fluorescent reporter strain of *Lm* which produces GFP constitutively and expresses *rfp* under control of the *actA* promoter. We first tested the ability of this reporter strain to detect intracellular *Lm* by flow cytometry. Using standard infection conditions of a multiplicity of infection (MOI) of 1 for 1 hour resulted in only ~5% of macrophages becoming GFP^+ (Figure 8A). To determine whether the low percentage of GFP^+ macrophages was due to the infection conditions, we increased the MOI and length of infection time. Increasing both of these parameters led to a marked increase in GFP^+ macrophages, with a 4 hour infection at a MOI of 10 resulting in approximately 80% GFP^+ macrophages (Figure 8A).

Next, we gated on GFP^+ cells and detected RFP fluorescence as a measure of *actA* expression. For these experiments, we perturbed glutathione levels in both macrophages and *Lm* to determine if we could accurately detect changes in *actA* expression via RFP fluorescence. Depleting host cell glutathione using the chemical inhibitor buthionine sulfoximine (BSO) has no effect on ActA production, while preventing bacterial glutathione synthesis by disruption of *gshF* decreases ActA levels to 14% of wt *Lm*[29]. In the absence of both bacterial and host glutathione, ActA protein levels are nearly undetectable. We observed very similar phenotypes when detecting *actA* expression using our fluorescent reporter. BSO treatment had no effect on RFP expression, infection with a transposon mutant of *gshF* reduced *actA* expression by 75%, and iBMMs lacking both host and bacterial glutathione were ~96% RFP^- (Figure 8B). Collectively, these data

demonstrate the utility of our dual-fluorescence reporter strain in measuring both uptake of *Lm* and expression of *actA* in macrophages.

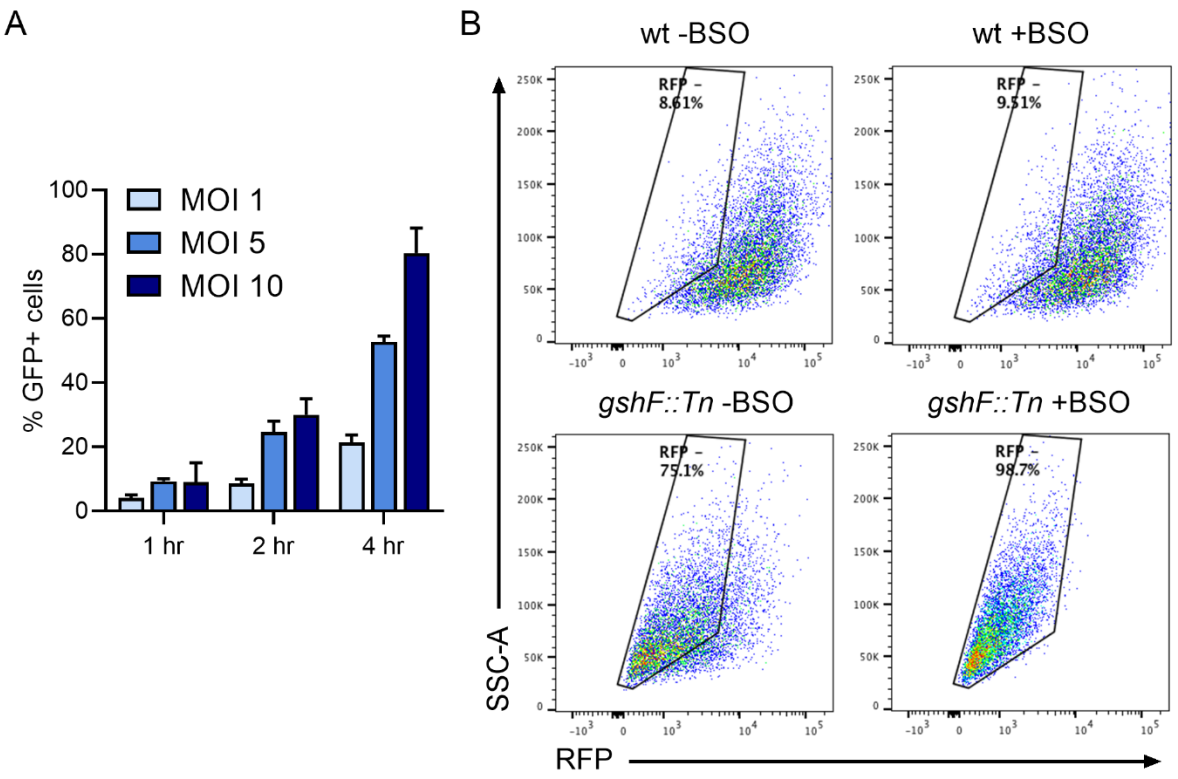

Figure 8. Optimization of CRISPR/Cas9 screen. (A) Optimization of infection efficiency. iBMMs were infected with the P*actA*-RFP reporter strain for the indicated MOI and time, gentamicin was added to kill extracellular *Lm*, and GFP$^+$ cells were quantified by flow cytometry 6 hours post-infection. Data are means and SEM of at least two independent experiments. (B) Detection of *actA* expression by RFP fluorescence. iBMMs were infected with *Lm* expressing the P*actA* reporter in either a wt or *gshF::Tn* background for 4 hours at MOI=10. Gentamicin was added to kill extracellular *Lm*, and cells were analyzed by flow cytometry 6 hours post-infection. Representative dot plots show the percentage of RFP-negative cells in GFP$^+$ populations. Where indicated, cells were plated overnight in the presence of 2 mM BSO.

The genome-wide CRISPR/Cas9 screen was performed as depicted in Figure 9. iBMMs expressing Cas9 were transduced with the murine Brie sgRNA library and transductants were selected with antibiotics. Transduced cells were then infected with mock or the P*actA* reporter strain of *Lm* and two populations were isolated using FACS: GFP$^-$RFP$^-$ cells (phagocytosis-deficient) and GFP$^+$RFP$^-$ cells (*actA*-deficient). sgRNAs were amplified from sorted cells and mock-infected control libraries and abundance in each population was measured by Illumina sequencing. To maintain coverage of the library, cells were transduced and infected at 1000-fold coverage of the library, and ~500-fold coverage was sorted.

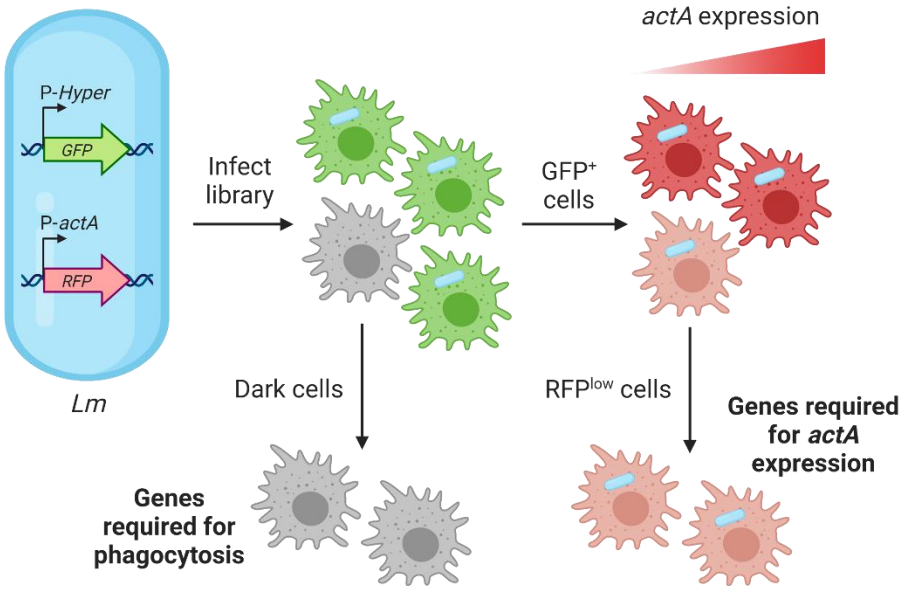

Figure 9. Genome-wide CRISPR screen to identify host genes required for phagocytosis of *Lm* and PrfA activation. Schematic of the CRISPR/Cas9 screen in iBMMs. Three independent iBMM knockout libraries were generated using the genome-wide Brie sgRNA library. Cells were infected with mock or *Lm* expressing fluorescent reporters at MOI=10 for 4 hours. 6 hours post-infection, uninfected cells (GFP^-) and *actA*-deficient cells (GFP^+RFP^-) were isolated by FACS. sgRNA abundances in sorted cells versus mock-infected controls were measured by Illumina sequencing and MAGeCK analysis.

Analysis of sgRNAs enriched in the GFP^+RFP^- (*actA*-deficient) population

Using Model-based Analysis of Genome-wide CRISPR/Cas9 Knockout (MAGeCK)[99], we identified sgRNAs targeting 197 genes enriched in the GFP^+RFP^- population (Table 2, Figure 10A). Among the candidate genes, multiple members of the protocadherin gene family (*Pcdhga8*, *Pcdh1*, and *Pcdh10*), the SEC gene family (*Sec22b*, *Sec22c*, and *Sec31a*), and SET domain-containing proteins (*Setd5* and *Setd8*) were identified. In addition, we performed gene ontology analysis using Metascape to identify pathways enriched in our data set[100]. 14 pathways were identified representing a variety of biological processes; the top enriched pathway included genes in the endomembrane system, and 3 other identified pathways were involved in vacuolar or endoplasmic reticulum trafficking (Figure 10B).

To validate the screen, individual knockout cell lines of a subset of genes were generated using 2 sgRNAs per gene and genome editing was confirmed using Inference of CRISPR Edits (ICE) analysis[101]. Knockout iBMMs were infected with the *Lm* P*actA* reporter strain in the same manner as the original screen, and both GFP and RFP were quantified using flow cytometry. While some of the cell lines tested had decreased RFP fluorescence during infection, these cells exhibited an almost identical decrease in GFP fluorescence (Figure 10C and 10D) indicating that there was a decrease in overall *Lm* burden in these cells rather than a defect in *actA* expression. Most of these effects were small in magnitude, however cells expressing sgRNAs targeting *Pten* exhibited a larger decrease in both GFP and RFP fluorescence (Figure 10C and 10D).

Interestingly, *Pten* was also identified in our screen for phagocytosis-deficient cells as described below, suggesting that this gene is required for proper uptake of *Lm* by macrophages. Overall, these data indicate that none of the tested candidate genes are required for *actA* expression by *Lm*.

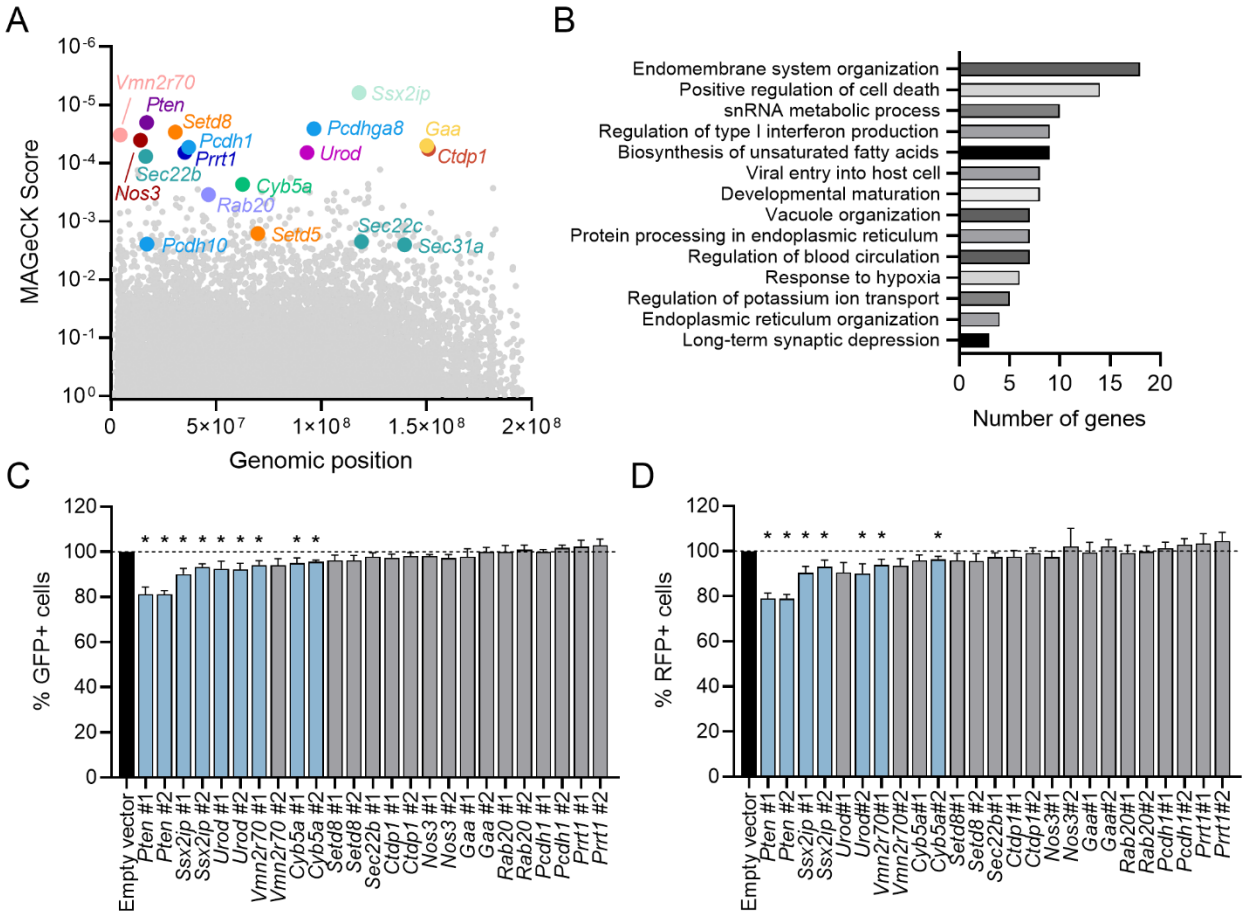

Figure 10. Candidate genes identified in GFP⁺RFP⁻ populations. (A) MAGeCK score of each gene in the Brie library from three independent screen replicates. Gene names are depicted for the top 13 hits (lowest MAGeCK scores) and related genes. (B) Hits with $p<0.01$ (n=197) were analyzed by Metascape. The number of genes belonging to each biological process is depicted. (C-D) iBMMs were transduced with empty vector or sgRNAs targeting selected hits. For each gene, two sgRNAs were used to generate two knockout cell lines. Cell lines were infected with the P*actA* reporter strain of *Lm* and both GFP (C) and RFP (D) were quantified by flow cytometry. Data are normalized to iBMMs transduced with empty vector. Data are means and SEM of three independent experiments. *$p<0.05$ as determined by unpaired *t* tests.

Analysis of sgRNAs enriched in GFP$^-$ (phagocytosis-deficient) population

Overall, we identified 557 sgRNAs enriched in the GFP$^-$ population compared to the mock-infected libraries, corresponding to 235 genes (Table 3, Figure 11A). Initial examination of these candidates found several sets of genes belonging to the same protein family or protein complex: TFIID complex proteins (*Taf1d, Taf2, Taf3, Taf4a, Taf5, Taf8, Taf10,* and *Taf13*); SAGA complex proteins (*Usp22, Supt7l, Supt20, Taf5l, Taf6l, Atxn7l3, Tada2b,* and *Tada1*); negative elongation factor (*Nelfa, Nelfb, Nelfcd,* and *Nelfe*); Ras-related GTP-binding proteins (*Rraga* and *Rragc*); glycogen synthase kinase 3 (*Gsk3a* and *Gsk3b*); and translation initiation factors (*Eif3h, Eif4g2,* and *Eif5*). Identification of many independent genes within the same complex suggests that our genome-wide screen was robust. Pathway enrichment analysis using Metascape identified 20 biological pathways enriched in the dataset (Figure 11C). Several enriched pathways were involved in chromatin remodeling, mRNA transcription, and mRNA processing, suggesting that proper host cell transcription may be required for phagocytosis of *Lm*. Interestingly, we also identified signaling pathways involving major regulators of cell proliferation and survival, including PTEN (*Pten*), p53 (*Trp53*), and NF-κB (*Rela*).

To validate the screen, individual knockout cell lines of a subset of genes were generated as described above. Knockout iBMMs were infected with GFP-expressing *Lm* in the same manner as the original screen, and GFP$^+$ cells were quantified using flow cytometry. Of the eleven candidate genes tested, eight exhibited significantly reduced intracellular *Lm* with both sgRNAs and one with a single sgRNA (Figure 11B). The two candidate genes which had no change in *Lm* uptake with either sgRNA (*Nelfcd* and *Taf13*) had <30% CRISPR-InDel frequency, as measured by ICE analysis, or were unable to be confirmed by sequencing. Together, these data validate our screen for phagocytosis regulators as a whole and suggest that the other candidate genes identified by the screen are likely to also affect *Lm* infection of macrophages.

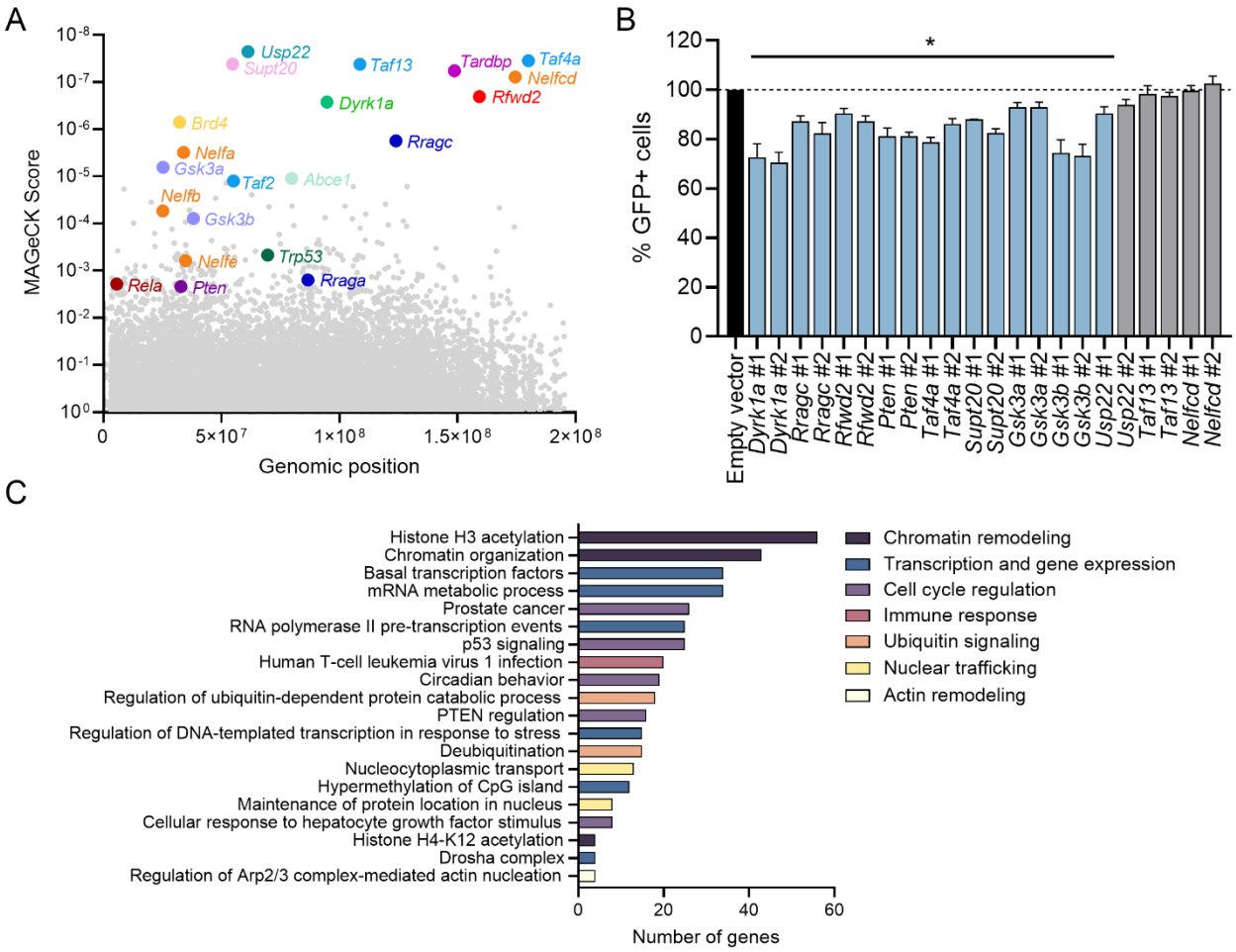

Figure 11. sgRNAs in GFP$^-$ population identify candidate genes important for phagocytosis of *Lm*. (A) MAGeCK score of each gene in the Brie library from three independent screen replicates. Gene names are depicted for the top 14 hits and related genes. (B) iBMMs were transduced with empty vector or sgRNAs targeting selected hits. For each gene, two sgRNAs were used to generate two knockout cell lines. Cell lines were infected with the P*actA* reporter strain of *Lm* and GFP was quantified by flow cytometry. Data are normalized to iBMMs transduced with empty vector. Data are means and SEM of three biological replicates. *p* values for significant results (blue bars) range from <0.0001 to 0.025. (C) Hits with $p<0.01$ were analyzed by Metascape. The number of genes belonging to each biological process is depicted.

Host cell transcription and translation modulate uptake of *Lm*

Many of the genes that we identified have not been previously implicated in phagocytosis of bacteria. Therefore, we hypothesized that *Lm* is taken up by macrophages using a novel and distinct phagocytosis pathway compared to other bacterial species. To test this possibility, we assessed uptake of various *Listeria* species using a gentamicin protection assay. iBMMs were infected with *Lm,* gentamicin was added 30 minutes post-infection to kill extracellular bacteria, and intracellular bacteria were enumerated 1 hour post-infection. *Lm* was internalized more efficiently by iBMMs than either *Listeria ivanovii* or *Listeria innocua*, with *L. innocua* being taken up only ~15% as efficiently as *Lm* (Figure 12A). These experiments were repeated in primary

bone marrow-derived macrophages (BMDMs), and we observed very similar phenotypes (data not shown). These results suggest distinct mechanisms of phagocytosis between *Listeria* species under non-opsonizing conditions.

We hypothesized that some of the candidate genes identified in our screen were responsible for mediating enhanced uptake of *Lm* by macrophages compared to other species. To assess the contribution of the identified pathways to species-specific phagocytosis, gentamicin protection assays were used to measure internalization of *Lm*, *L. innocua*, and the related Gram-positive bacterium *Bacillus subtilis*. As an orthologous approach to genetic knockouts, we used chemical inhibitors targeting transcription (actinomycin D), translation (cycloheximide), PTEN [bpV(pic)], GSK3 (CHIR99021), and NF-κB (parthenolide). All inhibitors tested blocked internalization of *Lm* during the 1-hour infection, suggesting the involvement of these pathways in uptake of *Lm* (Figure 12B). Interestingly, inhibitors targeting transcription, PTEN, and GSK3 had no effect on uptake of *L. innocua* or *B. subtilis*, indicating their specificity for internalization of *Lm*. We also found that host cell translation and NF-κB were required for uptake of all three species. Collectively, these data demonstrate the breadth of our screen in identifying regulators of phagocytosis both specific to *Lm* and involved more broadly in phagocytosis of bacteria.

Inhibiting host cell transcription impaired uptake of *Lm* by macrophages, but not *L. innocua* or *B. subtilis*, while host cell translation appears to be important for uptake of multiple bacterial species (Figure 12B). Inhibiting transcription or translation is likely to have major effects on cellular function and may be impairing the basal phagocytic machinery in macrophages. To test the phagocytic capacity of macrophages during transcription and translation inhibition, IgG-opsonized FITC-labeled latex beads were added to macrophages and uptake of the beads was measured by detecting FITC fluorescence using flow cytometry. Surprisingly, macrophages treated with actinomycin D or cycloheximide took up fluorescent beads similar to vehicle-treated cells (Figure 12C), indicating that phagocytic machinery is intact during transcription and translation inhibition.

We next wanted to determine whether host cell transcription and translation are important for invasion of *Lm* into non-phagocytic cells. TIB73 murine hepatocytes were treated with transcription and translation inhibitors and invasion was measured via gentamicin protection assay. Similar to macrophages, transcription inhibition reduced invasion of *Lm* into TIB73 cells (Figure 12D). However, inhibition of translation had the opposite effect, with significantly increased invasion of *Lm*. Overall, these data indicate that host transcription is required for uptake of *Lm* by multiple cell types, while the role of host translation in uptake of bacteria may be macrophage-specific.

To further investigate the role of transcription in *Lm* internalization, we employed an immunofluorescence strategy to quantify intracellular and extracellular bacteria over time during macrophage infection. iBMMs were cultured on glass coverslips and infected with mCherry-expressing *Lm* to visualize all adherent and intracellular bacteria. At various timepoints, coverslips were washed to remove non-adhered bacteria, fixed, and immunostained under non-permeabilizing conditions to label only extracellular adherent bacteria. Importantly, gentamicin was not used in these experiments, allowing simultaneous measurement of both adherence and internalization. While treatment of iBMMs with actinomycin D did not decrease overall adherence of *Lm* to the macrophages, we observed a decreased rate of internalization during transcription inhibition (Figure 12E and 12F). These data suggest that host transcription promotes internalization of *Lm* by host cells.

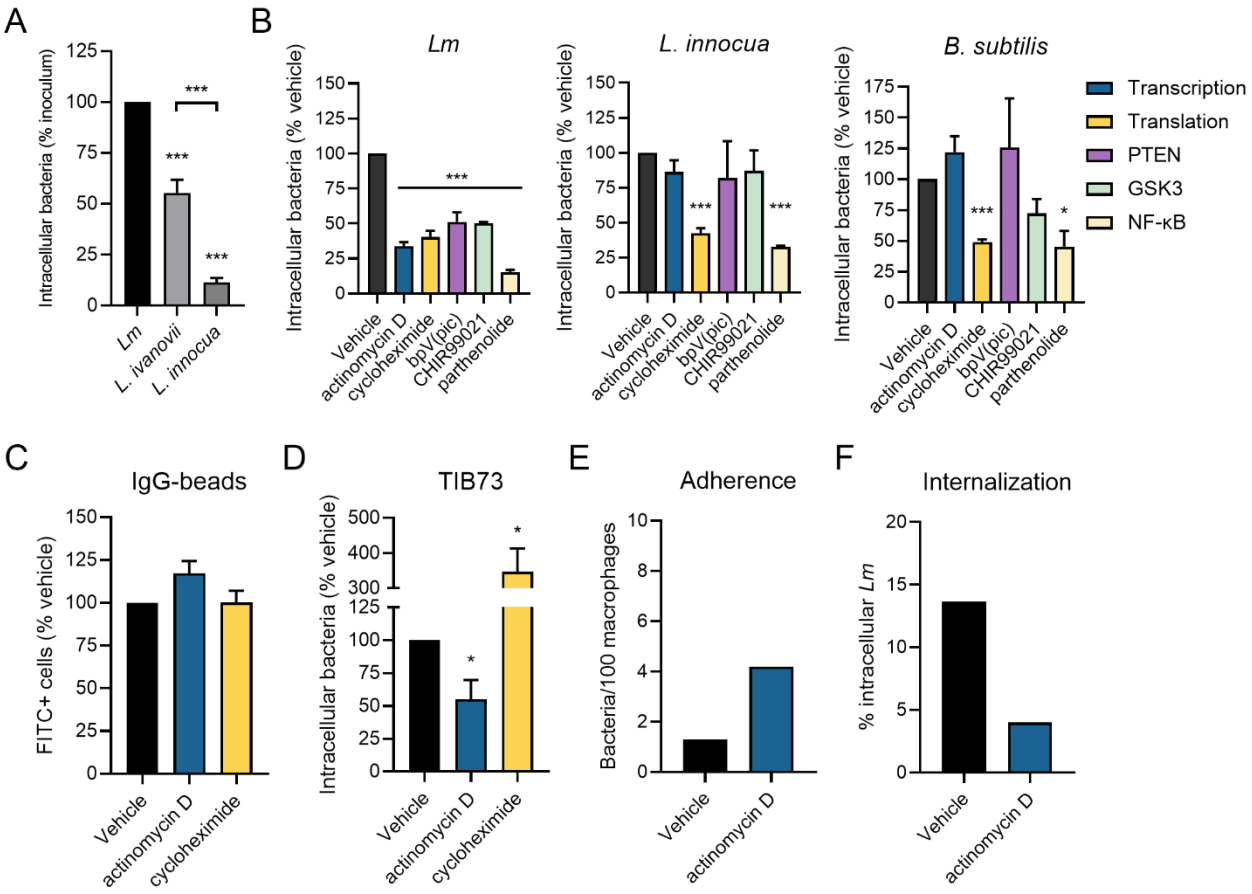

Figure 12. Role of transcription and translation in species-specific phagocytosis. (A) Gentamicin protection assay measuring bacterial uptake by iBMMs 1 hour post-infection. Data are normalized to uptake of *Lm*. (B) Gentamicin protection assay measuring bacterial uptake by iBMMs treated with 10 μg/mL actinomycin D, 1 μg/mL cycloheximide, 5 μM bpV(pic), 10 μM CHIR99021, or 10 μM parthenolide. iBMMs were infected at MOI=1 for 30 minutes and CFU were quantified 1 hour post-infection. Data are normalized to vehicle-treated cells. (C) Uptake of IgG-opsonized FITC-labeled latex beads by iBMMs treated with actinomycin D and cycloheximide. Beads were added to cells for 30 minutes and uptake was quantified by flow cytometry. Data are normalized to vehicle-treated cells. (D) Gentamicin protection assay measuring uptake of *Lm* by TIB73 cells. Cells were infected at MOI=50 for 1 hour and CFU were quantified 90 min post-infection. Data are normalized to vehicle-treated cells. (E-F) Cells were infected with mCherry-*Lm* at MOI=5 and fixed 30 min post-infection. Extracellular bacteria were labeled with *Listeria* antisera and a fluorescent secondary antibody. (E) The total number of bacteria per 100 macrophages was counted for at least three fields of view to quantify adherence. (F) The percentage of intracellular bacteria was calculated for at least three fields of view per condition to quantify internalization. All data are means and SEM of at least three biological replicates, except panels E and F which represent a single experiment. *p<0.05, ***p<0.001 as determined by unpaired t tests.

Discussion

Host determinants of both virulence gene expression in *Lm* and initiation of cellular infection in macrophages are underexplored. Here, we performed a genome-wide CRISPR/Cas9 screen for host-encoded regulators of *Lm* macrophage infection and identified hundreds of genes which have not been previously implicated in *Lm* pathogenesis. Although we were unable to identify any candidate genes impacting *actA* expression, we validated the role of several genes in promoting uptake of *Lm* by macrophages. Interestingly, our screen identified biological pathways involved in phagocytosis of *Lm* specifically, as well as Gram-positive bacteria broadly. In particular, host cell transcription was required for uptake of *Lm* by macrophages but is dispensable for uptake of other bacteria or opsonized beads. The host gene *Pten* was also found to be specifically required for phagocytosis of *Lm* and this phenotype is extensively characterized in Chapter 4. Overall, our unbiased forward genetic screen in macrophages constitutes a major step towards comprehensively identifying the host cell determinants of *Lm* infection.

Our flow cytometry-based fluorescent reporter system accurately detects *actA* expression intracellularly as evidenced by correlation with previously reported changes in ActA protein levels upon glutathione perturbation[29]. Therefore, we were surprised that our screen was unable to identify genes impacting *actA* expression. One possible explanation for this is that PrfA activation by the host is multifactorial. The work presented in Chapter 2 found that a protein component of the host cytosol is required for PrfA activation, however this may be due to the action of multiple proteins and deletion of any one single gene would have no effect. In addition, our dataset generated 197 candidate genes, only 13 of which we tested further. Even if multiple host genes are involved in regulating *actA*, it is likely that only a small number of genes may be involved in maintaining a specific host signal or cue. Performing a sub-pool CRISPR screen, in which a defined library of sgRNAs targeting only the significant hits from the genome-wide screen is used, would be valuable to determine if any of our 197 candidates impact PrfA activation.

In contrast to the *actA* expression screen, our screen for regulators of phagocytosis successfully identified several genes impacting uptake of *Lm* by macrophages. Importantly, we used a long infection time and high MOI in order to ensure that the majority of the macrophage population was infected and maintain coverage of the CRISPR library. Therefore, it is certainly possible that genes impacting other stages of cellular infection, such as vacuolar escape and cytosolic growth, may be represented in our list of candidate genes. However, we validated the role of several biological pathways in initial uptake of *Lm* using gentamicin protection assays. Nonetheless, characterizing candidate genes which impact infection downstream of phagocytosis will be valuable to reveal novel aspects of both *Lm* pathogenesis and host biology.

A large number of candidate genes were involved in chromatin modification and general mRNA transcription, including several TAF proteins and members of the SAGA complex. In accordance with these results, we found that host cell transcription was important for uptake of *Lm* by macrophages. Interestingly, this was specific to *Lm* uptake, as internalization of *L. innocua* and *B. subtilis* were unaffected by transcriptional inhibition in macrophages. It is possible that inhibition of macrophage transcription prevents expression of transcripts that are important for initial detection and internalization of *Lm,* or blocks transcription of genes induced in response to *Lm* infection. *Lm* induces a specific transcriptional response in macrophages which can be detected within the first hour of infection[102]. This early response is dominated by TLR and NF-κB

signaling, the latter of which was identified by our initial screen and subsequent studies as required for phagocytosis of *Lm*. However, NF-κB was required for uptake of all bacteria tested suggesting that host transcription and NF-κB regulate *Lm* uptake using distinct mechanisms. While there is some evidence that NF-κB promotes phagocytosis of bacteria downstream of TLRs, this has not been thoroughly characterized[103,104]. The precise roles of host cell transcription and NF-κB signaling in regulating phagocytosis of *Lm* warrant further investigation.

Overall, the genome-wide CRISPR screen described here identified hundreds of candidate genes important for macrophage infection by *Lm*. These data provide a valuable resource to investigate *Lm* pathogenesis and phagocytosis of bacteria more broadly. We focused our studies largely on *Pten* (Chapter 4), however our preliminary data on the role of host transcription in promoting phagocytosis of *Lm* demonstrates that this is a promising area of study. In addition, the numerous other genes identified by our screen are likely to reveal novel host-*Lm* interactions and inform our understanding of the host determinants of *Lm* infection.

Table 2. Candidate genes identified by sgRNAs enriched in the GFP$^+$RFP$^-$ (*actA*-deficient) population (p<0.01).

Gene symbol	Gene Name	Enriched sgRNAs	MAGeCK Score	*p*-value
Ssx2ip	Afadin- and alpha-actinin-binding protein	3	6.2E-06	2.4E-05
Pten	Phosphatase and tensin homolog	3	2.0E-05	8.1E-05
Pcdhga8	Protocadherin gamma A8	1	2.6E-05	1.0E-04
Setd8	Lysine methyltransferase 5A	3	2.9E-05	1.2E-04
Vmn2r70	Vomeronasal 2, receptor 70	4	3.2E-05	1.3E-04
Nos3	Endothelial NOS (eNOS)	4	4.0E-05	1.6E-04
Gaa	Lysosomal alpha glucosidase	3	5.0E-05	2.0E-04
Pcdh1	Protocadherin 1	4	5.3E-05	2.1E-04
Ctdp1	RNA polymerase II subunit A C-terminal domain phosphatase	2	5.7E-05	2.2E-04
Prrt1	Proline rich transmembrane protein 1	2	6.5E-05	2.6E-04
Urod	Uroporphyrinogen III decarboxylase	3	6.5E-05	2.6E-04
Sec22b	SEC22 homolog B, vesicle trafficking protein	3	7.7E-05	3.1E-04
Znhit3	Zinc finger hit domain-containing protein 3	3	1.3E-04	5.1E-04
Cadm2	Cell adhesion molecule 2	4	1.3E-04	5.2E-04
Srp68	Signal recognition particle 68	3	1.6E-04	6.3E-04
Rsrp1	Arginine/serine rich protein 1	1	1.8E-04	6.9E-04
Ccar1	Cell division cycle and apoptosis regulator 1	4	2.3E-04	8.7E-04
Cyb5a	Cytochrome b5	1	2.3E-04	8.8E-04
Spred1	Sprouty protein with EVH-1 domain 1, related sequence	3	2.7E-04	1.0E-03
Oosp2	Oocyte-secreted protein 2	4	2.7E-04	1.0E-03
Ncbp3	Nuclear cap binding subunit 3	4	2.7E-04	1.0E-03
Socs2	Suppressor of cytokine signaling 2	1	2.8E-04	1.1E-03
Lce1i	Late cornified envelope 1	3	3.1E-04	1.2E-03
Atl2	Atlastin GTPase 2	4	3.1E-04	1.2E-03

Snrpd2	Small nuclear ribonucleoprotein D2	2	3.2E-04	1.2E-03
Adat3	Adenosine deaminase tRNA specific 3	4	3.2E-04	1.2E-03
Med11	Mediator complex subunit 11	1	3.3E-04	1.2E-03
Rab20	Ras-related protein Rab20	2	3.4E-04	1.3E-03
Mageb16	MAGE family member B16	2	3.8E-04	1.4E-03
Magea1	MAGE family member A1	3	4.0E-04	1.5E-03
Mtch1	Mitochondrial carrier homolog 1	3	4.0E-04	1.5E-03
Mtpn	Myotrophin	3	4.1E-04	1.5E-03
Col5a1	Collagen type V alpha 1 chain	3	4.1E-04	1.5E-03
Pus7	Pseudouridylate synthase 7	4	4.2E-04	1.6E-03
Sprr1a	Small proline-rich protein 1A; Cornifin A	3	4.3E-04	1.6E-03
Kdm3b	Lysine demethylase 3B	4	4.4E-04	1.6E-03
Tmem106a	Transmembrane protein 106A	4	4.7E-04	1.7E-03
Tril	TLR4 interactor with leucine rich repeats	3	4.8E-04	1.8E-03
Cog4	Conserved oligomeric golgi complex subunit 4	2	4.9E-04	1.8E-03
Mrpl30	Mitochondrial ribosomal protein L30	4	4.9E-04	1.8E-03
Cd209e	CD209 antigen-like protein E	3	5.2E-04	1.9E-03
Rpn2	Ribophorin II	2	5.4E-04	2.0E-03
Olfr479	Olfactory receptor 479	4	5.7E-04	2.1E-03
Bace1	Beta-site APP cleaving enzyme 1	4	5.7E-04	2.1E-03
Trim42	Tripartite motif-containing 42	3	5.9E-04	2.2E-03
Olfr1183	Olfactory receptor 1183	4	5.9E-04	2.2E-03
1700022I11Rik	RIKEN cDNA 1700022I11 gene	3	5.9E-04	2.2E-03
Hoxb2	Homeobox B2	4	6.0E-04	2.2E-03
Ano6	Anoctamin 6	3	6.1E-04	2.3E-03
Bfsp1	Beaded filament structural protein 1, in lens-CP94	2	6.2E-04	2.3E-03
Negr1	Neuronal growth regulator 1	1	6.4E-04	2.4E-03
Ccdc142	Coiled-coil domain containing 142	4	6.7E-04	2.4E-03
Olfr128	Olfactory receptor 128	3	6.7E-04	2.4E-03
Tbck	TBC1 domain-containing kinase	2	6.7E-04	2.5E-03
Irf2bp2	Interferon regulatory factor 2 binding protein 2	3	6.8E-04	2.5E-03
Epo	Erythropoietin	2	6.9E-04	2.5E-03
Henmt1	HEN methyltransferase 1	4	7.0E-04	2.6E-03
Dnaja3	DnaJ heat shock protein family (Hsp40) member A3	3	7.2E-04	2.6E-03
Pdia6	Protein disulfide isomerase A6	2	7.3E-04	2.7E-03
Gm9	Predicted gene 9	2	7.5E-04	2.7E-03
Ranbp10	Ran-binding protein 10	2	7.9E-04	2.9E-03
Adamtsl4	ADAMTS-like protein 4	4	8.2E-04	3.0E-03
Dagla	Diacylglycerol lipase, alpha	1	8.4E-04	3.1E-03
Ywhaq	Tyrosine 3-monooxygenase/tryptophan 5-monooxygenase activation protein theta	4	8.6E-04	3.1E-03
Lhcgr	Luteinizing hormone/choriogonadotropin receptor	3	8.6E-04	3.1E-03
Inmt	Indolethylamine N-methyltransferase	2	8.9E-04	3.2E-03
Rpl19	Ribosomal protein L19	2	9.1E-04	3.3E-03

Tradd	TNFRSF1A-associated via death domain	4	9.4E-04	3.4E-03
Clec1b	C-type lectin domain family 1 member B	1	9.4E-04	3.4E-03
Lgi3	Leucine-rich repeat LGI family member 3	2	9.9E-04	3.6E-03
Klk1b21	Kallikrein 1-related peptidase b21	4	1.0E-03	3.6E-03
Thsd1	Thrombospondin, type I, domain 1	2	1.0E-03	3.6E-03
Nap1l3	Nucleosome assembly protein 1-like 3	4	1.0E-03	3.7E-03
Gm813	Ferritin domain containing 1	4	1.0E-03	3.8E-03
Dhx15	DEAH (Asp-Glu-Ala-His) box polypeptide 15	3	1.0E-03	3.8E-03
Mterf4	Mitochondrial transcription termination factor 4	4	1.1E-03	3.9E-03
Cct3	T-complex protein 1 subunit gamma	2	1.1E-03	4.0E-03
Vmn1r123	Vomeronasal 1 receptor 123	3	1.1E-03	4.0E-03
Anks1	Ankyrin repeat and SAM domain containing 1	3	1.1E-03	4.0E-03
Gnb1	Guanine nucleotide binding protein (G protein), beta 1	4	1.1E-03	4.0E-03
Mast3	Microtubule associated serine/threonine kinase 3	3	1.1E-03	4.1E-03
Adgrb1	Adhesion G protein-coupled receptor B1	2	1.1E-03	4.1E-03
Dpysl3	Dihydropyrimidinase-related protein 3	3	1.1E-03	4.2E-03
Smim14	Small integral membrane protein 14	1	1.1E-03	4.2E-03
Cgref1	Cell growth regulator with EF hand domain protein 1	4	1.2E-03	4.2E-03
Svs2	Semenogelin 1	4	1.2E-03	4.3E-03
Rttn	Rotatin	2	1.2E-03	4.3E-03
Dpyd	Dihydropyrimidine dehydrogenase	3	1.2E-03	4.3E-03
Casp1	Caspase 1	4	1.2E-03	4.3E-03
Kcnj13	Potassium inwardly-rectifying channel, subfamily J, member 13	3	1.2E-03	4.4E-03
Tmem159	Lipid droplet assembly factor 1	2	1.2E-03	4.5E-03
Mcrs1	Microspherule protein 1	3	1.3E-03	4.6E-03
Ubxn2a	UBX domain-containing protein 2A	4	1.3E-03	4.6E-03
Acot1	Acyl-CoA thioesterase 1	4	1.3E-03	4.6E-03
Mei1	Meiotic double-stranded break formation protein 1	3	1.3E-03	4.7E-03
Vps35	Vacuolar protein sorting-associated protein 35	4	1.3E-03	4.9E-03
Zcchc16	Retrotransposon Gag like 4	2	1.4E-03	4.9E-03
Tmem50a	Transmembrane protein 50A	2	1.4E-03	4.9E-03
Tmem38a	Transmembrane protein 38A	4	1.4E-03	5.0E-03
Pacsin1	Protein kinase C and casein kinase substrate in neurons 1	2	1.4E-03	5.0E-03
Srrm3	Serine/arginine repetitive matrix 3	3	1.4E-03	5.1E-03
Sap30bp	SAP30 binding protein	3	1.4E-03	5.2E-03
Gm4214	Vomeronasal 1 receptor 258	2	1.5E-03	5.2E-03
Ufd1l	Ubiquitin recognition factor in ER-associated degradation 1	2	1.5E-03	5.2E-03
Nedd9	Neural precursor cell expressed, developmentally down-regulated gene 9	2	1.5E-03	5.3E-03
Ctsh	Cathepsin H	4	1.5E-03	5.5E-03

Meox1	Mesenchyme homeobox 1	4	1.5E-03	5.5E-03
Tmem173	Stimulator of interferon response cGAMP interactor 1 (STING)	3	1.5E-03	5.5E-03
4932429P05Rik	RIKEN cDNA 4932429P05 gene	4	1.5E-03	5.5E-03
Kif1b	Kinesin family member 1B	3	1.5E-03	5.6E-03
Mettl4	Methyltransferase like 4	2	1.6E-03	5.6E-03
Commd3	COMM domain containing 3	4	1.6E-03	5.6E-03
Rsc1a1	Regulatory solute carrier protein, family 1, member 1	3	1.6E-03	5.7E-03
Setd5	SET domain containing 5	3	1.6E-03	5.8E-03
Trappc13	Trafficking protein particle complex 13	4	1.6E-03	5.8E-03
Vta1	Vesicle (multivesicular body) trafficking 1	3	1.6E-03	5.8E-03
Hscb	Iron-sulfur cluster co-chaperone	4	1.6E-03	5.9E-03
3110040N11Rik	RIKEN cDNA 3110040N11 gene	2	1.7E-03	5.9E-03
Uba2	Ubiquitin-like modifier activating enzyme 2	4	1.7E-03	6.0E-03
Rbmx2	RNA binding motif protein, X-linked 2	2	1.7E-03	6.1E-03
Scd4	Stearoyl-coenzyme A desaturase 4	1	1.7E-03	6.1E-03
Dnajc1	DnaJ heat shock protein family (Hsp40) member C1	4	1.7E-03	6.2E-03
Snapc1	Small nuclear RNA activating complex, polypeptide 1	4	1.7E-03	6.2E-03
Thap2	THAP domain containing, apoptosis associated protein 2	3	1.8E-03	6.3E-03
Tcea2	Transcription elongation factor A (SII), 2	2	1.8E-03	6.3E-03
Olfr166	Olfactory receptor family 2 subfamily L member 13	4	1.8E-03	6.3E-03
Lrrc48	Dynein regulatory complex subunit 3	3	1.8E-03	6.5E-03
Cep85	Centrosomal protein 85	4	1.8E-03	6.5E-03
B3galnt1	UDP-GalNAc:betaGlcNAc beta 1,3-galactosaminyltransferase, polypeptide 1	4	1.8E-03	6.5E-03
Nhsl2	NHS-like 2	2	1.9E-03	6.6E-03
Tns1	Tensin 1	3	1.9E-03	6.7E-03
Prr32	Proline rich 32	4	1.9E-03	6.7E-03
Smg8	SMG8 nonsense mediated mRNA decay factor	4	1.9E-03	6.8E-03
Zfp748	Zinc finger protein 748	4	1.9E-03	6.8E-03
Usp18	Ubiquitin specific peptidase 18	1	1.9E-03	6.8E-03
Nsl1	NSL1, MIS12 kinetochore complex component	2	1.9E-03	6.9E-03
Gm14351	BTB domain containing 35, family member 10	1	7.0E-03	6.9E-03
Slc22a28	Solute carrier family 22, member 28	2	2.0E-03	7.0E-03
Akap6	A kinase (PRKA) anchor protein 6	4	2.0E-03	7.0E-03
Avpr1b	Arginine vasopressin receptor 1B	2	2.0E-03	7.2E-03
Pla2g15	Phospholipase A2, group XV	4	2.1E-03	7.4E-03
Tm2d3	TM2 domain containing 3	2	2.1E-03	7.4E-03
Olfr229	Olfactory receptor family 8 subfamily G member 2	1	2.1E-03	7.4E-03
Llcfc1	LLLL and CFNLAS motif containing 1	4	2.1E-03	7.5E-03
Rp1l1	Retinitis pigmentosa 1 homolog like 1	2	2.1E-03	7.6E-03

Ctgf	Cellular communication network factor 2	3	2.1E-03	7.6E-03
Jazf1	JAZF zinc finger 1	2	2.1E-03	7.6E-03
Fbxo16	F-box protein 16	3	2.2E-03	7.8E-03
Clec4g	C-type lectin domain family 4, member g	4	2.2E-03	7.8E-03
Erich3	Glutamate rich 3	3	2.2E-03	7.8E-03
Zkscan8	Zinc finger with KRAB and SCAN domains 8	2	2.2E-03	7.9E-03
Fbln2	Fibulin 2	4	2.2E-03	7.9E-03
BC021891	Mitogen-activated protein kinase kinase kinase 21	3	2.2E-03	7.9E-03
Sec22c	SEC22 homolog C, vesicle trafficking protein	3	2.2E-03	7.9E-03
Kcnk3	Potassium channel, subfamily K, member 3	4	2.2E-03	8.1E-03
Gm10767	Predicted gene 10767	1	2.3E-03	8.1E-03
Mrpl51	Mitochondrial ribosomal protein L51	4	2.3E-03	8.3E-03
Mt3	Metallothionein 3	2	2.3E-03	8.3E-03
Mtmr6	Myotubularin related protein 6	3	2.3E-03	8.3E-03
Dhx36	DEAH (Asp-Glu-Ala-His) box polypeptide 36	2	2.3E-03	8.3E-03
Acad9	Acyl-CoA dehydrogenase family, member 9	3	2.3E-03	8.4E-03
Hspa1l	Heat shock protein 1-like	3	2.4E-03	8.4E-03
Slc25a2	Solute carrier family 25 (mitochondrial carrier, ornithine transporter) member 2	3	2.4E-03	8.4E-03
Xpo4	Exportin 4	3	2.4E-03	8.5E-03
Mgll	Monoglyceride lipase	3	2.4E-03	8.5E-03
Slc1a7	Solute carrier family 1 (glutamate transporter), member 7	3	2.4E-03	8.6E-03
Pih1d2	PIH1 domain containing 2	3	2.4E-03	8.6E-03
Olfr124	Olfactory receptor family 2 subfamily B member 4	1	2.4E-03	8.7E-03
Pcdh10	Protocadherin 10	4	2.4E-03	8.7E-03
Mcl1	Myeloid cell leukemia sequence 1	2	2.5E-03	8.8E-03
Cldn23	Claudin 23	4	2.5E-03	8.9E-03
Peli3	Pellino 3	2	2.5E-03	8.9E-03
Hacd2	3-hydroxyacyl-CoA dehydratase 2	4	2.5E-03	8.9E-03
Slc35d3	Solute carrier family 35, member D3	3	2.5E-03	8.9E-03
Sec31a	SEC31 homolog A, COPII coat complex component	3	2.5E-03	9.0E-03
Vps18	VPS18 CORVET/HOPS core subunit	1	2.5E-03	9.0E-03
Zfyve27	Zinc finger, FYVE domain containing 27	4	2.5E-03	9.0E-03
Dusp2	Dual specificity phosphatase 2	4	2.5E-03	9.0E-03
Poc5	POC5 centriolar protein	3	2.5E-03	9.1E-03
Ppib	Peptidylprolyl isomerase B	4	2.6E-03	9.1E-03
Exd1	Exonuclease 3'-5' domain containing 1	1	2.6E-03	9.2E-03
Vmn1r56	Vomeronasal 1 receptor 56	4	2.6E-03	9.2E-03
Cspp1	Centrosome and spindle pole associated protein 1	2	2.6E-03	9.2E-03
Acsbg2	Acyl-CoA synthetase bubblegum family member 2	3	2.6E-03	9.3E-03
Ints9	Integrator complex subunit 9	2	2.6E-03	9.3E-03

Snrpc	U1 small nuclear ribonucleoprotein C	4	2.6E-03	9.4E-03
Cep89	Centrosomal protein 89	2	2.6E-03	9.4E-03
Ndufb5	NADH:ubiquinone oxidoreductase subunit B5	3	2.6E-03	9.4E-03
Vmn1r80	Vomeronasal 1 receptor 80	3	2.6E-03	9.4E-03
Srsf9	Serine and arginine-rich splicing factor 9	2	2.6E-03	9.4E-03
Ptov1	Prostate tumor over expressed gene 1	3	2.7E-03	9.5E-03
Rpl37	Ribosomal protein L37	3	2.7E-03	9.6E-03
Sirt4	Sirtuin 4	3	2.7E-03	9.6E-03
Sars	Seryl-aminoacyl-tRNA synthetase	2	2.7E-03	9.7E-03
Vmn1r219	Vomeronasal 1 receptor 219	2	2.8E-03	9.8E-03
Spop	Speckle-type BTB/POZ protein	2	2.8E-03	9.9E-03

Table 3. Candidate genes identified by sgRNAs enriched in the GFP^{-} (phagocytosis-deficient) population (p<0.01).

Gene symbol	Gene name	Enriched sgRNAs	MAGeCK score	p-value
Usp22	Ubiquitin specific peptidase 22	4	2.2E-08	2.5E-07
Taf4a	TATA-box binding protein associated factor 4	4	3.5E-08	2.5E-07
Supt20	SPT20 SAGA complex component	3	4.1E-08	2.5E-07
Taf13	TATA-box binding protein associated factor 13	4	4.2E-08	2.5E-07
Tardbp	TAR DNA-binding protein	3	5.7E-08	2.5E-07
Nelfcd	Negative elongation factor complex member C/D	4	7.8E-08	2.5E-07
Rfwd2	COP1 E3 ubiquitin ligase	4	2.0E-07	7.5E-07
Dyrk1a	Dual specificity tyrosine-phosphorylation regulated kinase 1A	4	2.7E-07	1.3E-06
Brd4	Bromodomain containing 4	3	7.1E-07	2.3E-06
Rragc	Ras-related GTP-binding C	3	1.8E-06	5.8E-06
Nelfa	Negative elongation factor complex member A	3	3.1E-06	1.2E-05
Gsk3a	Glycogen synthase kinase 3 alpha	4	6.4E-06	2.4E-05
Abce1	ATP-binding cassette sub-family E, member 1	3	1.1E-05	4.1E-05
Taf2	TATA-box binding protein associated factor 2	3	1.3E-05	5.1E-05
Eif3h	Eukaryotic translation initiation factor 3 subunit H	4	1.4E-05	5.6E-05
Taf10	TATA-box binding protein associated factor 10	3	1.6E-05	6.6E-05
Zc3h10	Zinc finger CCCH domain-containing protein 10	3	1.7E-05	6.7E-05
Taf6l	TATA-box binding protein associated factor 6 like	4	1.9E-05	7.5E-05
Ccar1	Cell division cycle and apoptosis regulator 1	3	2.5E-05	1.0E-04
Pcdhga8	Protocadherin gamma subfamily A, 8	1	2.6E-05	1.0E-04
Taf8	TATA-box binding protein associated factor 8	4	2.9E-05	1.2E-04
Kcnk16	Potassium channel subfamily K member 16	3	3.5E-05	1.4E-04
Ino80	INO80 complex subunit	3	3.9E-05	1.5E-04
Atxn7l3	Ataxin-7-like 3	3	4.3E-05	1.7E-04

Ptbp1	Polypyrimidine tract-binding protein 1	4	4.3E-05	1.7E-04
Mau2	Chromatid cohesion factor homolog	4	4.4E-05	1.7E-04
Cebpb	CCAAT/enhancer-binding protein beta	2	4.6E-05	1.8E-04
Tada2b	Transcriptional adapter 2B	3	5.2E-05	2.0E-04
Nelfb	Negative elongation factor complex member B	3	5.4E-05	2.1E-04
Eif4g2	Eukaryotic translation initiation factor 4 gamma 2	3	6.3E-05	2.5E-04
Morc3	MORC family CW-type zinc finger protein 3	3	7.5E-05	3.0E-04
Gsk3b	Glycogen synthase kinase 3 beta	4	7.8E-05	3.2E-04
Cnga4	Cyclic nucleotide-gated cation channel alpha-4	3	7.9E-05	3.2E-04
Pagr1a	PAXIP1-associated glutamate-rich protein 1A	3	8.9E-05	3.5E-04
Plekhb2	Pleckstrin homology domain-containing family B member 2	4	9.3E-05	3.7E-04
Drosha	Class 2 ribonuclease III	3	9.8E-05	3.9E-04
Arf1	ADP-ribosylation factor 1	4	1.0E-04	4.1E-04
Pcyt2	Ethanolamine-phosphate cytidylyltransferase	2	1.1E-04	4.2E-04
Erh	Enhancer of rudimentary homolog	3	1.1E-04	4.4E-04
Ankrd52	Ankyrin repeat domain 52	4	1.1E-04	4.5E-04
Ifi205	Interferon-activated gene 205	4	1.2E-04	4.6E-04
Stxbp3a	Syntaxin-binding protein 3	4	1.2E-04	4.9E-04
Cdkn1a	Cyclin dependent kinase inhibitor 1A	3	1.3E-04	5.2E-04
Prdm13	PR domain containing 13	4	1.6E-04	6.3E-04
Ikbkg	Inhibitor of nuclear factor kappa-B kinase gamma	2	1.7E-04	6.6E-04
Spi1	Spleen focus forming virus (SFFV) proviral integration oncogene	3	2.2E-04	8.5E-04
Prss42	Serine protease 42	4	2.3E-04	8.6E-04
Dscaml1	DS cell adhesion molecule like 1	1	2.3E-04	8.8E-04
Ccdc60	Coiled-coil domain containing 60	4	2.5E-04	9.4E-04
Actr8	Actin-related protein 8	3	2.6E-04	9.8E-04
Smg6	SMG6 nonsense mediated mRNA decay factor	4	2.7E-04	1.0E-03
Vmn1r53	Vomeronasal 1 receptor 53	4	2.7E-04	1.0E-03
Ipo13	Importin-13	4	2.7E-04	1.0E-03
Egr1	Early growth response protein 1	4	2.8E-04	1.1E-03
Ambra1	Autophagy/beclin 1 regulator 1	3	2.8E-04	1.1E-03
Kdm3b	KDM3B lysine demethylase 3B	3	2.9E-04	1.1E-03
Gm6484	Angiopoietin-like 8	4	3.1E-04	1.1E-03
Ggct	Gamma-glutamyl cyclotransferase	3	3.1E-04	1.2E-03
Ric8	RIC8 guanine nucleotide exchange factor	4	3.3E-04	1.2E-03
Spin1	Spindlin-1	4	3.4E-04	1.3E-03
Irak4	Interleukin-1 receptor-associated kinase 4	4	3.4E-04	1.3E-03
Olfr1030	Olfactory receptor family 5 subfamily M member 5	4	3.4E-04	1.3E-03

Pced1b	PC-esterase domain-containing protein 1B	4	3.5E-04	1.3E-03
Tcf7	Transcription factor 7, T cell specific	3	3.6E-04	1.3E-03
Gtf2h5	General transcription factor IIH subunit 5	4	3.8E-04	1.4E-03
Tada1	Transcriptional adaptor 1	4	3.8E-04	1.4E-03
Fan1	FANCD2/FANCI-associated nuclease 1	4	3.9E-04	1.4E-03
Tars2	Threonyl-tRNA synthetase 2, mitochondrial (putative)	4	4.2E-04	1.6E-03
Hes6	Transcription cofactor HES-6	4	4.3E-04	1.6E-03
Ly6g5c	Lymphocyte antigen 6 complex locus protein G5C	3	4.3E-04	1.6E-03
Nfrkb	Nuclear factor related to kappa-B-binding protein	2	4.3E-04	1.6E-03
Atp2b1	ATPase, Ca++ transporting, plasma membrane 1	3	4.4E-04	1.6E-03
Trp53	Cellular tumor antigen p53	3	4.7E-04	1.7E-03
Dhx15	DEAH-box RNA helicase 15	4	4.7E-04	1.7E-03
Olfr491	Olfactory receptor 491	3	4.8E-04	1.8E-03
Acly	ATP citrate lyase	3	4.8E-04	1.8E-03
Glis1	Glis family zinc finger 1	2	4.8E-04	1.8E-03
Uvssa	UV-stimulated scaffold protein A	2	4.8E-04	1.8E-03
Taf5l	TATA-box binding protein associated factor 5 like	2	4.8E-04	1.8E-03
Lrrc16b	Capping protein regulator and myosin 1 linker 3	3	5.2E-04	1.9E-03
Capns1	Calpain small subunit 1	4	5.2E-04	1.9E-03
Camp	Cathelicidin antimicrobial peptide	3	5.2E-04	1.9E-03
Supt7l	SPT7-like, STAGA complex gamma subunit	3	5.6E-04	2.1E-03
Cysltr1	Cysteinyl leukotriene receptor 1	4	5.8E-04	2.1E-03
Hemk1	HemK methyltransferase family member 1	3	5.9E-04	2.2E-03
Spock2	Sparc/osteonectin, cwcv and kazal-like domains proteoglycan 2	2	5.9E-04	2.2E-03
Psme4	Proteasome activator complex subunit 4	3	5.9E-04	2.2E-03
Ptges3l	Prostaglandin E synthase 3 like	4	5.9E-04	2.2E-03
Clp1	Cleavage and polyadenylation factor 1 subunit	4	6.0E-04	2.2E-03
Nelfe	Negative elongation factor complex member E	3	6.1E-04	2.3E-03
Usp5	Ubiquitin specific peptidase 5	3	6.3E-04	2.3E-03
Dad1	Defender against apoptotic cell death 1	3	6.9E-04	2.5E-03
Lamp2	Lysosome-associated membrane glycoprotein 2	4	7.1E-04	2.6E-03
Krtap5-1	Keratin-associated protein 5-1	4	7.6E-04	2.8E-03
Gpr82	G-protein coupled receptor 82	4	7.8E-04	2.8E-03
Mrpl17	Mitochondrial ribosomal protein L17	1	7.9E-04	2.9E-03
Aak1	AP2 associated kinase 1	3	7.9E-04	2.9E-03
Tsc2	TSC complex subunit 2	4	7.9E-04	2.9E-03
Lrrc74b	Leucine-rich repeat-containing protein 74B	4	8.1E-04	2.9E-03

Olfr1215	Olfactory receptor family 4 subfamily C member 110	4	8.3E-04	3.0E-03
Rnf138rt1	Ring finger protein 138, retrogene 1	4	8.3E-04	3.0E-03
Gm2863	BTB domain containing 35, family member 12	4	8.4E-04	3.0E-03
Mafg	Transcription factor MafG	4	8.4E-04	3.1E-03
Uchl5	Ubiquitin carboxyl-terminal hydrolase isozyme L5	4	8.4E-04	3.1E-03
Plekha4	Pleckstrin homology domain-containing family A member 4	4	8.5E-04	3.1E-03
Sod1	Superoxide dismutase 1	4	8.5E-04	3.1E-03
Upf3b	Regulator of nonsense transcripts 3B	4	8.5E-04	3.1E-03
Runx1	Runt-related transcription factor 1	4	8.6E-04	3.1E-03
Myo19	Myosin XIX	4	8.8E-04	3.2E-03
Taf3	TATA-box binding protein associated factor 3	4	8.9E-04	3.2E-03
Chaf1b	Chromatin assembly factor 1 subunit B	4	9.0E-04	3.3E-03
Yipf5	Yip1 domain family, member 5	4	9.1E-04	3.3E-03
Oxsr1	Oxidative-stress responsive 1	4	9.2E-04	3.3E-03
Hdgfl1	Hepatoma-derived growth factor-like protein 1	4	9.2E-04	3.3E-03
Rps16	40S ribosomal protein S16	4	9.4E-04	3.4E-03
Kat7	Lysine acetyltransferase 7	4	9.7E-04	3.5E-03
Cd3e	CD3 antigen, epsilon polypeptide	4	9.9E-04	3.6E-03
C330007P06Rik	STING1 ER exit protein 1	4	9.9E-04	3.6E-03
Ppil6	Peptidylprolyl cis-trans isomerase-like 6	4	1.0E-03	3.7E-03
Synpr	Synaptoporin	4	1.0E-03	3.7E-03
Thoc2	THO complex subunit 2	4	1.0E-03	3.7E-03
Sox10	SRY (sex determining region Y)-box 10	4	1.0E-03	3.7E-03
Ferd3l	Fer3-like bHLH transcription factor	4	1.0E-03	3.8E-03
Taf5	TATA-box binding protein associated factor 5	4	1.0E-03	3.8E-03
Ptgr2	Prostaglandin reductase 2	4	1.0E-03	3.8E-03
Ccdc101	SAGA complex associated factor 29	4	1.1E-03	3.9E-03
Psmd12	26S proteasome non-ATPase regulatory subunit 12	4	1.1E-03	4.0E-03
Rbm17	RNA binding motif protein 17	4	1.1E-03	4.1E-03
Polr3b	DNA-directed RNA polymerase III subunit RPC2	4	1.2E-03	4.2E-03
Rhbdf2	Rhomboid family member 2	4	1.2E-03	4.2E-03
Homer1	Homer scaffolding protein 1	4	1.2E-03	4.2E-03
Wasf2	Wiskott-Aldrich syndrome protein family member 2	4	1.2E-03	4.3E-03
Unc13b	Unc-13 homolog B	4	1.2E-03	4.3E-03
Senp5	Sentrin-specific protease 5	4	1.2E-03	4.4E-03
Pggt1b	Geranylgeranyl transferase type-1 subunit beta	4	1.2E-03	4.4E-03
Fubp3	Far upstream element-binding protein 3	4	1.2E-03	4.4E-03

Tet1	Tet methylcytosine dioxygenase 1	4	1.2E-03	4.4E-03
Xpo5	Exportin 5	4	1.2E-03	4.5E-03
Sftpa1	Surfactant associated protein A1	4	1.3E-03	4.5E-03
Gpr19	G-protein coupled receptor 19	4	1.3E-03	4.5E-03
Ap1m1	AP-1 complex subunit mu-1	4	1.3E-03	4.6E-03
Gpaa1	Glycosylphosphatidylinositol anchor attachment protein 1	4	1.3E-03	4.8E-03
Nxf2	Nuclear RNA export factor 2	4	1.3E-03	4.8E-03
Ropn1	Rhophilin associated protein 1	4	1.3E-03	4.8E-03
Brk1	BRICK1, SCAR/WAVE actin-nucleating complex subunit	4	1.3E-03	4.9E-03
Siah1b	E3 ubiquitin-protein ligase SIAH1B	4	1.3E-03	4.9E-03
Cst9	Cystatin 9	4	1.4E-03	5.0E-03
Cap1	Adenylyl cyclase-associated protein 1	4	1.4E-03	5.0E-03
Sumo2	Small ubiquitin-like modifier 2	4	1.4E-03	5.0E-03
Dhrs13	Dehydrogenase/reductase SDR family member 13	4	1.4E-03	5.1E-03
Tcp10c	T-complex protein 10c	4	1.4E-03	5.1E-03
Ptpn12	Protein tyrosine phosphatase, non-receptor type 12	4	1.4E-03	5.1E-03
Ing4	Inhibitor of growth protein 4	4	1.4E-03	5.2E-03
Tfpt	TCF3 fusion partner	4	1.4E-03	5.2E-03
Tut1	Terminal uridylyl transferase 1, U6 snRNA-specific	4	1.5E-03	5.2E-03
Atp6v0a4	ATPase, H+ transporting, lysosomal V0 subunit A4	4	1.5E-03	5.2E-03
Ahdc1	AT-hook DNA-binding motif-containing protein 1	4	1.5E-03	5.3E-03
Olfr710	Olfactory receptor family 2 subfamily D member 4	4	1.5E-03	5.3E-03
Olfr324	Olfactory receptor family 2 subfamily AB member 1	4	1.5E-03	5.5E-03
Akr1c18	Aldo-keto reductase family 1 member C18	4	1.5E-03	5.5E-03
Dscr3	VPS26 endosomal protein sorting factor C	4	1.6E-03	5.6E-03
Rraga	Ras-related GTP-binding protein A	4	1.6E-03	5.6E-03
2810474O19Rik	Retroelement silencing factor 1	4	1.6E-03	5.7E-03
Brd2	Bromodomain-containing protein 2	4	1.6E-03	5.7E-03
Vmn1r215	Vomeronasal 1 receptor 215	4	1.6E-03	5.8E-03
Tas2r122	Taste receptor, type 2, member 122	4	1.6E-03	5.8E-03
Nkd1	Naked cuticle 1	4	1.6E-03	5.9E-03
Upf2	Regulator of nonsense transcripts 2	4	1.6E-03	5.9E-03
Pigh	Phosphatidylinositol glycan anchor biosynthesis, class H	4	1.7E-03	5.9E-03
Dgcr8	DGCR8 microprocessor complex subunit	4	1.7E-03	5.9E-03

Crebbp	CREB-binding protein	4	1.7E-03	5.9E-03
Vmn1r212	Vomeronasal 1 receptor 212	4	1.7E-03	6.0E-03
Plat	Tissue-type plasminogen activator	4	1.7E-03	6.1E-03
Ppcdc	Phosphopantothenoylcysteine decarboxylase	4	1.7E-03	6.1E-03
Pou3f2	POU domain, class 3, transcription factor 2	4	1.7E-03	6.2E-03
Pde1b	Phosphodiesterase 1B, Ca2+-calmodulin dependent	4	1.8E-03	6.3E-03
Cbfb	Core-binding factor subunit beta	4	1.8E-03	6.5E-03
Larp4b	La ribonucleoprotein 4B	4	1.9E-03	6.7E-03
Smad4	SMAD family member 4	4	1.9E-03	6.7E-03
Fem1c	Fem 1 homolog C	4	1.9E-03	6.7E-03
U2af1l4	U2 small nuclear RNA auxiliary factor 1-like 4	4	1.9E-03	6.8E-03
3110082J24Rik	RIKEN cDNA 3110082J24 gene	4	1.9E-03	6.8E-03
Trmt10c	tRNA methyltransferase 10C, mitochondrial RNase P subunit	4	1.9E-03	6.8E-03
Cbx1	Chromobox 1	4	1.9E-03	6.9E-03
Rela	Nuclear factor NF-kappa-B p65 subunit	4	1.9E-03	6.9E-03
Edc3	Enhancer of mRNA-decapping protein 3	4	1.9E-03	6.9E-03
U2af1	U2 small nuclear ribonucleoprotein auxiliary factor 1	4	2.0E-03	7.0E-03
Gm5114	Predicted gene 5114	4	2.0E-03	7.1E-03
Col5a2	Collagen, type V, alpha 2	4	2.0E-03	7.1E-03
Sigirr	Single immunoglobulin and toll-interleukin 1 receptor (TIR) domain	4	2.1E-03	7.4E-03
Rpl12	60S ribosomal protein L12	4	2.1E-03	7.4E-03
Hectd1	HECT domain E3 ubiquitin protein ligase 1	4	2.1E-03	7.4E-03
Actrt1	Actin-related protein T1	4	2.1E-03	7.5E-03
Tacc2	Transforming acidic coiled-coil-containing protein 2	4	2.1E-03	7.6E-03
Poldip3	Polymerase delta-interacting protein 3	4	2.1E-03	7.7E-03
Cgrrf1	Cell growth regulator with RING finger domain protein 1	4	2.2E-03	7.7E-03
Pten	Phosphatase and tensin homolog	4	2.2E-03	7.8E-03
Galnt1	Polypeptide N-acetylgalactosaminyltransferase 1	4	2.2E-03	8.0E-03
Pmvk	Phosphomevalonate kinase	4	2.3E-03	8.1E-03
Haus2	HAUS augmin-like complex subunit 2	4	2.3E-03	8.1E-03
Tmem53	Transmembrane protein 53	4	2.3E-03	8.1E-03
Olfr508	Olfactory receptor family 5 subfamily P member 80	4	2.3E-03	8.2E-03
Plvap	Plasmalemma vesicle-associated protein	4	2.3E-03	8.2E-03
Yes1	YES proto-oncogene 1, Src family tyrosine kinase	4	2.3E-03	8.3E-03

Rgs13	Regulator of G-protein signaling 13	4	2.3E-03	8.3E-03
A630033H20Rik	Purinergic receptor P2Y, G-protein coupled 10B	4	2.3E-03	8.3E-03
Taf1d	TATA-box binding protein associated factor, RNA polymerase I, D	4	2.4E-03	8.6E-03
R3hdm1	R3H domain-containing protein 1	4	2.4E-03	8.6E-03
Trip12	Thyroid hormone receptor interactor 12	4	2.4E-03	8.6E-03
H1fx	H1.10 linker histone	4	2.4E-03	8.7E-03
Pigf	Phosphatidylinositol-glycan anchor biosynthesis class F	4	2.5E-03	8.8E-03
Fam217a	Family with sequence similarity 217, member A	4	2.5E-03	8.8E-03
Stk40	Serine/threonine-protein kinase 40	4	2.5E-03	8.8E-03
Gm20826	Predicated gene 20826	4	2.5E-03	8.8E-03
Olfr652	Olfactory receptor family 52 subfamily H member 7	4	2.5E-03	8.9E-03
Doc2g	Double C2-like domain-containing protein gamma	4	2.5E-03	8.9E-03
Id2	Inhibitor of DNA binding 2	4	2.5E-03	9.0E-03
Mief1	Mitochondrial elongation factor 1	4	2.5E-03	9.0E-03
Eif5	Eukaryotic translation initiation factor 5	4	2.6E-03	9.2E-03
Msra	Peptide methionine sulfoxide reductase A	4	2.6E-03	9.2E-03
Dhx38	DEAH (Asp-Glu-Ala-His) box polypeptide 38	4	2.6E-03	9.3E-03
Det1	De-etiolated homolog 1	4	2.6E-03	9.3E-03
Cpne8	Copine 8	4	2.7E-03	9.5E-03
Arhgap30	Rho GTPase-activating protein 30	4	2.7E-03	9.5E-03
Lamtor4	Late endosomal/lysosomal adaptor, MAPK and MTOR activator 4	4	2.7E-03	9.5E-03
Sf3b3	Splicing factor 3B subunit 3	4	2.7E-03	9.6E-03
Phc1	Polyhomeotic-like protein 1	4	2.7E-03	9.6E-03
Bub1b	Mitotic checkpoint serine/threonine-protein kinase BUB1 beta	4	2.7E-03	9.6E-03
Sptlc1	Serine palmitoyltransferase, long chain base subunit 1	4	2.7E-03	9.7E-03
Tmem208	Transmembrane protein 208	4	2.7E-03	9.8E-03
Vmn2r35	Vomeronasal 2, receptor 35	4	2.8E-03	9.8E-03
Olfr477	Olfactory receptor family 5 subfamily P member 56	4	2.8E-03	9.8E-03
Arhgap1	Rho GTPase-activating protein 1	4	2.8E-03	9.8E-03
Gse1	Genetic suppressor element 1	3	2.8E-03	7.7E-03
Setd5	SET domain containing 5	4	2.8E-03	9.9E-03

Chapter 4: PTEN is required for phagocytosis by macrophages and promotes myeloid restriction of *Lm*

Introduction

The genome-wide CRISPR screen described in Chapter 3 identified the PTEN regulation pathway as important for phagocytosis of *Lm* (Figure 11C). Indeed, two members of this pathway, GSK3 and PTEN itself, were required for uptake of *Lm* by macrophages (Figures 11B and 12B). Interestingly, this was specific to *Lm* as PTEN and GSK3 were dispensable for uptake of *L. innocua* and *B. subtilis*. We hypothesize that *Lm* is phagocytosed by macrophages using a distinct, PTEN-dependent pathway.

PTEN (phosphatase and tensin homolog) is a dual-specificity phosphatase primarily known for its tumor suppressor activity[105]. PTEN blunts the PI3K (phosphoinositide 3-kinase) signaling cascade as shown in Figure 13. Briefly, PI3K becomes activated downstream of ligand binding to receptor tyrosine kinases (RTKs). Activated PI3K phosphorylates phosphatidylinositol (4,5)-bisphosphate (PIP_2) to form phosphatidylinositol (3,4,5)-triphosphate (PIP_3). PIP_3 then acts as a second messenger to regulate many biological processes. One of the most well-studied roles of PIP_3 is in promoting cell survival and proliferation. Therefore, activation of this pathway must be tightly controlled to prevent aberrant cell division and oncogenesis. PTEN's primary function is to dephosphorylate PIP_3 back to PIP_2 and terminate PI3K signaling, thus acting as a tumor suppressor[106,107]. While PTEN's tumor suppressor function is the most well-studied aspect of this enzyme, PTEN also exhibits protein phosphatase activity against tyrosine or serine/threonine residues which regulates cell division and other cellular processes[108–110].

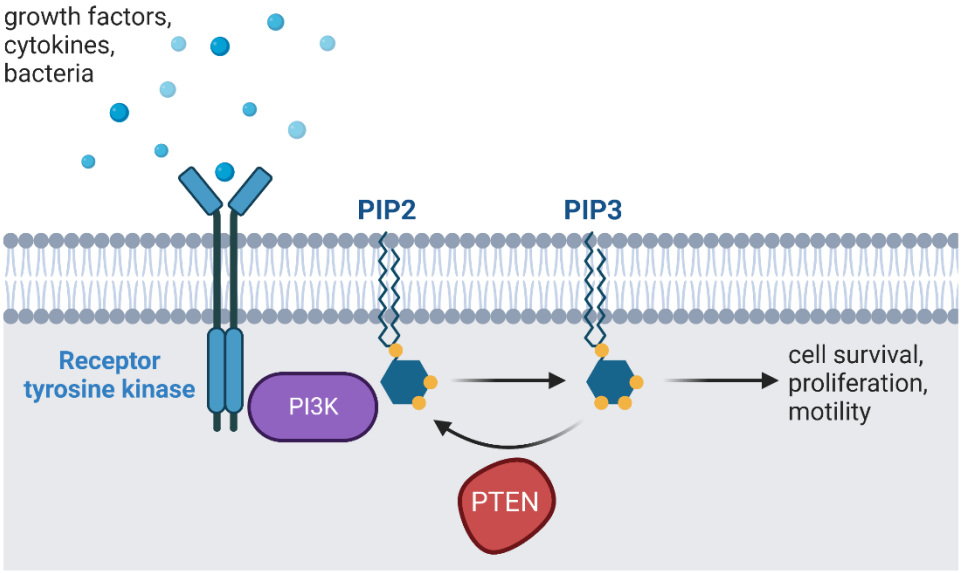

Figure 13. PI3K/PTEN signaling axis. PI3K becomes activated downstream of surface receptors and produces PIP_3. PIP_3 regulates many downstream effectors to regulate cell survival and motility. PTEN dephosphorylates PIP_3 to antagonize PI3K signaling.

PTEN and PI3K also regulate phagocytosis and endocytosis through control of cytoskeletal dynamics and membrane phospholipids[111]. PI3K activity leads to activation of small GTPases which control actin polymerization at the cell membrane to direct internalization of substrates[112]. Accordingly, PI3K activation has been shown to be required for phagocytosis of various bacteria[113–116]. PI3K is also well known to be critical for internalization of *Lm* by non-phagocytes downstream of receptor binding[46,117]. As an antagonist of PI3K signaling, PTEN has been previously reported to repress phagocytosis of various substrates[118–121]. Our preliminary data showing promotion of phagocytosis of *Lm* by PTEN is intriguing, therefore we set out to characterize a potential novel function of PTEN in the regulation of phagocytosis.

In this study, we found that PTEN was required for uptake of *Lm* by human and mouse macrophages in a bacterial species- and serovar-dependent manner. PTEN promotes phagocytosis of *Lm* by enhancing adherence to macrophages and uptake through this pathway is more efficient than PTEN-independent mechanisms. Tight control of PIP_3 signaling regulates phagocytosis of *Lm*, as both PIP_3 production and turnover by PI3K and PTEN, respectively, are required for uptake. Using an oral murine listeriosis model in conditional *Pten* knockout mice, we demonstrate that myeloid PTEN is dispensable for dissemination from the GI tract and restricts *Lm* replication *in vivo*. Overall, this work revealed a novel function of PTEN in promoting phagocytosis of a bacterial pathogen and demonstrated a role for non-opsonic phagocytosis in anti-*Lm* immunity.

The majority of this chapter is published in: Glover RC, Schwardt NH, Leano SE, Sanchez ME, Thomason MK, Olive AJ, Reniere ML. 2023. A genome-wide screen in macrophages identifies PTEN as required for myeloid restriction of *Listeria monocytogenes* infection. *PLoS Pathogens*. 19(5): e1011058. 10.1371/journal.ppat.1011058.

Results

PTEN is required for uptake of *Lm* by macrophages

To elucidate the role of PTEN in the context of *Lm* infection, we first derived single-cell clones from an iBMM *Pten* CRISPR knockout population and confirmed the absence of PTEN protein by immunoblot for two independent clones (Figure 14A). A small amount of PTEN protein at a lower molecular weight was detected for Clone 2, however sequencing analysis revealed a 45 base pair deletion in the phosphatase domain of this clone. Each cell line was infected with *Lm* and uptake was assessed by gentamicin protection assay. Compared to wildtype (WT) iBMMs, *Pten*$^{-/-}$ iBMMs exhibited a dramatic reduction in *Lm* uptake (Figure 14B). As both clones had similar phenotypes, iBMM *Pten*$^{-/-}$ Clone 1 was used for the remainder of our experiments. To assess the overall phagocytic ability of *Pten*$^{-/-}$ iBMMs, we measured phagocytosis of fluorescently-labeled latex beads. IgG-opsonized FITC-labeled beads were added to WT and *Pten*$^{-/-}$ iBMMs for 30 minutes, after which excess beads were removed. Fluorescence of any remaining extracellular beads was quenched with trypan blue and FITC fluorescence was quantified by flow cytometry. Phagocytosis of fluorescent beads was not significantly different between WT and *Pten*$^{-/-}$ iBMMs (Figure 14C), indicating that basal phagocytic activity was not altered by loss of *Pten.* In addition, these results suggest that PTEN is not required for Fcγ receptor-mediated phagocytosis in iBMMs.

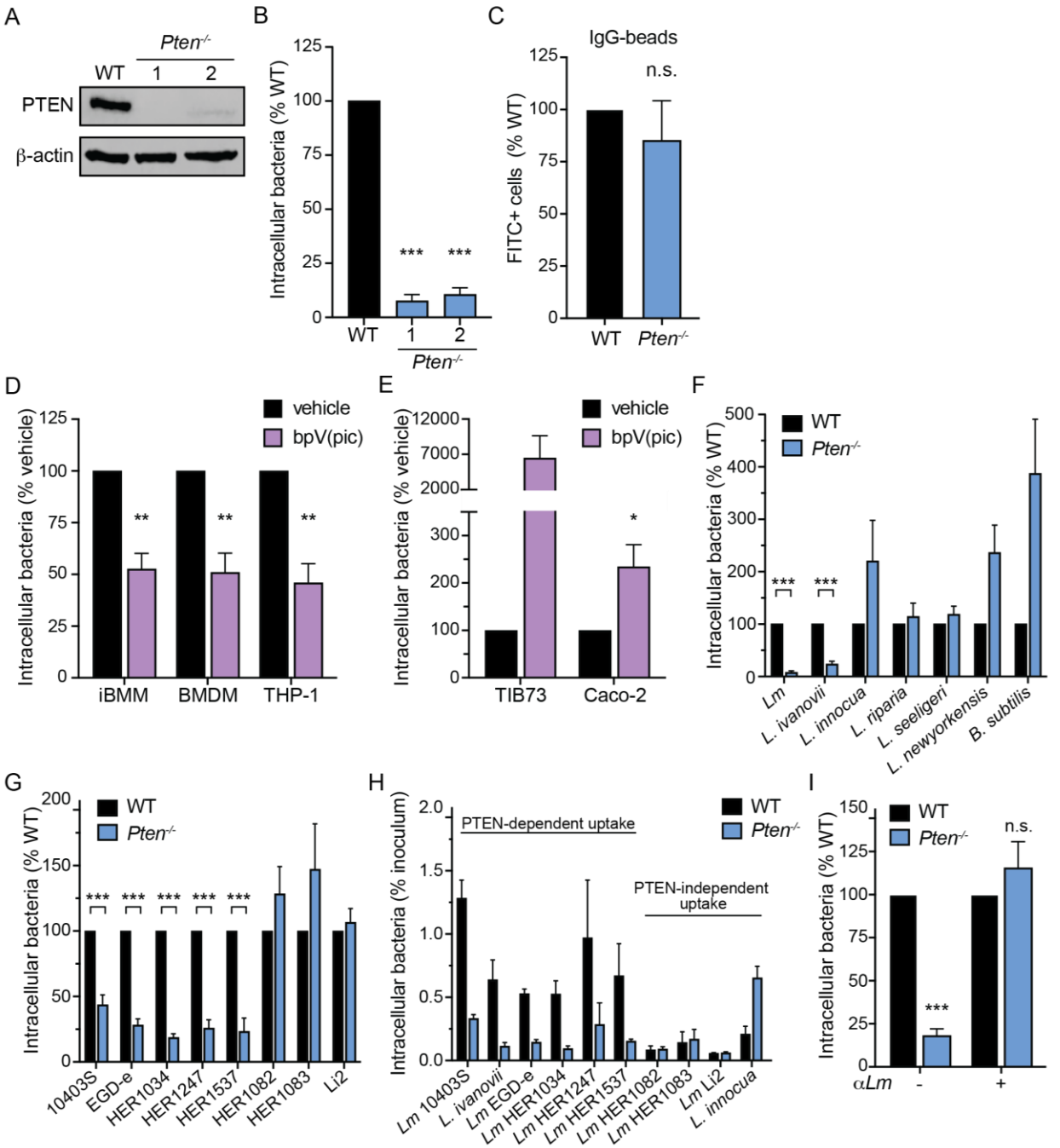

Figure 14. PTEN is a novel host factor which enhances phagocytosis of specific *Lm* strains. (A) Immunoblot of PTEN in WT and *Pten*$^{-/-}$ iBMM clones. β-actin is used as a loading control. (B) Gentamicin protection assay measuring uptake of *Lm* by *Pten*$^{-/-}$ iBMMs. iBMMs were infected at MOI=1 for 30 minutes and CFU were quantified 1 hour post-infection. Two independent single-cell clones were analyzed. Data are normalized to WT iBMMs. (C) Uptake of IgG-opsonized FITC-labeled latex beads by WT and *Pten*$^{-/-}$ iBMMs. Beads were added to cells for 30 minutes and uptake was quantified by flow cytometry. (D) Gentamicin protection assay measuring uptake of *Lm* by iBMMs, BMDMs, and PMA-differentiated THP-1 cells. Cells were treated with vehicle or 5 μM bpV(pic). Data are normalized to vehicle-treated cells. (E) Gentamicin protection assay measuring uptake of *Lm* by TIB73 and Caco-2 cells. Cells were infected at

MOI=10 (Caco-2) or MOI=50 (TIB73) for 1 hour and CFU were quantified 90 min post-infection. Cells were treated with vehicle or 5 μM bpV(pic). Data are normalized to vehicle-treated cells. (F) Gentamicin protection assay measuring uptake of bacteria by WT and *Pten*$^{-/-}$ iBMMs. Data are normalized to WT iBMMs for each species. (G) Gentamicin protection assay measuring uptake of *Lm* strains by WT and *Pten*$^{-/-}$ iBMMs. Data are normalized to WT iBMMs for each strain. (H) Gentamicin protection assay measuring uptake of *Lm* strains, *L. ivanovii*, and *L. innocua* by iBMMs. The initial inoculum of each strain was enumerated and the percentage of internalized bacteria was calculated. (I) Gentamicin protection assay measuring uptake of un-opsonized and antibody-opsonized *Lm* 10403S by WT and *Pten*$^{-/-}$ iBMMs. Data are normalized to WT iBMMs. All data are means and SEM of at least three biological replicates. *p<0.05, **p<0.01, ***p<0.001, n.s. = non-significant, as determined by unpaired *t* tests.

We next investigated the role of PTEN in *Lm* internalization in various cell types. iBMMs, BMDMs, and THP-1 human monocyte-derived macrophages were treated with the well-characterized potent competitive PTEN inhibitor bpV(pic)[122]. Uptake of *Lm* was reduced to similar levels in all three macrophage cell types tested (Figure 14D), indicating that regulation of *Lm* uptake by PTEN is conserved in primary murine macrophages as well as human macrophages. *Lm* also induces phagocytosis-like internalization into non-phagocytic cells[123]. In contrast to macrophages, TIB73 murine hepatocytes and Caco-2 human colonic epithelial cells exhibited increased *Lm* internalization following treatment with bpV(pic) (Figure 14E). These data demonstrate that PTEN is required for phagocytosis of *Lm* specifically by macrophages.

Chemical inhibition of PTEN specifically blocks uptake of *Lm* but not *L. innocua* or *B. subtilis*. To confirm the specificity of PTEN for regulation of *Lm* uptake, we assessed phagocytosis of various *Listeria* species and *B. subtilis* in WT and *Pten*$^{-/-}$ iBMMs. *Pten*$^{-/-}$ iBMMs were deficient for uptake of the pathogenic species *Lm* and *L. ivanovii*, but not the non-pathogens *L. innocua*, *L. riparia*, *L. seeligeri*, *L. newyorkensis*, or *B. subtilis* (Figure 14F). Given that *Lm* and *L. ivanovii* are taken up more efficiently by macrophages than *L. innocua*, we compared uptake efficiency in WT and *Pten*$^{-/-}$ iBMMs between these species by determining the percentage of the initial inoculum that was internalized under each condition. Uptake efficiency of *Lm* and *L. ivanovii* by *Pten*$^{-/-}$ iBMMs was reduced to that of *L. innocua* in WT cells (Figure 14H). These data suggest that enhanced macrophage uptake of *Lm* and *L. ivanovii* relative to *L. innocua* is PTEN-dependent. In addition to assessing uptake of different species, we also measured phagocytosis of various *Lm* strains in *Pten*$^{-/-}$ iBMMs. Similar to the lab strain 10403S used in all prior experiments, four other *Lm* strains exhibited reduced uptake in *Pten*$^{-/-}$ iBMMs (Figure 14G). In contrast, uptake of three *Lm* strains (HER1082, HER1083, and Li2) remained unchanged in *Pten*$^{-/-}$ iBMMs. Similar to our species-level analysis, *Lm* strains which required PTEN for uptake were internalized more efficiently by macrophages, and this advantage was lost in *Pten*$^{-/-}$ iBMMs (Figure 14H). Overall, these data demonstrate that PTEN enhances uptake of specific species and *Lm* strains by macrophages.

We hypothesized that specific bacterial factors present in these species and strains confer the ability to be taken up by PTEN-dependent phagocytosis. Bacterial factors required for PTEN-dependent phagocytosis could be secreted factors or surface molecules that directly interact with macrophages. To test this, we opsonized *Lm* 10403S with *Listeria* antisera to block direct binding to the *Lm* cell surface and force uptake through Fc receptors. Opsonized *Lm* no longer required PTEN for uptake (Figure 14I), indicating that direct interaction between the macrophage surface and *Lm* cell wall is required for uptake via PTEN-dependent phagocytosis.

PTEN promotes adherence of *Lm* to macrophages

Given that *Pten*$^{-/-}$ iBMMs have reduced intracellular CFU as early as 1 hour post-infection, we hypothesized that PTEN is not involved in escape from the vacuole. To directly test this, we compared uptake of wildtype *Lm* and an LLO-deficient strain (Δ*hly*), which is unable to escape the phagocytic vacuole. If the defect in *Pten*$^{-/-}$ iBMMs was due to impaired vacuolar escape, we would expect to see no difference in intracellular CFU between WT and *Pten*$^{-/-}$ iBMMs during infection with the Δ*hly* mutant that is trapped in the vacuole. However, the Δ*hly* strain displayed a similar reduction in CFU in *Pten*$^{-/-}$ iBMMs compared to wildtype *Lm* (Figure 15A), indicating that PTEN does not play a role in vacuolar escape of *Lm*. In addition, there was no difference in the intracellular growth rate of wildtype *Lm* between WT and *Pten*$^{-/-}$ iBMMs (Figure 15B). Taken together, these data confirm that while PTEN promotes internalization of *Lm*, PTEN is not important for *Lm* escape from the vacuole or replication in the host cytosol.

To further investigate the role of PTEN in *Lm* internalization, we employed an immunofluorescence strategy to quantify intracellular and extracellular bacteria over time during macrophage infection. WT and *Pten*$^{-/-}$ iBMMs were cultured on glass coverslips and infected with mCherry-expressing *Lm* to visualize all adherent and intracellular bacteria. At various timepoints, coverslips were washed to remove non-adhered bacteria, fixed, and immunostained under non-permeabilizing conditions to label only extracellular adherent bacteria. Importantly, gentamicin was not used in these experiments, allowing simultaneous measurement of both adherence and internalization. At 15 minutes post-infection, *Pten*$^{-/-}$ iBMMs had far fewer bacteria present overall (Figure 15C and 15D), indicating a defect in *Lm* adherence to *Pten*$^{-/-}$ macrophages relative to WT iBMMs. To measure efficiency of internalization, we calculated the percentage of total bacteria that were intracellular for each genotype. There was no difference in the percentage of intracellular bacteria between WT and *Pten*$^{-/-}$ macrophages (Figure 15E), suggesting that PTEN does not affect the internalization rate of *Lm*. Collectively, our data indicate that PTEN enhances phagocytosis by promoting adherence of *Lm* to macrophages.

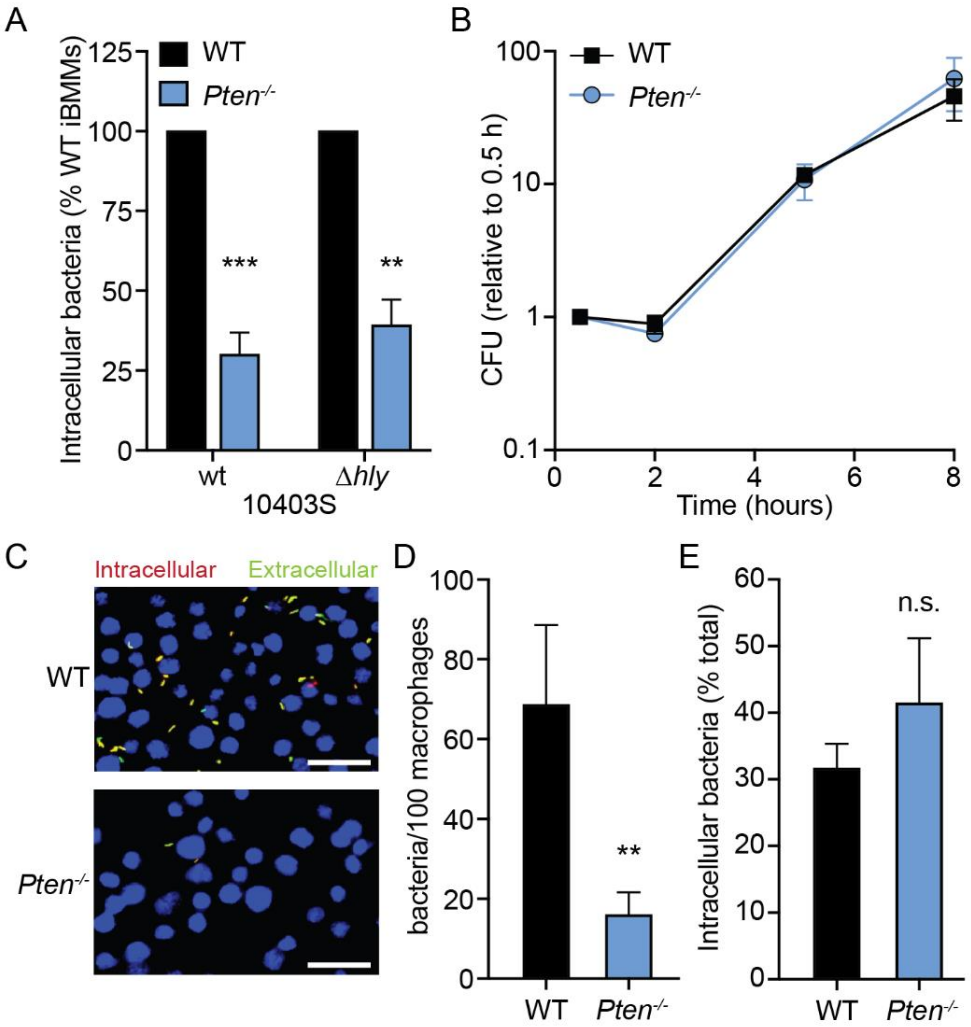

Figure 15. PTEN promotes adherence of *Lm* to macrophages. (A) Gentamicin protection assay measuring uptake of *Lm* wildtype (wt) and Δ*hly* strains by WT and *Pten*$^{-/-}$ iBMMs. iBMMs were infected at MOI=1 for 30 minutes and CFU were quantified 1 hour post-infection. Data are normalized to WT iBMMs for each strain. (B) Intracellular growth of wildtype *Lm* in WT and *Pten*$^{-/-}$ iBMMs. Data are normalized to CFU at 30 minutes for each genotype. (C) Immunofluorescence microscopy of infected WT or *Pten*$^{-/-}$ iBMMs. Cells were infected by centrifugation with mCherry-*Lm* at MOI=5 and fixed 15 min post-infection. Extracellular bacteria were labeled with *Listeria* antisera and a fluorescent secondary antibody. Macrophage nuclei were stained with DAPI. Scale bars indicate 25 μm. (D) Quantification of adherence in (C). The total number of bacteria per 100 macrophages was counted for at least three fields of view (approximately 600 macrophages) per genotype and averaged for each experiment. (E) Quantification of *Lm* internalization 1 hour post-infection. The percentage of intracellular bacteria was calculated for at least three fields of view per genotype and averaged for each experiment. All data are means and SEM of at least three biological replicates. ***p*<0.01, ****p*<0.001, n.s. = non-significant, as determined by unpaired *t* tests (A) or ratio paired *t* tests (D, E).

The lipid phosphatase activity of PTEN promotes *Lm* uptake

PTEN is a protein and lipid phosphatase which participates in major phospho-signaling cascades in mammalian cells[105]. To begin dissecting the PTEN-dependent signaling pathways involved in regulation of *Lm* adherence, we first investigated the enzymatic activity of PTEN required for *Lm* uptake. The following PTEN variants were constitutively expressed in *Pten*$^{-/-}$ iBMMs: a CRISPR-resistant PTEN allele (PTEN^{CR}); PTEN^{CR} G129E, which retains protein phosphatase activity but is unable to dephosphorylate lipids; or PTEN^{CR} G129R, which lacks both protein and lipid phosphatase activity[124]. Expression of each PTEN variant was confirmed at the protein level by immunoblot (Figure 16A). Each cell line was infected with *Lm* and uptake was measured by gentamicin protection assay. Ectopic expression of PTEN^{CR} in *Pten*$^{-/-}$ iBMMs restored uptake of *Lm* to that of WT iBMMs (Figure 16B). In contrast, neither the lipid phosphatase mutant (G129E) nor the enzymatically dead mutant (G129R) variants of PTEN rescued *Lm* uptake in *Pten*$^{-/-}$ iBMMs, demonstrating that the lipid phosphatase activity of PTEN is required for enhancement of *Lm* phagocytosis.

Class 1A PI3K activation is required for macrophage phagocytosis of *Lm*

The lipid phosphatase activity of PTEN specifically dephosphorylates the D3 position of 3-phosphorylated phosphatidylinositol species, mainly phosphatidylinositol (3,4,5)-triphosphate (PIP_3)[106]. PIP_3 is transiently produced upon phosphorylation of $PI(4,5)P_2$ (PIP_2) by activated PI3K and turnover of PIP_3 back to PIP_2 is mediated by PTEN via dephosphorylation[105]. We hypothesized that turnover of PIP_3 by PTEN is important for enhancement of *Lm* phagocytosis. To begin investigating the role of PIP_3 in *Lm* uptake, we first determined whether PIP_3 is produced during *Lm* infection of macrophages. Upon PI3K activation and subsequent PIP_3 production, Akt is recruited to the plasma membrane where it undergoes phosphorylation[125]; therefore, detection of phosphorylated Akt is a common method of measuring PI3K activation. Akt phosphorylation was measured by immunoblot analysis at 15, 30, and 60 minutes post-infection. Infection with *Lm* induced strong Akt phosphorylation 15 minutes post-infection, which waned at 30 minutes and returned to baseline levels by 60 minutes post-infection (Figure 16C). These data indicate that *Lm* rapidly and transiently activates PI3K and PIP_3 production during macrophage infection.

We next modulated PIP_3 levels during infection and measured the effect on *Lm* uptake. First, PIP_3 production was blocked by treating macrophages with the PI3K inhibitor wortmannin. iBMMs, BMDMs, and THP-1 cells all exhibited reduced *Lm* uptake when pre-treated with wortmannin (Figure 16D), indicating that PI3K activation is required for phagocytosis of *Lm* by macrophages. Given that PTEN was specifically required for uptake of *Lm* compared to other bacterial species, we also assessed the specificity of the requirement for PI3K. In contrast to PTEN, PI3K activation was required for uptake of *L. ivanovii*, *L. innocua*, and *B. subtilis* (Figure 16E), suggesting that PI3K activation is broadly important for phagocytosis of bacteria by macrophages.

In mammals, PI3Ks encompass a large family of enzymes consisting of three classes that phosphorylate different phosphoinositides, all of which are inhibited by wortmannin. The majority of PI3K isoforms belong to Class I, which produces PIP_3 from $PI(4,5)P_2$, while Class II and Class III PI3Ks produce other phosphoinositide species such as PI3P and $PI(3,4)P_2$[126]. The catalytic subunits of Class I PI3Ks are further divided into Class 1A isoforms (p110α, p110β, and p110δ)

and a single Class 1B isoform (p110γ). To identify whether PIP_3-producing PI3K isoforms are involved in promoting phagocytosis of *Lm*, we pre-treated iBMMs with isoform-specific PI3K inhibitors targeting all four Class I PI3K isoforms and measured uptake of *Lm*. Inhibition of p110β blocked uptake of *Lm* in iBMMs, while inhibition of p110α, p110δ, or p110γ had no effect (Figure 16F). Collectively, these data show that PIP_3 production by the Class 1A PI3K p110β is required for phagocytosis of *Lm* by macrophages.

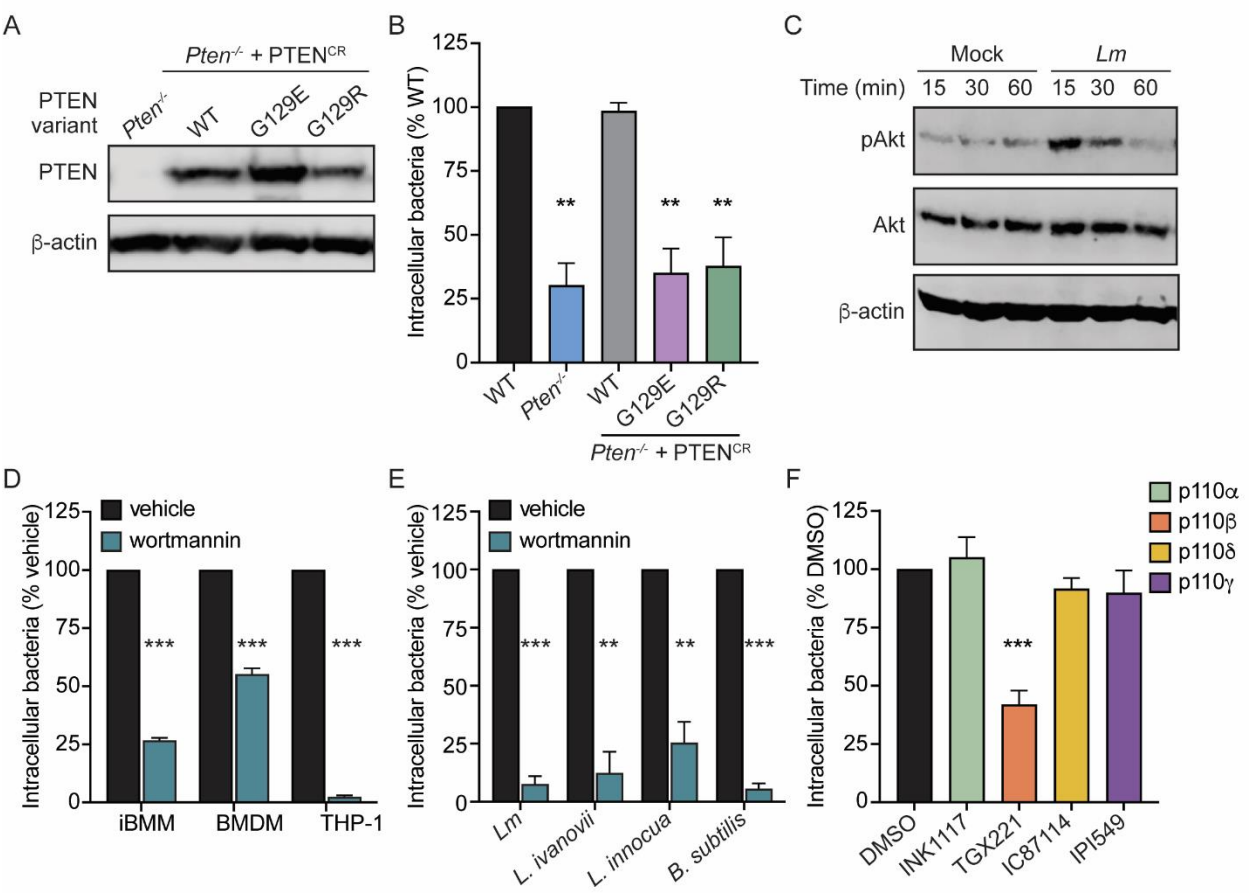

Figure 16. The role of PIP_3 in regulating phagocytosis of *Lm* by macrophages. (A) Immunoblot of PTEN in *Pten*$^{-/-}$ iBMMs expressing CRISPR-resistant PTEN (PTEN^{CR}), PTEN^{CR} G129E, or PTEN^{CR} G129R. β-actin was used as a loading control. (B) Gentamicin protection assay measuring uptake of *Lm* by WT iBMMs or *Pten*$^{-/-}$ iBMMs expressing PTEN variants. iBMMs were infected at MOI=1 for 30 minutes and CFU were quantified 1 hour post-infection. Data are normalized to WT iBMMs. (C) Immunoblot of phosphorylated Akt (Ser473) in BMDMs in response to *Lm* infection. BMDMs were mock infected or infected with MOI=100 and lysed at the indicated timepoints. Total Akt and β-actin were probed as loading controls. (D) Gentamicin protection assay measuring uptake of *Lm* by macrophages treated with 100 nM wortmannin. Data are normalized to vehicle-treated cells. (E) Gentamicin protection assay measuring uptake of bacteria by iBMMs in the presence of 100 nM wortmannin. Data are normalized to vehicle-treated cells. (F) Gentamicin protection assay measuring uptake of *Lm* by iBMMs in the presence of 1 μM INK1117, 10 μM TGX221, 10 μM IC87114, or 50 nM IPI549. Legend indicates the isoform of PI3K that each inhibitor targets. Data are normalized to DMSO-treated controls. All data are means and SEM of at least three biological replicates. $^{**}p<0.01$, $^{***}p<0.001$, as determined by unpaired *t* tests.

Class 1A PI3Ks are canonically activated by phosphorylated tyrosine residues on receptor tyrosine kinases and other cell surface receptors[126]. Additionally, Class 1A PI3Ks are activated downstream of toll-like receptors (TLRs) in response to bacterial infection[127,128]. Given that *Lm* is known to activate TLR2 and TLR5 on the surface of macrophages[129,130], we hypothesized that *Lm*-induced PI3K activation in macrophages is mediated by TLRs. To test this hypothesis, we measured uptake of *Lm* and PI3K activation in *Tlr2*$^{-/-}$ macrophages. For these studies, BMDMs from *Tlr2*$^{-/-}$ mice were isolated and absence of TLR2 was confirmed by immunoblot analysis (Figure 17A). Interestingly, uptake of *Lm* was unchanged in *Tlr2*$^{-/-}$ BMDMs compared to WT BMDMs (Figure 17B). While we did not directly test *Tlr5*$^{-/-}$ macrophages, studies from our lab have found that *Lm* lacking the TLR5 ligand *flaA* are taken up by macrophages with equal efficiency as wildtype *Lm*[131]. To account for the possibility of redundancy between TLR2 and TLR5, we infected WT and *Tlr2*$^{-/-}$ BMDMs with Δ*flaA* and found that uptake remained unchanged in the absence of TLR2 and TLR5 recognition (Figure 17C). These results indicate that phagocytosis of *Lm* is TLR-independent.

To test the role of TLRs in mediating PI3K/PTEN signaling in macrophages during *Lm* infection, we pre-treated WT and *Tlr2*$^{-/-}$ BMDMs with PI3K and PTEN inhibitors prior to infection with Δ*flaA.* Wortmannin and bpV(pic) inhibited uptake of Δ*flaA* to a similar extent in both WT and *Tlr2*$^{-/-}$ BMDMs (Figure 17D), suggesting that PI3K signaling is intact in the absence of TLR stimulation. To test this, we monitored Akt phosphorylation in WT and *Tlr2*$^{-/-}$ BMDMs infected with wildtype *Lm* and Δ*flaA* and observed Akt phosphorylation over background in the absence of TLR2 and TLR5 recognition (Figure 17E). Together, these data demonstrate that *Lm*-induced PI3K activation in macrophages occurs independently of TLR2 and TLR5. Given that specific *Lm* strains are phagocytosed using a distinct PTEN-dependent pathway compared to other *Lm* strains or *L. innocua*, we tested whether PTEN-independent uptake of the latter was mediated by TLRs. To that end, we compared uptake of *Lm* 10403S, *Lm* Li2, and *L. innocua* in WT and *Tlr2*$^{-/-}$ BMDMs and found that uptake of all three bacterial strains was TLR2-independent (Figure 17F). While we did not directly test a role for TLR5 in PTEN-independent uptake, *Lm* Li2 and *L. innocua* do not produce flagella at 37ºC[132,133], strongly suggesting that these strains do not engage TLR5 in our assays. Overall, our data show that uptake of *Listeria* species in murine macrophages is TLR-independent.

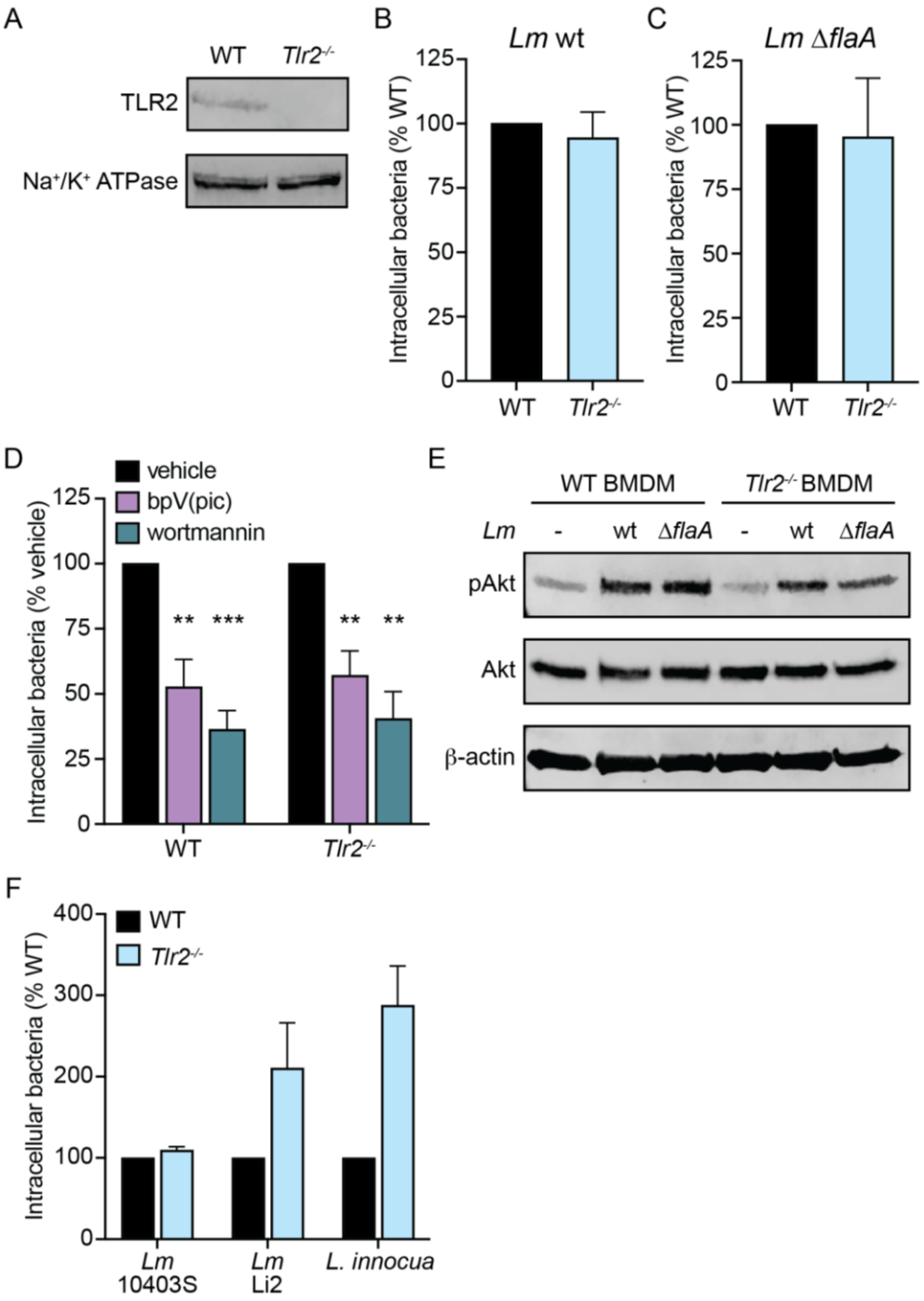

Figure 17. Uptake of *Listeria* by BMDMs is TLR-independent. (A) Immunoblot analysis of TLR2 in WT and *Tlr2*$^{-/-}$ BMDMs. Na^+/K^+ ATPase was used as a loading control for membrane proteins. (B) Gentamicin protection assay measuring uptake of wildtype (wt) *Lm* by WT and *Tlr2*$^{-/-}$ BMDMs. Cells were infected at MOI=1 for 30 minutes and CFU were quantified 1 hour post-infection. Data are normalized to WT BMDMs. (C) Gentamicin protection assay measuring uptake of *Lm* Δ*flaA* by WT and *Tlr2*$^{-/-}$ BMDMs. Data are normalized to WT BMDMs. (D) Gentamicin protection assay measuring uptake of *Lm* Δ*flaA* by WT and *Tlr2*$^{-/-}$ BMDMs in the presence of 5 μM bpV(pic) or 100 nM wortmannin. Data are normalized to vehicle-treated

cells. (E) Immunoblot of phosphorylated Akt (Ser473) in WT and *Tlr2*$^{-/-}$ BMDMs mock-infected or infected with *Lm* wt or Δ*flaA* strains. BMDMs were infected with MOI=100 and lysed 15 minutes post-infection. Total Akt and β-actin were used as loading controls. (F) Gentamicin protection assay measuring uptake of *Lm* 10403S, *Lm* Li2, or *L. innocua* by WT and *Tlr2*$^{-/-}$ BMDMs. Data are normalized to WT BMDMs for each strain. All data are means and SEM of at least three biological replicates except (F) which consists of two biological replicates. ***p*<0.01, ****p*<0.001, as determined by unpaired *t* tests.

Myeloid PTEN promotes bacterial restriction during murine foodborne listeriosis

To investigate the role of PTEN-dependent phagocytosis of *Lm in vivo*, we generated myeloid-specific conditional *Pten* knockout mice. C57BL/6 mice expressing Cre recombinase from the myeloid-specific *Lyz2* promoter (*LysM*-Cre$^{+/+}$) were crossed with C57BL/6 mice containing *loxP* sites flanking exon 5 of *Pten* (*Pten*$^{fl/fl}$) to produce *LysM*-Cre$^{+/+}$ *Pten*$^{fl/fl}$ myeloid knockout mice (PTEN$^{M\text{-}KO}$). *LysM*-Cre$^{+/+}$ *Pten*$^{wt/wt}$ mice which express Cre but do not contain *Pten loxP* sites (PTEN$^{M\text{-}WT}$) were included as controls. We used a foodborne model of listeriosis to ensure passage through the intestinal lamina propria where *Lm* is engulfed by resident macrophages, which are hypothesized to promote dissemination of *Lm* to peripheral organs[71,78]. 8-10 week old PTEN$^{M\text{-}WT}$ and PTEN$^{M\text{-}KO}$ sex- and age-matched mice were given streptomycin in their drinking water for 48 hours and fasted for 16 hours prior to infection to increase susceptibility to oral infection[10,134]. Mice were then fed 10^8 *Lm* in PBS and body weight was recorded over the course of 5 days as an overall measurement of disease severity. To assess bacterial burdens throughout the infection, mice were euthanized at 1, 3, and 5 days post-infection (dpi) and CFU were enumerated from organs. In addition, ilea and colons were fractionated to separate the mucus layer, epithelial cells, and lamina propria compartments and CFU were enumerated from each fraction.

At 1 dpi, we observed significantly increased bacterial burdens in the epithelial cells and lamina propria of the ileum in PTEN$^{M\text{-}KO}$ mice compared to PTEN$^{M\text{-}WT}$ mice (Figure 18A). There was no difference in CFU in the ileum mucus layer (Figure 18A), suggesting that higher bacterial burdens in the epithelial cells and lamina propria were not due to overall increased colonization of the ileal lumen. In contrast to the lamina propria, there were no differences in CFU between PTEN$^{M\text{-}WT}$ and PTEN$^{M\text{-}KO}$ mice in the mesenteric lymph nodes (MLN), spleen, or liver 1 dpi (Figure 19D-F), indicating that myeloid PTEN is dispensable for initial dissemination of *Lm* to peripheral organs. We also observed no difference in CFU in the feces or cecum between PTEN$^{M\text{-}WT}$ and PTEN$^{M\text{-}KO}$ mice throughout the experiment (Figure 19B-C), demonstrating that PTEN does not affect colonization of the GI tract or fecal shedding. Together, these data show that myeloid expression of PTEN restricts *Lm* replication in the epithelial cells and lamina propria of the ileum early during infection, however increased bacterial burdens in these compartments does not affect dissemination.

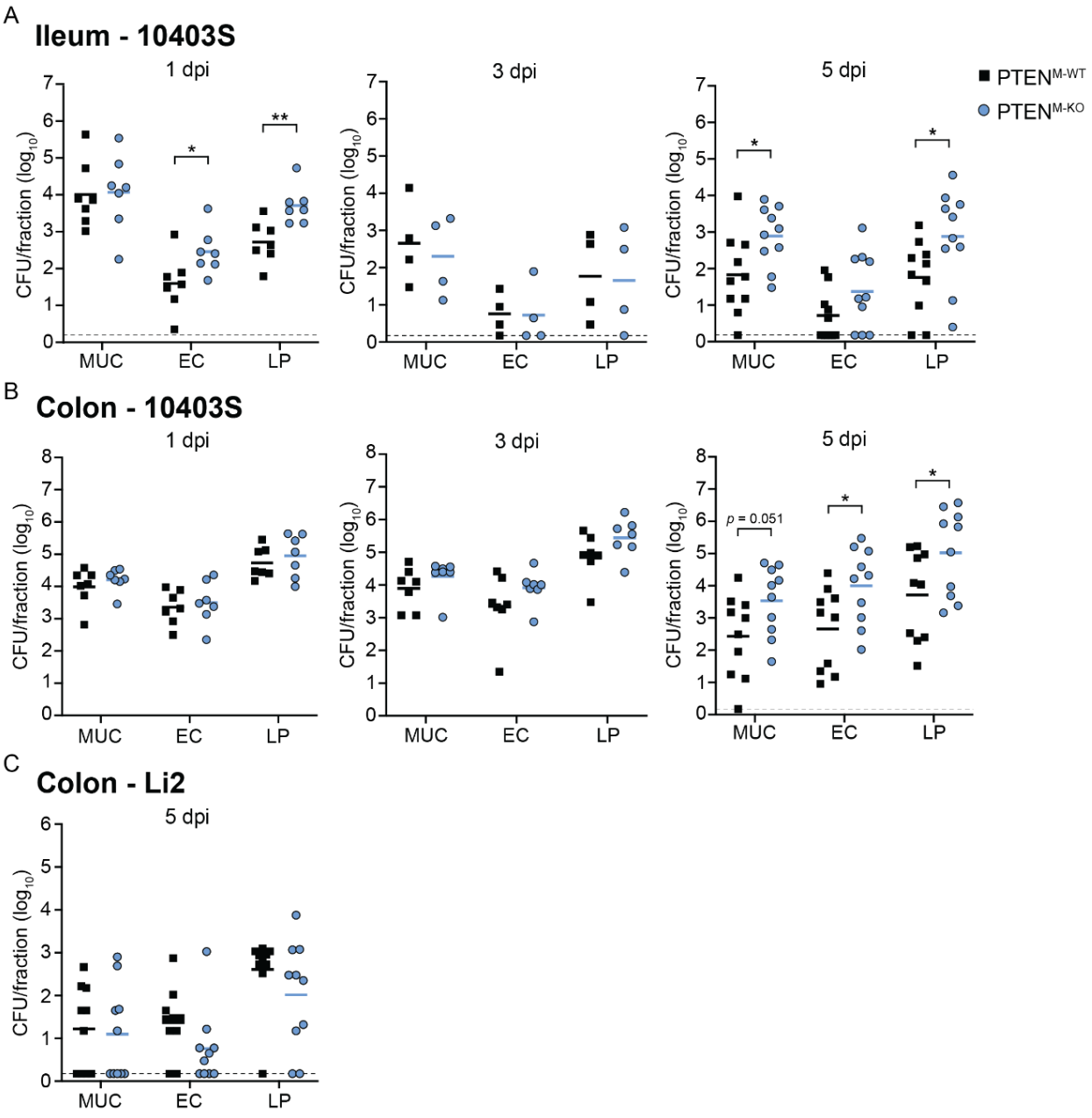

Figure 18. Myeloid PTEN restricts bacterial replication in the intestinal lamina propria. Mice were orally infected with 10^8 *Lm* 10403S or 5 x 10^8 *Lm* Li2. Intestinal fractions were isolated from ilea or colons 1, 3, or 5 dpi (MUC = mucus layer, EC = epithelial cells, LP = lamina propria). (A) Ileal fractions and (B) colon fractions from 10403S-infected mice. (C) Colon fractions from Li2-infected mice 5 dpi. Each data point represents a single mouse. Data are combined from two independent experiments per timepoint. Solid lines indicate geometric means. Dashed lines indicate the limit of detection (l.o.d.). *p<0.05, **p<0.01 as determined by unpaired t tests of natural log-transformed values.

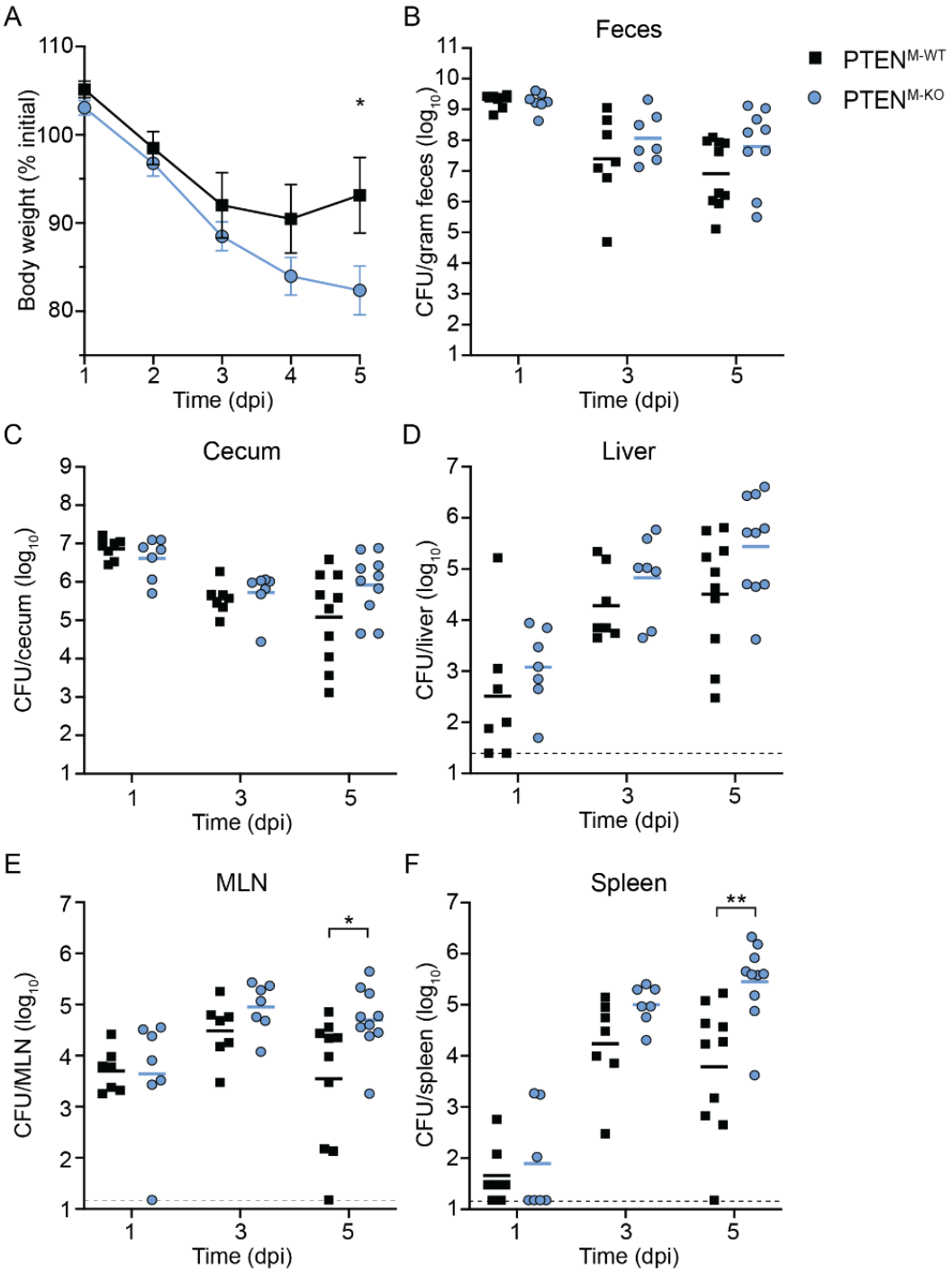

Figure 19. Myeloid PTEN promotes bacterial clearance during murine foodborne listeriosis. (A) Body weights of infected mice over time, reported as the percent of initial weight before streptomycin treatment. Data are means and SEM of n = 10 mice at each timepoint. (B-F) Mice were orally infected with 10^8 *Lm* 10403S and CFU from tissues were enumerated at 1, 3, and 5 dpi. Each data point represents a single mouse. Data for each time point represents two independent experiments. Solid lines indicate geometric means. Dashed lines represent the l.o.d. *p<0.05, **p<0.01 as determined by unpaired t tests of untransformed (A) or natural log-transformed (B-F) values.

There were no differences in weight loss or bacterial burdens in any organs tested at 3 dpi (Figures 18A-B and 19A-F). By 5 dpi, however, PTEN$^{M\text{-}WT}$ mice lost ~7% of their initial body weight while PTEN$^{M\text{-}KO}$ mice lost nearly 18% of their initial weight (Figure 19A), indicating that PTEN$^{M\text{-}KO}$ mice experienced more severe disease during the later stages of infection. Consistent with increased weight loss, PTEN$^{M\text{-}KO}$ mice displayed significantly increased bacterial burdens in the MLN (~1-log) and spleen (~2-logs) compared to PTEN$^{M\text{-}WT}$ mice at 5 dpi (Figure 19E-F). While not statistically significant, CFU were also elevated in the livers of PTEN$^{M\text{-}KO}$ mice compared to PTEN$^{M\text{-}WT}$ mice at 5 dpi (~1 log; $p = 0.07$) (Figure 19D). In addition, the lamina propria of both the ileum and colon as well as the ileal mucus layer and colonic epithelium of PTEN$^{M\text{-}KO}$ mice also contained higher *Lm* burdens compared to PTEN$^{M\text{-}WT}$ mice at 5 dpi (Figure 18A-B), suggesting that PTEN$^{M\text{-}KO}$ mice contained higher bacterial burdens overall in these organs. Taken together, these data demonstrate that myeloid PTEN limits disease severity and restricts *Lm* growth during later stages of foodborne listeriosis.

To specifically assess the contribution of PTEN-regulated phagocytosis to controlling *Lm* infection, we infected mice with the *Lm* strain Li2, which is phagocytosed using a PTEN-independent mechanism (Figure 14G). We reasoned that any global effects of myeloid PTEN loss would impact both strains equally, while phagocytosis-specific phenotypes would not affect *Lm* Li2 infection. In contrast to mice infected with *Lm* 10403S, there were no significant differences in CFU in the MLN, spleen, or colon fractions between PTEN$^{M\text{-}WT}$ and PTEN$^{M\text{-}KO}$ mice infected with *Lm* Li2 at 5 dpi (Figures 18C and 20D-E). These data indicate that restriction of *Lm* 10403S by myeloid PTEN in these organs is largely driven by PTEN-dependent phagocytosis. However, we observed increased bacterial burdens in livers of PTEN$^{M\text{-}KO}$ mice infected with *Lm* Li2 (Figure 20C), suggesting that PTEN limits CFU in this organ independently of its regulation of phagocytosis.

To determine whether passage through the gastrointestinal tract is necessary for restriction of *Lm* by myeloid PTEN in peripheral organs, we evaluated the role of myeloid PTEN during i.v. infection. At 2 dpi, PTEN$^{M\text{-}KO}$ mice infected through the i.v. route exhibited increased bacterial burdens in the spleen, but not the liver, compared to PTEN$^{M\text{-}WT}$ mice (Figure 20F-G). These data suggest that control of *Lm* by myeloid PTEN in the spleen is independent of dissemination from the gastrointestinal tract, and provide further evidence that PTEN-dependent phagocytosis contributes to anti-*Lm* immunity during the systemic phase of infection.

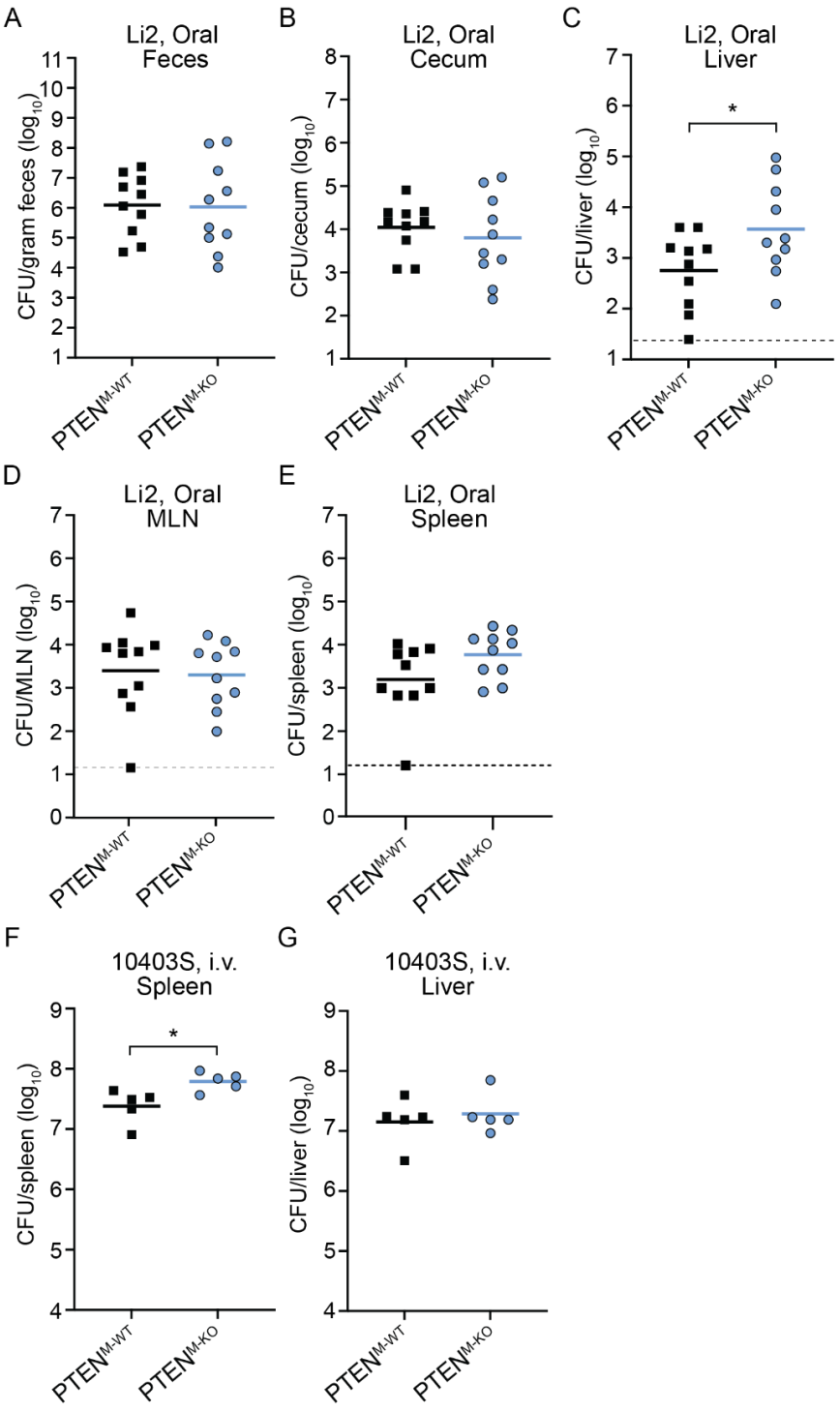

Figure 20. Restriction of *Lm* by myeloid PTEN is driven by PTEN-dependent phagocytosis. (A-E) Mice were orally infected with $5x10^8$ *Lm* Li2 and CFU from tissues were enumerated at 5 dpi. Each data point represents a single mouse from two independent experiments. Solid lines indicate geometric means. Dashed lines represent the l.o.d. (F-G) Mice were infected intravenously with 1.5×10^5 *Lm* 10403S via retro-orbital injection and CFU from tissues were enumerated at 2 dpi. Each data point represents a single mouse. Solid lines indicate geometric means. *$p<0.05$ as determined by unpaired *t* tests of natural log-transformed values.

Discussion

Host determinants of non-opsonic phagocytosis of *Lm* have not previously been studied. Here, we found that PTEN promoted phagocytosis of *Lm* by enhancing adherence of the bacteria to macrophages. Both PIP_3 production by the type 1A PI3K p110β and the lipid phosphatase activity of PTEN are required for phagocytosis, strongly suggesting that PIP_3 turnover is important for enhancement of *Lm* uptake. The role of PTEN-dependent phagocytosis *in vivo* was assessed using an oral *Lm* infection of myeloid conditional knockout mice. Myeloid PTEN limits bacterial burdens in the lamina propria early during infection, however this does not impact initial dissemination to internal organs. During later stages of infection, myeloid PTEN promotes bacterial restriction in several organs and protects against severe disease. Taken together, our results indicate a novel role for PTEN in regulating phagocytosis of *Lm* and begin to characterize the contributions of opsonin-independent phagocytosis *in vivo*.

Our results demonstrate that PTEN promotes phagocytosis of *Lm* specifically by macrophages. These data are surprising and intriguing for a few reasons. First, it is well-documented that class I PI3Ks are required for the phagocytic activity of macrophages due to PIP_3 regulation of actin polymerization at the phagocytic cup[135]. Consistent with this, we and others have found that phagocytosis of several bacterial species is dependent on PI3K activation[113–116], suggesting that PI3K activation and PIP_3 production are common features of bacterial recognition by macrophages. PTEN has thus been characterized as a repressor of phagocytosis due to PIP_3 dephosphorylation and antagonism of PI3K signaling[118–121]. To our knowledge, this is the first report that PTEN can promote phagocytosis of bacteria by macrophages. In addition, PTEN appears to play opposing roles in regulating uptake of *Lm* by phagocytes and non-phagocytes. PI3K activation is also required for internalin-mediated uptake of *Lm* into non-phagocytic cells[46], suggesting that PTEN would act as a repressor of this process. Indeed, we found that inhibition of PTEN increased uptake of *Lm* by hepatocytes and intestinal epithelial cells. Our finding that PTEN promotes phagocytosis of *Lm* by enhancing adherence to macrophages provides a possible explanation for these cell type differences, whereby PTEN regulates macrophage-specific *Lm* adherence factors. Overall, our results support a model in which PI3K activation and PIP_3 production are broadly required for internalization of bacteria, including *Lm*, and PTEN functions distinctly to promote adherence of *Lm* to macrophages.

The factors mediating adherence of *Lm* to macrophages are not well understood. We hypothesize that PTEN affects adherence to human and murine macrophages by increasing availability of one or more surface receptors which bind *Lm*. Elevated baseline PIP_3 levels in *Pten*$^{-/-}$ cells may serve in a signaling capacity to regulate expression of *Lm*-specific receptors or altered membrane dynamics may affect surface presentation of adherence factors. Alternatively, turnover of PIP_3 by PTEN may be important for regeneration of $PI(4,5)P_2$, which is capable of acting in a signaling capacity to regulate membrane dynamics[136,137]. Our data indicate that TLRs do not serve as primary phagocytic receptors for *Lm*, as phagocytosis of *Lm* and *L. innocua* were TLR-independent. We demonstrated that the class 1A PI3K p110β was specifically required for phagocytosis of *Lm*, and p110β is canonically activated by receptor tyrosine kinases (RTKs)[126], suggesting that phagocytosis of *Lm* may involve one or more RTKs. Very few macrophage receptors have been previously implicated in phagocytosis of non-opsonized *Lm*. Fcγ-receptor 1A (FcγR1a or CD64) mediates antibody-independent uptake of *Lm* specifically by human

macrophages, although murine FcγR1a was not involved in internalization of *Lm*[68]. The macrophage scavenger receptor SR-A I/II (*Msr1*) reportedly promotes phagocytosis of *Lm* by peritoneal macrophages and Kupffer cells during i.v. infection of mice, however internalization via this pathway is listericidal[69]. The identity of *Lm*-specific receptor(s) which activate PI3K and lead to cytosolic *Lm* replication in both human and mouse macrophages remains to be determined.

The finding that different strains of *Lm* undergo distinct mechanisms of uptake is intriguing and indicates that both host and bacterial factors regulate phagocytosis of *Lm*. Interestingly, the strains of *Lm* internalized via PTEN-dependent phagocytosis belong to serovar 1/2, while strains whose uptake is PTEN-independent belong to serovar 4 (Table 4). The 16 serovars of *Lm* are differentiated by the chemical composition of the cell wall-associated teichoic acids[138]. Thus, while this is not an exhaustive characterization of *Lm* serovars, our data suggest that differences in bacterial surface molecules dictate whether *Lm* is phagocytosed primarily via a PTEN-dependent or -independent mechanism, likely through recognition by distinct receptors. *Lm* serovar is associated with disease severity, with the majority of human listeriosis cases caused by serovar 4b strains[139]. Recently, specific modifications of wall teichoic acids on serovar 4b strains were found to be important for pathogenesis by promoting invasion of non-phagocytic cells[140]. Given that PTEN-dependent phagocytosis is a host defense against listeriosis, as discussed below, it is possible that avoidance of phagocytosis through this pathway by serovar 4b strains may contribute to their virulence.

To dissect the role of PTEN-dependent phagocytosis *in vivo*, we infected myeloid PTEN conditional knockout mice ($PTEN^{M\text{-}KO}$) via the oral inoculation route. This approach gave us a unique opportunity to study the contribution of macrophage phagocytosis to *Lm* disease progression during foodborne listeriosis. In the absence of myeloid PTEN, bacterial burdens were elevated in the ileal lamina propria early during infection. These results were surprising, as macrophages are thought to be the main growth-permissive cell type in the lamina propria, leading us to predict reduced bacterial burdens in $PTEN^{M\text{-}KO}$ mice as a result of reduced uptake into macrophages. It was recently demonstrated that infection of specific macrophage subsets in the lamina propria is important for early production of IFNγ and promotes bacterial restriction in this compartment[141]. It is therefore possible that reduced macrophage phagocytosis in $PTEN^{M\text{-}KO}$ mice blunts local immune responses that normally restrict replication of *Lm* in the lamina propria. Nonetheless, the localization of *Lm* in the lamina propria of $PTEN^{M\text{-}KO}$ mice is currently unknown. The majority of bacteria in the lamina propria are extracellular following oral infection[78], suggesting that *Lm* may be able to more efficiently replicate in the extracellular space in the absence of macrophage phagocytosis. Alternatively, lymphocytes support intracellular growth of *Lm in vivo*[142], and may serve as a replicative niche in the lamina propria of $PTEN^{M\text{-}KO}$ mice. *Lm* does not replicate in dendritic cells or monocytes in the gut[62,63], so these populations are unlikely to serve as a replication niche. While the exact cell types responsible for promoting *Lm* growth and dissemination from the lamina propria are not well understood, our data suggest that macrophages play a primarily protective role in the gut.

Overall, our *in vivo* studies demonstrate that macrophage phagocytosis is not important for dissemination but is required for growth restriction and clearance of *Lm* during foodborne listeriosis. Mice lacking myeloid PTEN had higher bacterial burdens in the ilea, colons, MLNs, and spleens during later stages of infection. Importantly, these differences were not observed during oral infection of the *Lm* serovar 4b strain Li2, indicating that this phenotype is driven by PTEN-

regulated phagocytosis rather than global effects of myeloid PTEN loss. In addition, increased bacterial burdens in the spleens of PTEN$^{M\text{-}KO}$ mice after i.v. infection further demonstrate that macrophage phagocytosis is not required for dissemination from the GI tract but control of *Lm* during later stages of infection. These data are consistent with the demonstrated role of macrophages in host protection during *Lm* infection, in which IFNγ-primed macrophages are critical[86,87,141]. We hypothesize that IFNγ-activated macrophages lacking PTEN are unable to efficiently phagocytose and clear *Lm*, leading to increased bacterial burdens in PTEN$^{M\text{-}KO}$ mice. Alternatively, reduced uptake by macrophages early during infection may dampen cytokine production by these cells, which are important for establishing a robust immune response.

Restriction of *Lm* infection by PTEN in the liver appears to be distinct from other organs. Myeloid PTEN restricts *Lm* growth in the liver independently of PTEN-regulated phagocytosis, as the serovar 4b strain Li2 replicated to higher numbers in the livers of PTEN$^{M\text{-}KO}$ mice. Control of *Lm* in the liver involves uptake and killing by Kupffer cells through scavenger receptors[143], which may not be a PTEN-regulated pathway. Less is known about the role of macrophages in the hepatic response to *Lm* during foodborne infection, and our oral infection data suggests that myeloid cells are important for clearance of *Lm* in the liver in a PTEN-dependent manner.

Taken together, the data presented in this chapter characterize PTEN as a novel host factor required for proper phagocytosis of *Lm* by macrophages. In contrast to the current understanding of bacterial phagocytosis as a process driven by recognition of conserved PAMPs[144,145], our work demonstrates that highly related bacteria are internalized via functionally distinct mechanisms, even down to the strain level. Finally, we have defined a role for macrophages as an important host defense during foodborne listeriosis and provide the first evidence that non-opsonic phagocytosis contributes to *Lm* pathogenesis. Although few studies have investigated the immune response to *Lm* during oral infection[146], development of foodborne infection models of murine listeriosis has paved the way for studying interactions between *Lm* and immune cells in a physiologically relevant system[147]. Our infection studies have contributed to this body of work by demonstrating the protective role of macrophages during oral infection and providing a unique murine model to study macrophage phagocytosis of *Lm in vivo*.

Chapter 5: Future directions

Introduction

In this thesis, components of the host cell which influence the *Lm* intracellular lifecycle were investigated. Using cell-free extracts, I found that one or more proteins present in eukaryotic cytosol are required for *actA* expression. While these proteins remain unknown, I developed biochemical and genetic systems using cell-free extracts and CRISPR/Cas9 screening to identify proteins involved in regulation of *actA*. In addition, I applied CRISPR screening to investigate another unexplored area of *Lm* research and identified macrophage genes required for phagocytosis of *Lm*. These studies characterized the function of PTEN in promoting *Lm* uptake by macrophages and revealed a role for non-opsonic phagocytosis in host protection during foodborne listeriosis. There is still much work to be done to fully understand these processes and this thesis has opened up exciting new areas of investigation in *Lm*-host interactions.

The cytosolic signal that activates PrfA remains unknown

It has long been hypothesized that a host-derived signal present in the cytosol of eukaryotic cells acts as a signal to *Lm* to induce expression of virulence genes via PrfA. Transcription of *actA* is nearly undetectable during broth growth and is induced over 200-fold during intracellular infection[31]. Concerted efforts to study the environmental cues which mediate this transition have identified a number of biomolecules which influence PrfA activation during growth in broth[32–34,98,148]. However, all of these studies were limited in that they did not recapitulate their results in a native cytosolic environment. In Chapters 2 and 3, I developed biochemical and genetic systems to identify PrfA-activating molecules in more biologically relevant systems. Experiments in Chapter 2 revealed that none of the previously identified external signals were sufficient to induce *actA* transcription in cell-free extracts. While the identity of host-derived PrfA-activating signals remains unknown, I propose that *Xenopus* cell-free extracts and CRISPR/Cas9 screening are ideal systems to address this problem.

Biochemical and genetic systems each have their limitations; however, using both approaches simultaneously may help overcome these limitations to narrow down the identities of PrfA-activating factors. One major limitation of the CRISPR/Cas9 screening approach is that essential genes will not be represented in the macrophage knockout library. Considering that the ability of the host cytosol to activate PrfA is conserved between insects, frogs, and mammals, it is certainly possible that required components of this signal are essential and therefore, CRISPR-mediated gene deletion would not be feasible. If this is the case, then fractionation of *Xenopus* extracts would overcome this limitation as this technique can identify essential proteins. However, the success of chromatography separation to identify these unknown proteins relies in being able to isolate low-complexity fractions. Our attempts thus far have resulted in fractions containing a large number of different proteins, making it difficult to identify any one particular protein involved in the PrfA activation phenotype. Overall, our current methods for both fractionation of cell-free extracts and CRISPR screening have resulted in a high number of false positive results.

Improvements and optimization of both of these techniques could be made to reduce the number of candidate genes or proteins identified. For fractionation of *Xenopus* extracts, we only used anion-exchange chromatography to isolate active protein fractions. Application of other chromatography techniques may help to decrease the complexity of active fractions. If interaction of more than one component of the extracts is required for activating PrfA, then it may not be possible to generate a low-complexity fraction that retains activity. However, even isolation of additional high-complexity fractions would be beneficial. The protein content of active fractions isolated using different chromatographical methods are likely to be different from one another, and identification of proteins common amongst all active fractions would significantly reduce the number of candidate proteins. For the CRISPR/Cas9 screen, a sub-pool screen using a custom sgRNA library would determine if any of the 197 candidate genes identified in the original screen have any impact on PrfA activation. This would be a much smaller library than the genome-wide Brie library which would significantly reduce the time and cost to perform these additional screens. Finally, candidate genes identified by CRISPR screening whose gene products are also identified by cell-free extract fractionation are compelling candidates to test. In our initial rounds of screening, peptidylprolyl isomerase B (Ppib) was identified by both extract fractionation and CRISPR screening and is therefore a strong candidate for follow up studies.

Working towards a complete picture of *Lm* phagocytosis

Lm is phagocytosed more efficiently by macrophages than highly related species, suggesting distinct mechanisms of uptake. The genome-wide CRISPR screen performed in Chapter 3 identified 235 macrophage genes important for mediating phagocytosis of *Lm*. While we extensively characterized the role of PTEN in promoting phagocytosis of *Lm*, the involvement of the other 234 genes remains to be investigated. Many of these genes belonged to general transcriptional complexes or chromatin remodeling complexes, and we found that host cell transcription is involved in an uptake pathway specific to *Lm*. Elucidating the mechanism by which transcription promotes phagocytosis of *Lm* is an intriguing area of future study.

While transcription as a whole is a diverse and complex process, performing additional experiments on the nature of this interaction will help narrow down what aspect of transcription may be involved. First, using fluorescence microscopy to determine the dynamics by which transcription inhibition blocks uptake of *Lm*, as well as its role in adhesion versus internalization, would reveal the stage of phagocytosis that requires transcription. If transcription is required at a later timepoint, then expression of a specific gene or set of genes in response to initial *Lm* binding may signal to increase the internalization rate. Transcription being involved during the initial stages of uptake would suggest that transcription of a *Lm*-specific adhesion factor prior to infection is required. Second, determining the specific transcriptional complexes involved may shed light on the transcripts that are important for *Lm* uptake. Actinomycin D is non-specific and blocks expression of all transcripts by intercalating DNA. Using more specific chemical inhibitors or targeting individual transcription factors using CRISPR/Cas9 could be paired with RNA-seq to identify specific transcripts involved. Finally, we found in Chapter 4 that the pathway mediating enhanced phagocytosis of *Lm* by macrophages is PTEN-dependent. Determining whether transcription promotes *Lm* uptake through the same pathway as PTEN or a distinct mechanism

would either provide additional characterization of the PTEN-dependent phagocytosis pathway or reveal that uptake of *Lm* into macrophages is mediated through multiple distinct pathways.

Beyond transcription, our screen identified many other genes involved in various biological processes. These include several hubs of major signaling axes, including NF-κB (p65), p53, GSK3, and mTORC1. Interestingly, all of these proteins lie downstream of PI3K/PTEN signaling[149], suggesting that they may be promoting phagocytosis of *Lm* through the same pathway. However, we found that inhibition of NF-κB also blocked uptake of *L. innocua* and *B. subtilis*, suggesting that NF-κB regulates phagocytosis independently of PTEN. Similarly to the role of transcription, investigating whether these signaling components participate in PTEN-dependent or -independent phagocytosis is an important future direction of this work. Overall, our CRISPR screen to identify host factors required for phagocytosis of *Lm* has identified many genes not previously implicated in *Lm* pathogenesis, and additional studies on these genes have the potential to open up new lines of investigation.

Elucidating mechanisms of PTEN-dependent phagocytosis

In Chapter 4, we characterized the role of PTEN in promoting phagocytosis of *Lm* by macrophages. While we began to dissect the PTEN-dependent signaling pathway involved in phagocytosis, much work remains to elucidate the mechanism by which PTEN promotes *Lm* uptake. We found that dephosphorylation of PIP_3 by PTEN is important for phagocytosis by promoting adherence of *Lm* to macrophages. This suggests that PTEN regulates the expression or availability of adhesion factors on the macrophage surface. Signaling downstream of PIP_3 ultimately leads to changes in gene expression, therefore PTEN could regulate expression of *Lm*-specific receptors at the transcriptional level. Altered phosphoinositide composition of the cell membrane could also affect trafficking and surface presentation of receptors. Paradoxically, production of PIP_3 by PI3K was also found to be required for phagocytosis. This points to the possibility that it is not depletion of PIP_3 that is important for phagocytosis, but rather regeneration of PIP_2, which also acts as a second messenger in a variety of signaling pathways[136,137]. Determining the relative roles of PIP_2 and PIP_3 is a critical next step in characterizing the PTEN-dependent signaling involved in phagocytosis of *Lm*. These phosphoinositides can be exogenously added to cells and inserted into the membrane using a carrier system to study their effects on phagocytosis[150]. PIP_2 and PIP_3 levels can also be altered using genetics. The phosphatase SHIP1 also dephosphorylates PIP_3 but converts it to a different form of PIP_2, $PI(3,4)P_2$[151]. Overexpressing SHIP1 in *Pten*$^{-/-}$ iBMMs would reveal whether regeneration of the $PI(4,5)P_2$ form of PIP_2 is important for phagocytosis or if depletion of PIP_3 is sufficient.

PTEN regulates *Lm*-specific adherence factors, however surface components important in binding and internalizing *Lm* are currently unknown. Identification of one or more receptors which initiates uptake through the PTEN-dependent pathway is an important future direction of this work. Our findings that *Lm* activates type 1A PI3K upon infection of macrophages suggest that *Lm* engages an RTK to initiate intracellular signaling. A previous report found that *Lm*-induced Akt phosphorylation in macrophages is TLR2-dependent, although TLR2 did not mediate adherence of *Lm* to macrophages[70]. However, we found no role for TLR2 in uptake or PI3K activation. Importantly, the previous study used a strain of *Lm* with a constitutively active PrfA variant, which may impact the interpretation of their data. Scavenger receptors have been

reported to impact phagocytosis of *Lm*[69,152], therefore it is important to test whether these receptors are responsible for activating PI3K and mediating PTEN-dependent phagocytosis. In addition, several pathogens are internalized by macrophages through C-type lectin receptors, which recognize glycosylation patterns on bacterial surfaces[153–155]. As discussed below, we found that phagocytosis of *Lm* differed based on serovar, which is designated by distinct sugar residues on wall teichoic acids[138]. The possibility that PTEN-dependent phagocytosis of *Lm* is mediated by C-type lectins should be investigated. Finally, unbiased approaches could be used to identify macrophage receptors involved in phagocytosis of *Lm*. Our CRISPR screen identified genes encoding plasma membrane proteins, including *Pcdhga8*, *Dscaml1*, *Ly6g5c*, *Atp2b1*, *Cysltr1*, *Cd3e*, *Sigirr*, and multiple uncharacterized GPCRs. Although none of these proteins are RTKs, the potential of these proteins to act as receptors for *Lm* in macrophages is worthy of investigation. Proximity-based biochemical screens have successfully identified cell surface receptors for other bacteria[156] and could be applied to *Lm* for identification of macrophage receptors.

Characterization of macrophage receptors which bind *Lm* will inform on the cognate bacterial ligands, and vice versa. We found that the cell surface of *Lm* is responsible for mediating PTEN-dependent uptake, and that this is dependent on *Lm* serovar. Serovar 1/2 strains are unique in that their WTA is decorated with rhamnose residues, while serovar 4b and 4e strains have exposed glucose residues[138]. Manipulation of the glycosylation pattern of *Lm* WTA by genetic deletion of enzymes involved in sugar decoration would determine whether WTA modifications are important in mediating PTEN-dependent uptake. Testing whether additional *Lm* serovars are taken up through PTEN-dependent or -independent mechanisms would also inform on specific WTA modifications involved in phagocytosis. It is possible that other cell surface components outside of WTA are responsible for strain-dependent differences in phagocytosis. Comparative analysis of genomes between strains and species which undergo PTEN-dependent or -independent phagocytosis may reveal bacterial genes which participate in PTEN-dependent uptake pathways. Preliminary analysis between *Lm* strains 10403S, EGD-e, HER1247, and Li2 revealed 85 genes present in all serovar 1/2 strains and absent in serovar 4b Li2, including 5 members of the internalin gene family (*lmo0409*, *lmo2026*, *lmo2027*, *lmo0171*, and *lmo0801*). Further genomic analysis of additional strains would narrow down this list and present candidate genes for phenotypic studies. Global genetic approaches, such as transposon sequencing (Tn-Seq) screening, would also be effective methods for identification of *Lm* surface factors involved in phagocytosis.

Understanding the role of macrophage phagocytosis *in vivo*

Generation of myeloid conditional *Pten* knockout mice presented a unique opportunity to study the role of non-opsonic phagocytosis to *Lm* pathogenesis *in vivo*. In addition, the contribution of macrophages to dissemination of *Lm* versus host protection were investigated in the context of the natural foodborne route of infection for the first time. We found that non-opsonic phagocytosis of *Lm* played a protective role during foodborne listeriosis as $PTEN^{M\text{-}KO}$ had higher bacterial burdens overall. Interestingly, this was even the case in the intestinal lamina propria, a compartment previously thought to contain macrophages which are important for supporting replication of *Lm*. Further characterization of *Lm* survival and persistence in the lamina propria is an intriguing area of future study. In particular, determining the cell types which harbor intracellular

Lm in the lamina propria and whether or not they support replication of *Lm* may reveal *Lm*-host interactions important for dissemination beyond the GI tract. Additionally, it is possible that *Lm* replicates efficiently in the extracellular space of the lamina propria. It is increasingly becoming appreciated that extracellular growth of *Lm* in various organs is an important aspect of *Lm* pathogenesis[79,157], and may also contribute to dissemination from the lamina propria.

A major unanswered question from our *in vivo* studies is how PTEN-dependent phagocytosis contributes to anti-*Lm* immunity. Given the strong evidence in the literature for IFNγ-activated macrophages being critical for clearance of *Lm*[86,88,158], we hypothesize that these inflammatory phagocytes exhibit deficient uptake and killing of *Lm* in $PTEN^{M\text{-}KO}$ mice during foodborne infection. To directly test this model, depletion of IFNγ by administration of IFNγ-specific antibodies should increase bacterial burdens in $PTEN^{M\text{-}WT}$ mice but have a minimal effect in $PTEN^{M\text{-}KO}$ mice. Additionally, it is likely that reduced phagocytosis early during infection alters the inflammatory response in a way that affects clearance later on. Analysis of pro-inflammatory cytokine production and immune cell recruitment and differentiation in $PTEN^{M\text{-}KO}$ mice would provide insight into additional mechanisms by which phagocytosis of *Lm* contributes to immunity. Very little investigation of the immune response to *Lm* has been done using oral infection models; the experiments proposed here would not only contribute to our understanding of PTEN-dependent phagocytosis, but also provide valuable characterization of immunological dynamics during foodborne listeriosis.

Final remarks

Overall, the work presented in this thesis has shed light on mechanisms by which *Lm* senses and adapts to the host cell environment, as well as how host cells, particularly macrophages, influence the outcome of infection. While open questions remain, the experiments reported here have set the foundation for many new areas of investigation in *Lm*-host interactions and developed model systems to better study critical aspects of listeriosis. Beyond the utility of *Lm* as a model system for studying basic biology, invasive listeriosis is a significant public health risk which does not currently have adequate treatment options. A better understanding of how the biology of the host influences disease outcome will reveal possible avenues for therapeutic invention.

Chapter 6: Materials & methods

Bacterial strains and culture conditions

All bacterial strains used in this work are summarized in Table 4. Bacteria were cultured on brain heart infusion (BHI) agar (*Listeria spp.*) or LB agar (*B. subtilis, E. coli*) at 37ºC. Unless otherwise stated, bacteria were grown in BHI broth overnight at 37ºC with shaking prior to experiments. Antibiotics were used at the following concentrations: streptomycin, 200 µg/mL; chloramphenicol, 10 µg/mL (*E. coli*) and 7.5 µg/mL (*Lm*); tetracycline, 2 µg/mL; and carbenicillin, 100 µg/mL. Plasmids were transformed into chemically competent *E. coli* using heat shock.

Table 4. Bacterial strains used in this work.

Name	Species	Strain	Description	Reference or source
MLR-E0848	*E. coli*	SM10	pPL1.P*hyper*-GFP	This work
MLR-E0868	*E. coli*	SM10	pPL2t.P*hyper*-RFP	This work
MLR-E1095	*E. coli*	SM10	pPL2t.P*actA*-RFP	This work
MLR-E1096	*E. coli*	XL1	lentiCRISPR.*Taf4a*-sgRNA1	This work
MLR-E1097	*E. coli*	XL1	lentiCRISPR.*Taf4a*-sgRNA2	This work
MLR-E1098	*E. coli*	XL1	lentiCRISPR.*Supt20*-sgRNA1	This work
MLR-E1099	*E. coli*	XL1	lentiCRISPR.*Supt20*-sgRNA2	This work
MLR-E1100	*E. coli*	XL1	lentiCRISPR.*Rfwd2*-sgRNA1	This work
MLR-E1101	*E. coli*	XL1	lentiCRISPR.*Rfwd2*-sgRNA2	This work
MLR-E1102	*E. coli*	XL1	lentiCRISPR.*Dyrk1A*-sgRNA1	This work
MLR-E1103	*E. coli*	XL1	lentiCRISPR.*Dyrk1a*-sgRNA2	This work
MLR-E1104	*E. coli*	XL1	lentiCRISPR.*Rragc*-sgRNA1	This work
MLR-E1105	*E. coli*	XL1	lentiCRISPR.*Rragc*-sgRNA2	This work
MLR-E1106	*E. coli*	XL1	lentiCRISPR.*Pten*-sgRNA1	This work
MLR-E1107	*E. coli*	XL1	lentiCRISPR.*Pten*-sgRNA2	This work
MLR-E1108	*E. coli*	XL1	sgOpti.*Gsk3a*-sgRNA1	This work
MLR-E1109	*E. coli*	XL1	sgOpti.*Gsk3a*-sgRNA2	This work
MLR-E1110	*E. coli*	XL1	sgOpti.*Gsk3a*-sgRNA3	This work
MLR-E1111	*E. coli*	XL1	sgOpti.*Gsk3b*-sgRNA1	This work
MLR-E1112	*E. coli*	XL1	sgOpti.*Gsk3b*-sgRNA2	This work
MLR-E1113	*E. coli*	XL1	sgOpti.*Gsk3b*-sgRNA3	This work
MLR-E1114	*E. coli*	XL1	lentiCRISPR.*Usp22*-sgRNA1	This work
MLR-E1115	*E. coli*	XL1	lentiCRISPR.*Usp22*-sgRNA2	This work
MLR-E1116	*E. coli*	XL1	lentiCRISPR.*Taf13*-sgRNA1	This work
MLR-E1117	*E. coli*	XL1	lentiCRISPR.*Taf13*-sgRNA2	This work
MLR-E1118	*E. coli*	XL1	lentiCRISPR.*Nelfcd*-sgRNA1	This work
MLR-E1119	*E. coli*	XL1	lentiCRISPR.*Nelfcd*-sgRNA2	This work

MLR-E1120	*E. coli*	XL1	pLV.*Pten*-CR	This work
MLR-E1121	*E. coli*	XL1	pLV.*Pten*-CR-G129E	This work
MLR-E1122	*E. coli*	XL1	pLV.*Pten*-CR-G129R	This work
MLR-L0001	*L. monocytogenes*	10403S	serovar 1/2a	159,160
MLR-L0017	*L. monocytogenes*	10403S	Δ*actA* Δ*inlB* pPL2.P*actA*-cre *loxP*-oriC ("suicide strain")	29,97
MLR-L1123	*L. monocytogenes*	10403S	Δ*actA*, phage-cured	This work
MLR-L1124	*L. monocytogenes*	10403S	Δ*actA* pPL1.P*hyper*-GFP pPL2t.P*hyper*-RFP	This work
MLR-L1125	*L. monocytogenes*	10403S	Δ*actA* pPL1.P*hyper*-GFP pPL2t.P*actA*-RFP ("P*actA* reporter")	This work
RCG-L0067	*L. monocytogenes*	10403S	P*actA* reporter *gshF::himar1*	This work
MLR-L0551	*L. monocytogenes*	10403S	pPL2.P*hyper*-mCherry	161
MLR-L1068	*L. monocytogenes*	10403S	Δ*flaA*	131
MLR-L0022	*L. monocytogenes*	10403S	Δ*hly*	162
MLR-L0216	*L. monocytogenes*	EGD-e	serovar 1/2a	159
MLR-L1126	*L. monocytogenes*	HER1034	serovar 1/2c	163
MLR-L1127	*L. monocytogenes*	HER1082	serovar 4b	163
MLR-L1128	*L. monocytogenes*	HER1083	serovar 4e, ATCC 19118	163
MLR-L1129	*L. monocytogenes*	HER1247	serovar 1/2a	163
MLR-L1130	*L. monocytogenes*	HER1537	serovar 1/2a	163
MLR-L1131	*L. monocytogenes*	Li2	serovar 4b, ATCC 19115	163
MLR-L0516	*L. ivanovii*			163
MLR-L0432	*L. innocua*	CLIP11262		164
MLR-L1132	*L. seeligeri*	SLCC3954		163,165
MLR-L1133	*L. riparia*			163
MLR-L1134	*L. newyorkensis*	FSL M6-635		163
MLR-B0704	*B. subtilis*	MB4		166

Mammalian cell lines

Cas9-expressing immortalized bone marrow-derived macrophages (iBMMs) were described previously[167]. THP-1, TIB73, and Caco-2 cell lines were obtained from Dr. Joshua Woodward (University of Washington)[168]. HEK293T cells were purchased from ATCC and obtained from Dr. Jennifer Hyde (University of Washington). Cell lines were cultured at 37ºC and 5% CO_2. iBMMs, TIB73, and HEK293T cells were grown in high glucose (4.5 g/L) Dulbecco's modified Eagle's medium (DMEM) supplemented with 10% heat-inactivated fetal bovine serum (FBS) (Cytiva), 1 mM sodium pyruvate, 2 mM L-glutamine, and 100 U/mL penicillin-streptomycin (D-10). Caco-2 cells were cultured high glucose DMEM supplemented with 20% FBS, 1 mM sodium pyruvate, 2 mM L-glutamine, and 100 U/mL penicillin-streptomycin (D-20). THP-1 cells were grown in RPMI 1640 supplemented with 10% FBS, 1 mM sodium pyruvate, 2 mM L-glutamine, and 100 U/mL penicillin-streptomycin (RP-10). Cells were plated in medium without penicillin-streptomycin for infections. Cells were determined to be Mycoplasma-free using PCR[169].

Antibiotics were used at the following concentrations: gentamicin, 50 μg/mL; puromycin, 5 μg/mL; blasticidin, 10 μg/mL; and Geneticin (G418), 1000 μg/mL.

Primary cells

Bone marrow-derived macrophages (BMDMs) were cultured as above and grown in high glucose DMEM supplemented with 20% heat-inactivated FBS, 1 mM sodium pyruvate, 2 mM L-glutamine, 10% 3T3 cell supernatant (from M-CSF-producing 3T3 cells), and 55 μM β-mercaptoethanol (BMDM medium). BMDMs were isolated as previously described[6]. Briefly, femurs and tibias from 6-8 week old female C57BL/6 mice were crushed with a mortar and pestle in 20 mL BMDM medium and strained through 70 μm cell strainers. Cells were plated in 150 mm untreated culture dishes, supplemented with fresh BMDM medium at day 3, and harvested by pipetting in cold PBS at day 7. BMDMs were aliquoted in 80% BMDM medium, 10% FBS, and 10% DMSO and stored in liquid nitrogen.

Mice

Animal experiments were carried out in strict accordance with the recommendations in the Guide for the Care and Use of Laboratory Animals of the National Institutes of Health. All protocols were reviewed and approved by the Institutional Animal Care and Use Committee (IACUC) at the University of Washington (Protocol 4410–01). Animals were group-housed in University of Washington Department of Comparative Medicine facilities under specific pathogen-free conditions. 6 week old wildtype (#000664) and *Tlr2*$^{-/-}$ (#004650) female C57BL/6J mice were purchased from The Jackson Laboratory for isolating BMDMs. To generate *Pten* conditional knockout mice, male *LysM*-Cre$^{+/+}$ mice (#004781) and female *Pten*$^{fl/fl}$ mice (#006440) were purchased from The Jackson Laboratory and bred to produce double heterozygotes. Female heterozygotes were bred back to male *LysM*-Cre$^{+/+}$ mice to generate *LysM*-Cre$^{+/+}$ *Pten*$^{fl/wt}$ breeders, which were then bred together to produce *LysM*-Cre$^{+/+}$ *Pten*$^{fl/fl}$ knockout mice (PTEN$^{M\text{-}KO}$) and *LysM*-Cre$^{+/+}$ *Pten*$^{wt/wt}$ controls (PTEN$^{M\text{-}WT}$). Genotyping was performed by isolating gDNA from ear biopsies and following PCR protocols provided by The Jackson Laboratory. 8-10 week old male and female mice were used for infection studies. Animals were assigned to experimental groups by age-, sex, and littermate-matching and groups were co-housed when possible.

Bacterial strain construction

For the CRISPR/Cas9 screen, we constructed a Δ*actA* strain expressing GFP constitutively and RFP under control of the *actA* promoter. GFP driven by the constitutive P*hyper* promoter was cloned into the integrative vector pPL1[170] by restriction cloning (pPL1.P*hyper*-GFP). RFP was cloned downstream of the *actA* promoter into the integrative plasmid pPL2t[171] by restriction cloning (pPL2t.P*actA*-RFP). To integrate pPL1.P*hyper*-GFP into Δ*actA* (DPL3078)[172], this strain was cured of its endogenous prophage at the *comK-attBB'* site as previously described[170]. Δ*actA* was grown overnight in BHI broth at 37ºC with shaking. The next day, 8.5 x 10^8 U153 phage was combined with 4.25 x 10^7 bacteria (MOI = 20) in a total of 3 mL BHI containing 5 mM $CaCl_2$ and incubated at 37ºC with shaking for 75 minutes. The mixture was then diluted 1:100 and 1:10,000 into 2 mL BHI in separate culture tubes. Each tube was incubated at

37ºC with shaking for several hours until the 1:100 dilution reached an OD of approximately 0.1. At this point, the 1:10,000 dilution was diluted and spread plated to obtain single colonies. Colonies were screened by PCR with primers specific for *comK-attBB'* for presence of a 417 bp band to indicate successful phage curing. pPL1.P*hyper*-GFP and pPL2t.P*actA*-RFP were integrated into phage-cured Δ*actA* via trans-conjugation from *E. coli* SM10, generating the strain designated as P*actA*-reporter.

Preparation of cell-free extracts from *X. tropicalis* eggs

X. tropicalis frogs were housed and handled in strict accordance with protocols reviewed and approved by the IACUC at the University of Washington. Procedures performed directly on live animals were carried out by members of the Wills Lab in the Department of Biochemistry at the University of Washington. Ovulation of adult female *X. tropicalis* was performed as previously described[173] and eggs were collected into a 150 mm dish. Eggs were washed three times with Marc's Modified Ringer's buffer (MMR) and de-jellied in 1/9X MMR containing 3% cysteine for 5-10 minutes. Eggs were then washed three times in Extract Buffer (XB) (100 mM KCl, 1 mM $MgCl_2$, 100 μM $CaCl_2$, 10 mM HEPES pH 7.7, 50 mM sucrose) and three times in XB containing 2 mM $MgCl_2$ and 5 mM EGTA (CSF-XB). The final CSF-XB wash was carefully decanted off of the eggs and 50 mL of CSF-XB containing 10 μg/mL leupeptin, pepstatin, and chymostatin was added to the eggs. A plastic pasteur pipette with the tip cut off was used to collect eggs and transfer them to microcentrifuge tubes. The eggs were packed by centrifuging at 200 x g for 1 minute followed by 500 x g for 30 seconds, and excess buffer was aspirated off the top of the packed eggs. To lyse the eggs and separate the cytosolic fraction, eggs were centrifuged at max speed (>18,000 x g) for 15 minutes at 16ºC. The middle cytosolic fraction was carefully collected using a gel-loading pipette tip. Extracts were supplemented with 10 μg/mL leupeptin, pepstatin, and chymostatin, aliquoted, and stored at -80ºC.

Measuring PrfA activity in *Xenopus* extracts

Wildtype *Lm* and the suicide strain were grown overnight in BHI broth at 30ºC statically. Energy mix (150 mM creatine phosphate, 20 mM ATP, 2 mM EGTA, 20 mM $MgCl_2$; stored at -20ºC) was diluted 1:40 into 2X BHI (2X BHI-e). Extracts were thawed and diluted 1:2.5 into PBS. The PBS-extract mixture was then combined 1:1 with 2X BHI-e and 18 μL of the final mixture was aliquoted into PCR tubes. Bacterial overnight cultures were diluted 1:100 (wt) or 1:50 (suicide strain) in PBS and 2 μL of diluted cultures were added to each tube. 5 μL of sample were removed immediately after inoculation and after 4 hours of incubation at 37ºC, serially diluted, and plated to enumerate CFU. For enzymatic treatments, enzymes were added to extracts at the following concentrations: Benzonase, 0.156 U/μL; Proteinase K, 8 U/μL; Trypsin, 12.5 ng/μL; and biotinylated CIP, 50 ng/μL. Extracts were treated for 1 hour at 37ºC prior to diluting in PBS. Proteinase K was inactivated by adding 2 mM PMSF to treated extracts and incubating at room temperature for 20 minutes. Biotinylated CIP was removed from treated extracts using 25 μL Streptavidin magnetic beads per 100 μL extract. When indicated, Proteinase K-treated extracts were diluted 1:2.5 into untreated extract instead of PBS.

Fractionation of *Xenopus* extracts by FPLC

FPLC separation of *Xenopus* extracts was carried out using a 5 mL HiTrap Capto Q anion-exchange column. The column was equilibrated prior to each run with 5 column volumes of PBS. 1-2 mL of extract was applied to the column and the column was washed with 10 mL of PBS. A 0-100% gradient of 0.4 M NaCl was applied over 20 column volumes to elute proteins, and 2 mL fractions were collected. To test fractions for activity, 9 µL of each fraction was combined with 9 µL of 2X BHI-e and inoculated with 2 µL of diluted bacteria as described above.

Mass spectrometry

Samples were combined with 8 volumes of cold (-20ºC) acetone and vortexed. 1 volume of cold trichloroacetic acid was added, samples were vortexed, and precipitated at -20ºC overnight. Precipitated samples were centrifuged at 15,000 x g for 15 minutes at 4ºC and supernatants discarded. Protein pellets were washed three times with 200 µL cold acetone and air-dried until all acetone was evaporated. Samples were resuspended in 50 µL of 8 M urea and 0.4 M ammonium bicarbonate. 2 µL of 100 mM DTT was added and samples were incubated at 50ºC for 30 minutes. 3 µL of 300 mM iodoacetamide was then added and samples were incubated at room temperature for 30 minutes in the dark. Sample volume was brought up to 200 µL with water and samples were digested with 1 µg Trypsin overnight at 37ºC rotating. Samples were desalted with C18 columns, completely evaporated using a SpeedVac, and resuspended in 30 µL of 5% acetonitrile and 0.1% formic acid in water. Mass spectrometry of prepared samples was performed by the Northwestern University Proteomics Core.

Lentiviral transduction

HEK293T cells were transfected with pVSV-G (Addgene #138479), psPAX2 (Addgene #12260), and a lentiviral vector at a 2:2:1 molar ratio. The following day, culture media was replaced with fresh D-10 supplemented with non-essential amino acids (Cytiva) and 25 mM HEPES. Lentivirus-containing supernatant was collected 48 hours post-transfection, spun at 300 x g for 8 minutes to remove cell debris, aliquoted, and frozen at -80ºC. For transductions, cells were plated with lentiviral supernatants in the presence of 8 µg/mL polybrene, and antibiotics were added 48 hours post-transduction. Transduced cells were passaged in the presence of antibiotics for at least 1 week to allow complete selection.

Construction of knockout cell lines using CRISPR/Cas9

Individual sgRNAs (2 per gene) from the Brie library or designed using Benchling were cloned into lentiGuide-Puro (Addgene #52963), lentiCRISPR v2-blast (Addgene #98293), or sgOpti (Addgene #85681) as previously described[167,174–176]. Briefly, sgRNAs were annealed, phosphorylated with T4 Polynucleotide Kinase, digested with BsmBI, and ligated into lentiGuide-Puro, lentiCRISPR v2-blast, or sgOpti. Plasmids were packaged into lentivirus and transduced into iBMM-Cas9 cells as described above. To confirm genome-editing, gDNA was isolated using Zymo Quick-DNA Miniprep kits, cut sites were amplified by PCR, and Sanger sequencing performed. Sequences were analyzed using ICE analysis[101] to estimate InDel and knockout

efficiency. Clonal cell lines were derived from *Pten* knockout iBMMs (sgRNA1) for further analysis by single-cell sorting.

Intracellular growth curves

5 x 10^5 iBMMs per well were plated in 24-well plates overnight. *Lm* cultures were grown overnight at 30ºC stationary. The next day, overnight cultures were washed twice with PBS, diluted in cell culture medium, and added to cell monolayers at MOI = 1. After 30 minutes, cells were washed twice and medium containing gentamicin was added to kill extracellular bacteria. At various timepoints (0.5, 2, 5, and 8 hours post-infection), cells were washed twice with PBS and lysed in 250 µL cold 0.1% Triton-X in PBS. Lysates were serially diluted and plated to enumerate intracellular CFU.

Flow cytometry

iBMMs were plated at a density of 10^6 cells/well in 12-well plates and infected with *Lm* P*actA*-reporter. Unless otherwise indicated, cells were infected at MOI = 10. After 4 hours (or the designated time point), cells were washed twice with PBS and medium containing gentamicin was added for an additional 2 hours. Cells were then washed twice with PBS, harvested with 0.05% trypsin-EDTA, and fixed with 1% formaldehyde in Flow Buffer (PBS containing 5% FBS) for 10 minutes. Samples were washed twice with Flow Buffer and stored in Flow Buffer at 4ºC overnight. The next day, samples were analyzed on a BD LSRII flow cytometer. GFP or RFP fluorescence were measured and quantified by setting a gate for GFP or RFP-positive cells on uninfected cells with 5% background.

CRISPR/Cas9 screen

The mouse Brie pooled sgRNA library on the lentiGuide-Puro backbone was obtained from David Root and John Doench (Addgene #73633)[177]. The Brie library contains 78,637 sgRNAs, including 1000 non-targeting controls, and targets 19,674 genes using 4 sgRNAs per gene. The sgRNA library was packaged into lentivirus and transduced into iBMMs at MOI = 0.3 to ensure single integration events. Transduced cells were selected with puromycin for 1 week and maintained at 1000-fold coverage of the library. Three independent knockout libraries were generated and screened.

Knockout libraries were plated at 1000-fold coverage in 150 mm tissue culture dishes. The P*actA*-reporter strain was grown overnight in BHI broth at 30ºC stationary, washed twice with sterile PBS, and used to infect the knockout library at MOI = 10; sterile PBS was added to mock-infected control cells. At 4 hours post-infection cells were washed twice with PBS, and medium containing gentamicin was added to kill extracellular bacteria. At 6 hours post-infection cells were washed twice with PBS, harvested with 0.05% trypsin-EDTA, and fixed with 1% formaldehyde in PBS for 10 min. Fixed cells were washed twice with Flow Buffer and stored at 4ºC overnight. The following day, fluorescence-activated cell sorting (FACS) was performed using a BD FACSAria II cell sorter. To isolate uninfected cells, gates were drawn based on mock-infected cells (negative control) and wildtype cells infected with Δ*actA* pPL1.P*hyper*-GFP pPL2t.P*hyper*-RFP (positive

control). Double-negative cells ($GFP^{-}RFP^{-}$) and RFP-negative cells ($GFP^{+}RFP^{-}$) were collected from the infected knockout libraries.

Genomic DNA (gDNA) was isolated from mock-infected and sorted populations from three biological replicates as previously described[178]. The sgRNA locus was amplified and barcoded by PCR using KAPA HiFi polymerase and Ultramer DNA Oligos from IDT. Enough gDNA was amplified from mock-infected libraries to maintain 1000-fold coverage of the library, using an estimation of 6.6 µg gDNA per 10^6 cells; for sorted populations, all gDNA was amplified. PCR mixes were split into multiple 50 µL reactions, each containing 5 µg gDNA, and cycled 23 times according to manufacturer recommendations. Amplicons were purified using AMPure XP beads, pooled at 1:1 molar ratios, and sequenced on an Illumina HiSeq2500. sgRNAs enriched in the double-negative or RFP-negative populations were identified using MAGeCK as previously described[99]. Gene ontology analysis was performed using Metascape[100].

Measuring bacterial uptake via gentamicin protection assay

Cells were plated the day before infection at the following densities: 5 x 10^5 (iBMM and THP-1), 6 x 10^5 (BMDM), and 2 x 10^5 (Caco-2) per well in 24-well plates, or 5 x 10^5 (TIB73) per well in 12-well plates. THP-1 cells were plated in the presence of 100 ng/mL phorbol 12-myristate 13-acetate (PMA) 48 hours prior to infection to differentiate cells. Overnight bacterial cultures were diluted in BHI to an OD of 0.05-0.1 and grown at 37ºC with shaking to an OD of 1-2. Bacteria were washed twice with PBS, diluted in cell culture medium, and added to cell monolayers at MOI = 1 (iBMM, BMDM, THP-1), 10 (Caco-2), or 50 (TIB73). Medium containing 0.1% FBS was used for TIB73 infections and replaced with D-10 for subsequent steps. For experiments comparing different bacterial strains or species, the inoculation medium was serially diluted and plated for enumeration. When indicated, 24-well plates were centrifuged for 3 minutes at 300 x g after adding bacteria to cells. Macrophages were incubated with bacteria for 30 minutes, washed twice with PBS, and incubated with medium containing gentamicin for an additional 30 minutes. Nonphagocytic cells were incubated with bacteria for 1 hour, washed twice with pre-warmed D-10, and incubated with medium containing gentamicin for an additional 30 minutes. To enumerate intracellular bacteria, cells were washed twice and lysed in 250 µL cold 0.1% Triton-X in PBS. Lysates were serially diluted and plated for CFU.

Chemical inhibitors

All chemical inhibitors were added to cells 1 hour prior to infection and kept in the culture medium throughout the experiment. To avoid inhibition of bacterial transcription by actinomycin D, cells pre-treated with actinomycin D were washed twice with PBS immediately prior to infection and medium without inhibitor was used for the remainder of the experiment. Inhibitors had no effect on *Lm* viability, as measured by exposing *Lm* to each inhibitor for 1 hour in D-10 and enumerating CFU. All inhibitors were dissolved in DMSO except bpV(pic) which was dissolved in water. Inhibitors were used at the following concentrations: actinomycin D (Sigma-Aldrich), 10 µg/mL; cycloheximide (Sigma-Aldrich), 1 µg/mL; bpV(pic) (Cayman Chemical Company), 5 µM; CHIR99021 (Cayman Chemical Company), 10 µM; parthenolide (Sigma-Aldrich), 10 µM; wortmannin (Santa Cruz Biotechnology), 100 nM; INK1117 (GlpBio), 1 µM; TGX221 (Cayman

Chemical Company), 10 μM; IC87114 (Cayman Chemical Company), 10 μM; and IPI549 (MedChemExpress), 50 nM.

Phagocytosis of fluorescent beads

Phagocytosis of fluorescence beads was measured using IgG FITC Phagocytosis Assay Kits (Cayman Chemical Company) according to manufacturer instructions. Briefly, FITC-labeled, IgG-opsonized beads were diluted 1:250 in cell culture medium and incubated with iBMMs for 30 minutes. Cells were washed once in assay buffer and incubated in 0.04% Trypan Blue in assay buffer for 2 minutes to quench fluorescence from extracellular beads. Cells were washed once more with assay buffer, harvested using 0.05% trypsin-EDTA, and resuspended in Flow Buffer. Samples were analyzed on a BD LSRII flow cytometer to quantify FITC-positive cells.

Immunofluorescence microscopy

iBMMs were plated onto 12 mm sterile glass coverslips in 24-well plates at a density of 5 x 10^5 cells per well. *Lm* constitutively expressing mCherry (pPL2.P*hyper*-mCherry)[161] was grown overnight in BHI at 37ºC shaking. The following day, overnight bacterial cultures were diluted in BHI to an OD of 0.05 and grown at 37ºC with shaking to an OD of 1-2. Bacteria were washed twice with PBS, diluted in cell culture medium, and added to cell monolayers at MOI = 5. Plates were centrifuged for 3 minutes at 300 x g to synchronize infection. At each timepoint, coverslips were washed twice with PBS, removed from the plate, and inverted onto 20 μL of 4% formaldehyde on parafilm. Cells were fixed for 10 minutes and washed by dipping into three 50 mL conicals of PBS, 10 times each. Coverslips were washed in this manner in between each of the following incubations. Fixed coverslips were blocked with 1% BSA in PBS (staining buffer) for 10 minutes and stored in staining buffer overnight at 4ºC. To block non-specific binding to Fc receptors, coverslips were incubated with mouse Fc Block (BD) diluted 1:50 in staining buffer for 30 minutes. For immunofluorescence staining, coverslips were incubated for 30 minutes with Listeria O Antisera (BD) diluted 1:100 in staining buffer, followed by goat anti-rabbit Alexa Fluor 488 secondary antibody (Invitrogen) diluted 1:200 in staining buffer. Stained coverslips were mounted on glass slides with ProLong Diamond Antifade Mountant with DAPI (Invitrogen) and imaged on a Keyence BZ-X710 fluorescence microscope at 40X magnification.

Antibody opsonization of *Lm*

Overnight cultures of *Lm* 10403S were diluted to an OD of 0.05 in BHI and grown at 37ºC shaking until reaching an OD of ~2. Bacteria were diluted to an OD of 1 in PBS, washed once with antibody buffer (PBS +5% FBS) and resuspended in either antibody buffer (un-opsonized) or Listeria O Antisera (BD) diluted 1:10 in antibody buffer (opsonized). Samples were incubated at room temperature for 30 minutes, washed twice with antibody buffer, and added to iBMMs at MOI = 1. Inocula were serially diluted and plated on BHI agar to enumerate CFU. Bacterial internalization was measured by gentamicin protection assay as described above.

Immunoblotting

For PTEN immunoblots, 10^6 iBMMs per well were plated in 12-well plates. The following day, cell lysates were prepared as described below. For pAkt immunoblots, 1.2 x 10^6 BMDMs per well were plated in 12-well plates. The following day, overnight bacterial cultures were diluted to an OD of 0.05 in BHI and grown at 37ºC with shaking to an OD of 1-2. To eliminate background Akt phosphorylation, BMDMs were serum-starved by incubating in FBS- and CSF-free BMDM medium for 2 hours prior to infection. Bacteria were washed twice with PBS, diluted in FBS- and CSF-free BMDM medium, and added to cell monolayers at MOI = 100. At each timepoint, cells were washed twice in PBS and lysed in 50-100 µL cold RIPA buffer containing Halt Protease and Phosphatase Inhibitor Cocktail (Thermo Scientific). Lysates were incubated on ice for 15 minutes and centrifuged at 15,000 x g for 15 minutes at 4ºC to pellet cell debris. Protein concentration of clarified lysates was quantified using a Pierce BCA Protein Assay Kit (Thermo Scientific).

30 µg of each sample were separated by SDS-PAGE and transferred to PVD-F membranes. Membranes were blocked for 1 hour at room temperature in Intercept (TBS) Blocking Buffer (LI-COR) for pAkt blots or Intercept (PBS) Blocking Buffer (LI-COR) for PTEN immunoblots. Blocked membranes were incubated overnight at 4ºC with anti-Phospho-Akt (Ser473) antibody (Cell Signaling Technology #9271) or anti-PTEN antibody (Cell Signaling Technology #9559) diluted 1:1,000 in TBS antibody buffer (50% TBS, 50% TBS Blocking Buffer) or PBS antibody buffer (50% PBS, 50% PBS Blocking Buffer), respectively. The following day, membranes were washed with TBST and incubated for 1 hour at room temperature with anti-β-Actin antibody (Cell Signaling Technology #3700) diluted 1:1,000 in PBS antibody buffer. Membranes were washed with TBST and incubated with goat anti-rabbit Alexa Fluor 680 (Invitrogen) and goat anti-mouse IRDye 800CW (LI-COR) antibodies diluted 1:5,000 in PBS antibody buffer for 1 hour at room temperature. Blotted membranes were washed a final time with TBST and imaged on a LI-COR Odyssey Fc imager. For pAkt blots, membranes were stripped by incubation at 55ºC in stripping buffer (62.5 mM Tris pH 6.8, 2% SDS, 0.8% β-mercaptoethanol) for 45 minutes followed by 5-10 washes in water. Membranes were reblocked with PBS Blocking Buffer and reprobed overnight at 4ºC with anti-Akt antibody (Cell Signaling Technology #9272) diluted 1:1,000 in PBS antibody buffer, followed by goat anti-rabbit Alexa Fluor 680 for 1 hour at room temperature.

Expression of PTEN variants in iBMMs

cDNA was prepared from wildtype iBMMs by extracting total RNA using TRIzol (Invitrogen) and reverse transcription with an iScript cDNA Synthesis Kit (Bio-Rad). PTEN coding sequence was PCR amplified from cDNA and cloned into pLV-EF1a-IRES-Neo (Addgene #85139)[179] using restriction cloning. To prevent CRISPR/Cas9-mediated genome editing in *Pten*$^{-/-}$ iBMMs which constitutively express Cas9 and *Pten*-specific sgRNA, synonymous point mutations were made in each amino acid within the sgRNA recognition site using site-directed mutagenesis to generate a CRISPR-resistant *Pten* allele (PTEN-CR). PTEN-CR was further mutagenized using site-directed mutagenesis to create G129E or G129R point mutations. Empty pLV-EF1a-IRES-Neo, pLV.PTEN-CR, pLV.PTEN-CR-G129E, or pLV.PTEN-CR-G129R were packaged into lentivirus and transduced into *Pten*$^{-/-}$ iBMMs or wildtype iBMMs (empty vector only) as described above.

After antibiotic selection, protein expression of each PTEN variant was confirmed by immunoblot as described above.

Mouse infections

Oral infections were performed as previously described[10,180]. 8-10 week old male and female mice were used for infections. 5 mg/mL streptomycin was added to drinking water for 48 hours to eliminate gut flora. Food and water were then removed 16 hours prior to infection to initiate overnight fasting. *Lm* was grown overnight in BHI at 30ºC statically. The following day, cultures were diluted 1:10 into 5 mL fresh BHI and grown at 37ºC with shaking for 2 hours. Bacteria were washed twice with PBS and 10^8 CFU in 20 µL was fed to mice via pipette. We found that *Lm* Li2 did not colonize mice as well as 10403S at the same infectious dose, which may be due to the presence of residual streptomycin in the mice at the time of infection[134]. To overcome this, we used a higher infectious dose of 5 x 10^8, which resulted in bacterial burdens similar to 10403S at 5 dpi. Food and water were returned immediately after infection. For i.v. infections, *Lm* was grown to mid-log as described above and diluted in PBS. Mice were anesthetized with isoflurane and 1.5 x 10^5 CFU in 200 µL were administered via retro-orbital injection. Prepared bacterial suspensions were serially diluted and plated immediately after infection to enumerate inocula. Mice were humanely euthanized at 1-5-days post-infection and tissues were collected. Tissues were homogenized in 0.1% NP-40 in the following volumes: MLN, 3 mL; cecum (contents removed and tissue rinsed with PBS), 4 mL; spleen, 3 mL; and liver, 5 mL. Feces were homogenized in 1 mL 0.1% NP-40 with a sterile stick. Gallbladders were ruptured in 500 µL 0.1% NP-40 with a sterile stick. Samples were serially diluted and plated to enumerate CFU in each organ.

Intestinal tissue fractionation

Fractionation of intestinal tissues was performed as previously described[78,181]. Luminal contents of colons and ilea (distal 12 cm of small intestine) were removed by gently squeezing tissues with forceps. Tissues were flushed with 10 mL PBS using a 25 G needle and stored in 15 mL conicals in 5 mL PBS at 4ºC overnight. The following day, tissues were cut longitudinally, incubated in 3 mL 6 mM N-acetylcysteine (NAC) for 2 minutes, and shaken vigorously to remove the mucus layer. The NAC wash was repeated twice more for 3 total washes, transferring tissues to fresh tubes each time. To remove epithelial cells, tissues were then cut into small pieces and added to 15 mL conicals with 5 mL RPMI containing 5% FBS, 5 mM EDTA, and 1 mM DTT. Samples were incubated at 37ºC with shaking for 20 min, vortexed gently, and filtered through a 70 µm cell strainer. This process was repeated twice more for 3 total EDTA/DTT washes. Tissue pieces were washed once with 10 mL PBS to remove DTT. To isolate lamina propria (LP) cells, tissue pieces were then added to 15 mL conicals with 3 mL RPMI containing 5% FBS, 1 mg/mL collagenase type IV (Sigma-Aldrich), and 40 µg/mL DNase I (Roche). Samples were incubated at 37ºC with shaking for 40 min, vortexed, and filtered through 70 µm cell strainers. This process was repeated once more if necessary, until no more large tissue pieces remained. Fractions (NAC washes, EDTA/DTT washes, and LP suspensions) were pooled, centrifuged at 12,000 x g for 20 minutes at 4ºC, and pellets resuspended in 150 µL 0.1% NP-40. Samples were serially diluted and plated to enumerate CFU in each fraction.

References

1. Quereda, J.J., Leclercq, A., Moura, A., Vales, G., Gómez-Martín, Á., García-Muñoz, Á., Thouvenot, P., Tessaud-Rita, N., Bracq-Dieye, H., and Lecuit, M. (2020). Listeria valentina sp. nov., isolated from a water trough and the faeces of healthy sheep. Int J Syst Evol Microbiol *70*, 5868–5879. 10.1099/ijsem.0.004494.

2. Camargo, A.C., Woodward, J.J., Call, D.R., and Nero, L.A. (2017). Listeria monocytogenes in Food-Processing Facilities, Food Contamination, and Human Listeriosis: The Brazilian Scenario. Foodborne Pathog Dis *14*, 623–636. 10.1089/fpd.2016.2274.

3. Listeria Outbreaks | Listeria | CDC (2023). https://www.cdc.gov/listeria/outbreaks/index.html.

4. CDC (2022). Foodborne Illnesses and Germs. Centers for Disease Control and Prevention. https://www.cdc.gov/foodsafety/foodborne-germs.html.

5. Ireton, K., Mortuza, R., Gyanwali, G.C., Gianfelice, A., and Hussain, M. (2021). Role of internalin proteins in the pathogenesis of Listeria monocytogenes. Mol Microbiol *116*, 1407–1419. 10.1111/mmi.14836.

6. Portnoy, D.A., Jacks, P.S., and Hinrichs, D.J. (1988). Role of hemolysin for the intracellular growth of Listeria monocytogenes. J Exp Med *167*, 1459–1471.

7. Marquis, H., Doshi, V., and Portnoy, D.A. (1995). The broad-range phospholipase C and a metalloprotease mediate listeriolysin O-independent escape of Listeria monocytogenes from a primary vacuole in human epithelial cells. Infect Immun *63*, 4531–4534. 10.1128/iai.63.11.4531-4534.1995.

8. Chen, G.Y., Pensinger, D.A., and Sauer, J.-D. (2017). Listeria monocytogenes cytosolic metabolism promotes replication, survival and evasion of innate immunity. Cell Microbiol *19*, 10.1111/cmi.12762. 10.1111/cmi.12762.

9. Tilney, L.G., and Portnoy, D.A. (1989). Actin filaments and the growth, movement, and spread of the intracellular bacterial parasite, Listeria monocytogenes. J Cell Biol *109*, 1597–1608. 10.1083/jcb.109.4.1597.

10. Louie, A., Zhang, T., Becattini, S., Waldor, M.K., and Portnoy, D.A. (2019). A Multiorgan Trafficking Circuit Provides Purifying Selection of Listeria monocytogenes Virulence Genes. mBio *10*, e02948-19. 10.1128/mBio.02948-19.

11. Maudet, C., Kheloufi, M., Levallois, S., Gaillard, J., Huang, L., Gaultier, C., Tsai, Y.-H., Disson, O., and Lecuit, M. (2022). Bacterial inhibition of Fas-mediated killing promotes neuroinvasion and persistence. Nature *603*, 900–906. 10.1038/s41586-022-04505-7.

12. Dramsi, S., Lévi, S., Triller, A., and Cossart, P. (1998). Entry of Listeria monocytogenesinto Neurons Occurs by Cell-to-Cell Spread: an In Vitro Study. Infect Immun *66*, 4461–4468. 10.1128/IAI.66.9.4461-4468.1998.

13. Qiu, Z., Khairallah, C., and Sheridan, B.S. (2018). Listeria Monocytogenes: A Model Pathogen Continues to Refine Our Knowledge of the CD8 T Cell Response. Pathogens *7*, 55. 10.3390/pathogens7020055.

14. Shen, H., Tato, C.M., and Fan, X. (1998). Listeria monocytogenes as a probe to study cell-mediated immunity. Curr Opin Immunol *10*, 450–458. 10.1016/S0952-7915(98)80120-9.

15. Lambrechts, A., Gevaert, K., Cossart, P., Vandekerckhove, J., and Van Troys, M. (2008). Listeria comet tails: the actin-based motility machinery at work. Trends Cell Biol *18*, 220–227. 10.1016/j.tcb.2008.03.001.

16. Chakraborty, T. (1999). Molecular and Cell Biological Aspects of Infection by Listeria Monocytogenes. Immunobiology *201*, 155–163. 10.1016/S0171-2985(99)80055-2.

17. Chaturongakul, S., Raengpradub, S., Wiedmann, M., and Boor, K.J. (2008). Modulation of stress and virulence in Listeria monocytogenes. Trends Microbiol *16*, 388–396. 10.1016/j.tim.2008.05.006.

18. Ruhland, B.R., and Reniere, M.L. (2019). Sense and sensor ability: redox-responsive regulators in Listeria monocytogenes. Curr Opin Microbiol *47*, 20–25. 10.1016/j.mib.2018.10.006.

19. Scortti, M., Monzó, H.J., Lacharme-Lora, L., Lewis, D.A., and Vázquez-Boland, J.A. (2007). The PrfA virulence regulon. Microbes Infect *9*, 1196–1207. 10.1016/j.micinf.2007.05.007.

20. Milohanic, E., Glaser, P., Coppée, J.-Y., Frangeul, L., Vega, Y., Vázquez-Boland, J.A., Kunst, F., Cossart, P., and Buchrieser, C. (2003). Transcriptome analysis of Listeria monocytogenes identifies three groups of genes differently regulated by PrfA. Mol Microbiol *47*, 1613–1625. 10.1046/j.1365-2958.2003.03413.x.

21. Marr, A.K., Joseph, B., Mertins, S., Ecke, R., Müller-Altrock, S., and Goebel, W. (2006). Overexpression of PrfA Leads to Growth Inhibition of Listeria monocytogenes in Glucose-Containing Culture Media by Interfering with Glucose Uptake. J Bacteriol *188*, 3887–3901. 10.1128/JB.01978-05.

22. Vasanthakrishnan, R.B., de las Heras, A., Scortti, M., Deshayes, C., Colegrave, N., and Vázquez-Boland, J.A. (2015). PrfA regulation offsets the cost of Listeria virulence outside the host. Environ Microbiol *17*, 4566–4579. 10.1111/1462-2920.12980.

23. Chakraborty, T., Leimeister-Wächter, M., Domann, E., Hartl, M., Goebel, W., Nichterlein, T., and Notermans, S. (1992). Coordinate regulation of virulence genes in Listeria monocytogenes requires the product of the prfA gene. J Bacteriol *174*, 568–574. 10.1128/jb.174.2.568-574.1992.

24. Freitag, N.E., Rong, L., and Portnoy, D.A. (1993). Regulation of the prfA transcriptional activator of Listeria monocytogenes: multiple promoter elements contribute to intracellular growth and cell-to-cell spread. Infect Immun *61*, 2537–2544. 10.1128/iai.61.6.2537-2544.1993.

25. Freitag, N.E., and Portnoy, D.A. (1994). Dual promoters of the Listeria monocytogenes prfA transcriptional activator appear essential in vitro but are redundant in vivo. Mol Microbiol *12*, 845–853. 10.1111/j.1365-2958.1994.tb01070.x.

26. Schwab, U., Bowen, B., Nadon, C., Wiedmann, M., and Boor, K.J. (2005). The Listeria monocytogenes prfAP2 promoter is regulated by sigma B in a growth phase dependent manner. FEMS Microbiol Lett *245*, 329–336. 10.1016/j.femsle.2005.03.025.

27. Johansson, J., Mandin, P., Renzoni, A., Chiaruttini, C., Springer, M., and Cossart, P. (2002). An RNA Thermosensor Controls Expression of Virulence Genes in Listeria monocytogenes. Cell *110*, 551–561. 10.1016/S0092-8674(02)00905-4.

28. Mengaud, J., Dramsi, S., Gouin, E., Vazquez-Boland, J.A., Milon, G., and Cossart, P. (1991). Pleiotropic control of Listeria monocytogenes virulence factors by a gene that is autoregulated. Mol Microbiol *5*, 2273–2283. 10.1111/j.1365-2958.1991.tb02158.x.

29. Reniere, M.L., Whiteley, A.T., Hamilton, K.L., John, S.M., Lauer, P., Brennan, R.G., and Portnoy, D.A. (2015). Glutathione activates virulence gene expression of an intracellular pathogen. Nature *517*, 170–173. 10.1038/nature14029.

30. Hall, M., Grundström, C., Begum, A., Lindberg, M.J., Sauer, U.H., Almqvist, F., Johansson, J., and Sauer-Eriksson, A.E. (2016). Structural basis for glutathione-mediated activation of the virulence regulatory protein PrfA in Listeria. Proc Natl Acad Sci *113*, 14733–14738. 10.1073/pnas.1614028114.

31. Moors, M.A., Levitt, B., Youngman, P., and Portnoy, D.A. (1999). Expression of Listeriolysin O and ActA by Intracellular and Extracellular Listeria monocytogenes. Infect Immun *67*, 131–139. 10.1128/IAI.67.1.131-139.1999.

32. Portman, J.L., Dubensky, S.B., Peterson, B.N., Whiteley, A.T., and Portnoy, D.A. (2017). Activation of the Listeria monocytogenes Virulence Program by a Reducing Environment. mBio *8*. 10.1128/mBio.01595-17.

33. Milenbachs, A.A., Brown, D.P., Moors, M., and Youngman, P. (1997). Carbon-source regulation of virulence gene expression in Listeria monocytogenes. Mol Microbiol *23*, 1075–1085. 10.1046/j.1365-2958.1997.2711634.x.

34. Park, S.F., and Kroll, R.G. (1993). Expression of listeriolysin and phosphatidylinositol-specific phospholipase C is repressed by the plant-derived molecule cellobiose in Listeria monocytogenes. Mol Microbiol *8*, 653–661. 10.1111/j.1365-2958.1993.tb01609.x.

35. Joseph, B., Mertins, S., Stoll, R., Schär, J., Umesha, K.R., Luo, Q., Müller-Altrock, S., and Goebel, W. (2008). Glycerol Metabolism and PrfA Activity in Listeria monocytogenes. J Bacteriol *190*, 5412–5430. 10.1128/JB.00259-08.

36. Stoll, R., Mertins, S., Joseph, B., Müller-Altrock, S., and Goebel, W. (2008). Modulation of PrfA activity in Listeria monocytogenes upon growth in different culture media. Microbiology *154*, 3856–3876. 10.1099/mic.0.2008/018283-0.

37. Mertins, S., Joseph, B., Goetz, M., Ecke, R., Seidel, G., Sprehe, M., Hillen, W., Goebel, W., and Müller-Altrock, S. (2007). Interference of Components of the Phosphoenolpyruvate Phosphotransferase System with the Central Virulence Gene Regulator PrfA of Listeria monocytogenes. J Bacteriol *189*, 473–490. 10.1128/JB.00972-06.

38. Taylor, C.M., Beresford, M., Epton, H.A.S., Sigee, D.C., Shama, G., Andrew, P.W., and Roberts, I.S. (2002). Listeria monocytogenes relA and hpt Mutants Are Impaired in Surface-Attached Growth and Virulence. J Bacteriol *184*, 621–628. 10.1128/JB.184.3.621-628.2002.

39. Geiger, T., and Wolz, C. (2014). Intersection of the stringent response and the CodY regulon in low GC Gram-positive bacteria. Int J Med Microbiol *304*, 150–155. 10.1016/j.ijmm.2013.11.013.

40. Bennett, H.J., Pearce, D.M., Glenn, S., Taylor, C.M., Kuhn, M., Sonenshein, A.L., Andrew, P.W., and Roberts, I.S. (2007). Characterization of relA and codY mutants of Listeria monocytogenes: identification of the CodY regulon and its role in virulence. Mol Microbiol *63*, 1453–1467. 10.1111/j.1365-2958.2007.05597.x.

41. Lobel, L., Sigal, N., Borovok, I., Belitsky, B.R., Sonenshein, A.L., and Herskovits, A.A. (2015). The metabolic regulator CodY links L. monocytogenes metabolism to virulence by directly activating the virulence regulatory gene, prfA. Mol Microbiol *95*, 624–644. 10.1111/mmi.12890.

42. Lobel, L., and Herskovits, A.A. (2016). Systems Level Analyses Reveal Multiple Regulatory Activities of CodY Controlling Metabolism, Motility and Virulence in Listeria monocytogenes. PLoS Genet *12*, e1005870. 10.1371/journal.pgen.1005870.

43. Krypotou, E., Scortti, M., Grundström, C., Oelker, M., Luisi, B.F., Sauer-Eriksson, A.E., and Vázquez-Boland, J. (2019). Control of Bacterial Virulence through the Peptide Signature of the Habitat. Cell Rep *26*, 1815-1827.e5. 10.1016/j.celrep.2019.01.073.

44. Mengaud, J., Ohayon, H., Gounon, P., Mege R-M, null, and Cossart, P. (1996). E-cadherin is the receptor for internalin, a surface protein required for entry of L. monocytogenes into epithelial cells. Cell *84*, 923–932. 10.1016/s0092-8674(00)81070-3.

45. Shen, Y., Naujokas, M., Park, M., and Ireton, K. (2000). InlB-dependent internalization of Listeria is mediated by the Met receptor tyrosine kinase. Cell *103*, 501–510. 10.1016/s0092-8674(00)00141-0.

46. Ireton, K., Payrastre, B., Chap, H., Ogawa, W., Sakaue, H., Kasuga, M., and Cossart, P. (1996). A Role for Phosphoinositide 3-Kinase in Bacterial Invasion. Science *274*, 780–782. 10.1126/science.274.5288.780.

47. Bierne, H., Gouin, E., Roux, P., Caroni, P., Yin, H.L., and Cossart, P. (2001). A role for cofilin and LIM kinase in Listeria-induced phagocytosis. J Cell Biol *155*, 101–112. 10.1083/jcb.200104037.

48. Sousa, S., Cabanes, D., Bougnères, L., Lecuit, M., Sansonetti, P., Tran-Van-Nhieu, G., and Cossart, P. (2007). Src, cortactin and Arp2/3 complex are required for E-cadherin-mediated internalization of Listeria into cells. Cell Microbiol *9*, 2629–2643. 10.1111/j.1462-5822.2007.00984.x.

49. Jiwani, S., Wang, Y., Dowd, G.C., Gianfelice, A., Pichestapong, P., Gavicherla, B., Vanbennekom, N., and Ireton, K. (2012). Identification of components of the host type IA phosphoinositide 3-kinase pathway that promote internalization of Listeria monocytogenes. Infect Immun *80*, 1252–1266. 10.1128/IAI.06082-11.

50. Ireton, K., Rigano, L.A., and Dowd, G.C. (2014). Role of host GTPases in infection by Listeria monocytogenes. Cell Microbiol *16*, 1311–1320. 10.1111/cmi.12324.

51. Parida, S.K., Domann, E., Rohde, M., Müller, S., Darji, A., Hain, T., Wehland, J., and Chakraborty, T. (1998). Internalin B is essential for adhesion and mediates the invasion of Listeria monocytogenes into human endothelial cells. Mol Microbiol *28*, 81–93. 10.1046/j.1365-2958.1998.00776.x.

52. Faralla, C., Bastounis, E.E., Ortega, F.E., Light, S.H., Rizzuto, G., Gao, L., Marciano, D.K., Nocadello, S., Anderson, W.F., Robbins, J.R., et al. (2018). Listeria monocytogenes InlP

interacts with afadin and facilitates basement membrane crossing. PLoS Pathog *14*, e1007094. 10.1371/journal.ppat.1007094.

53. Faralla, C., Rizzuto, G.A., Lowe, D.E., Kim, B., Cooke, C., Shiow, L.R., and Bakardjiev, A.I. (2016). InlP, a New Virulence Factor with Strong Placental Tropism. Infect Immun *84*, 3584–3596. 10.1128/IAI.00625-16.

54. Ghosh, P., Halvorsen, E.M., Ammendolia, D.A., Mor-Vaknin, N., O'Riordan, M.X.D., Brumell, J.H., Markovitz, D.M., and Higgins, D.E. (2018). Invasion of the Brain by Listeria monocytogenes Is Mediated by InlF and Host Cell Vimentin. mBio *9*, e00160-18. 10.1128/mBio.00160-18.

55. Arandjelovic, S., and Ravichandran, K.S. (2015). Phagocytosis of apoptotic cells in homeostasis. Nat Immunol *16*, 907–917. 10.1038/ni.3253.

56. Underhill, D.M., and Ozinsky, A. (2002). Phagocytosis of Microbes: Complexity in Action. Annu Rev Immunol *20*, 825–852. 10.1146/annurev.immunol.20.103001.114744.

57. Moretti, J., and Blander, J.M. (2014). Insights into phagocytosis-coupled activation of Pattern Recognition Receptors and Inflammasomes. Curr Opin Immunol *0*, 100–110. 10.1016/j.coi.2013.11.003.

58. Blander, J.M., and Medzhitov, R. (2004). Regulation of Phagosome Maturation by Signals from Toll-Like Receptors. Science *304*, 1014–1018. 10.1126/science.1096158.

59. Shin, O.S., Isberg, R.R., Akira, S., Uematsu, S., Behera, A.K., and Hu, L.T. (2008). Distinct Roles for MyD88 and Toll-Like Receptors 2, 5, and 9 in Phagocytosis of Borrelia burgdorferi and Cytokine Induction. Infect Immun *76*, 2341–2351. 10.1128/IAI.01600-07.

60. Fang, L., Wu, H.-M., Ding, P.-S., and Liu, R.-Y. (2014). TLR2 mediates phagocytosis and autophagy through JNK signaling pathway in Staphylococcus aureus-stimulated RAW264.7 cells. Cell Signal *26*, 806–814. 10.1016/j.cellsig.2013.12.016.

61. Descamps, D., Le Gars, M., Balloy, V., Barbier, D., Maschalidi, S., Tohme, M., Chignard, M., Ramphal, R., Manoury, B., and Sallenave, J.-M. (2012). Toll-like receptor 5 (TLR5), IL-1β secretion, and asparagine endopeptidase are critical factors for alveolar macrophage phagocytosis and bacterial killing. Proc Natl Acad Sci *109*, 1619–1624. 10.1073/pnas.1108464109.

62. Jones, G.S., and D'Orazio, S.E.F. (2017). Monocytes Are the Predominant Cell Type Associated with *Listeria monocytogenes* in the Gut, but They Do Not Serve as an Intracellular Growth Niche. J Immunol *198*, 2796–2804. 10.4049/jimmunol.1602076.

63. Jones, G.S., Smith, V.C., and D'Orazio, S.E.F. (2017). *Listeria monocytogenes* Replicate in Bone Marrow–Derived CD11c $^{+}$ Cells but Not in Dendritic Cells Isolated from the Murine Gastrointestinal Tract. J Immunol *199*, 3789–3797. 10.4049/jimmunol.1700970.

64. Drevets, D.A., and Campbell, P.A. (1991). Roles of complement and complement receptor type 3 in phagocytosis of Listeria monocytogenes by inflammatory mouse peritoneal macrophages. Infect Immun *59*, 2645–2652. 10.1128/iai.59.8.2645-2652.1991.

65. Drevets, D.A., Canono, B.P., and Campbell, P.A. (1992). Listericidal and nonlistericidal mouse macrophages differ in complement receptor type 3-mediated phagocytosis of L. monocytogenes and in preventing escape of the bacteria into the cytoplasm. J Leukoc Biol *52*, 70–79. 10.1002/jlb.52.1.70.

66. Drevets, D.A., Leenen, P.J.M., and Campbell, P.A. (1996). Complement Receptor Type 3 Mediates Phagocytosis and Killing of Listeria monocytogenes by a TNF-α- and IFN-γ-Stimulated Macrophage Precursor Hybrid. Cell Immunol *169*, 1–6. 10.1006/cimm.1996.0083.

67. Pierce, M.M., Gibson, R.E., and Rodgers, F.G. (1996). Opsonin-independent adherence and phagocytosis of Listeria monocytogenes by murine peritoneal macrophages. J Med Microbiol *45*, 258–262. 10.1099/00222615-45-4-258.

68. Perelman, S.S., Abrams, M.E., Eitson, J.L., Chen, D., Jimenez, A., Mettlen, M., Schoggins, J.W., and Alto, N.M. (2016). Cell-Based Screen Identifies Human Interferon-Stimulated Regulators of Listeria monocytogenes Infection. PLoS Pathog *12*, e1006102. 10.1371/journal.ppat.1006102.

69. Ishiguro, T., Naito, M., Yamamoto, T., Hasegawa, G., Gejyo, F., Mitsuyama, M., Suzuki, H., and Kodama, T. (2001). Role of Macrophage Scavenger Receptors in Response to Listeria monocytogenes Infection in Mice. Am J Pathol *158*, 179–188. 10.1016/S0002-9440(10)63956-9.

70. Shen, Y., Kawamura, I., Nomura, T., Tsuchiya, K., Hara, H., Dewamitta, S.R., Sakai, S., Qu, H., Daim, S., Yamamoto, T., et al. (2010). Toll-Like Receptor 2- and MyD88-Dependent Phosphatidylinositol 3-Kinase and Rac1 Activation Facilitates the Phagocytosis of Listeria monocytogenes by Murine Macrophages. Infect Immun *78*, 2857–2867. 10.1128/IAI.01138-09.

71. Melton-Witt, J.A., Rafelski, S.M., Portnoy, D.A., and Bakardjiev, A.I. (2011). Oral Infection with Signature-Tagged Listeria monocytogenes Reveals Organ-Specific Growth and Dissemination Routes in Guinea Pigs. Infect Immun *80*, 720–732. 10.1128/IAI.05958-11.

72. Lecuit, M., Vandormael-Pournin, S., Lefort, J., Huerre, M., Gounon, P., Dupuy, C., Babinet, C., and Cossart, P. (2001). A Transgenic Model for Listeriosis: Role of Internalin in Crossing the Intestinal Barrier. Science *292*, 1722–1725. 10.1126/science.1059852.

73. Pentecost, M., Otto, G., Theriot, J.A., and Amieva, M.R. (2006). Listeria monocytogenes Invades the Epithelial Junctions at Sites of Cell Extrusion. PLoS Pathog *2*, e3. 10.1371/journal.ppat.0020003.

74. Nikitas, G., Deschamps, C., Disson, O., Niault, T., Cossart, P., and Lecuit, M. (2011). Transcytosis of Listeria monocytogenes across the intestinal barrier upon specific targeting of goblet cell accessible E-cadherin. J Exp Med *208*, 2263–2277. 10.1084/jem.20110560.

75. Corr, S., Hill, C., and Gahan, C.G.M. (2006). An in vitro cell-culture model demonstrates internalin- and hemolysin-independent translocation of Listeria monocytogenes across M cells. Microb Pathog *41*, 241–250. 10.1016/j.micpath.2006.08.003.

76. Jensen, V.B., Harty, J.T., and Jones, B.D. (1998). Interactions of the Invasive PathogensSalmonella typhimurium, Listeria monocytogenes, and Shigella flexneri with M Cells and Murine Peyer's Patches. Infect Immun *66*, 3758–3766. 10.1128/IAI.66.8.3758-3766.1998.

77. Chiba, S., Nagai, T., Hayashi, T., Baba, Y., Nagai, S., and Koyasu, S. (2011). Listerial invasion protein internalin B promotes entry into ileal Peyer's patches in vivo. Microbiol Immunol *55*, 123–129. 10.1111/j.1348-0421.2010.00292.x.

78. Bou Ghanem, E.N., Jones, G.S., Myers-Morales, T., Patil, P.D., Hidayatullah, A.N., and D'Orazio, S.E.F. (2012). InlA Promotes Dissemination of Listeria monocytogenes to the Mesenteric Lymph Nodes during Food Borne Infection of Mice. PLoS Pathog *8*, e1003015. 10.1371/journal.ppat.1003015.

79. Jones, G.S., Bussell, K.M., Myers-Morales, T., Fieldhouse, A.M., Bou Ghanem, E.N., and D'Orazio, S.E.F. (2015). Intracellular Listeria monocytogenes Comprises a Minimal but Vital Fraction of the Intestinal Burden following Foodborne Infection. Infect Immun *83*, 3146–3156. 10.1128/IAI.00503-15.

80. Drevets, D.A. (1999). Dissemination of Listeria monocytogenesby Infected Phagocytes. Infect Immun *67*, 3512–3517. 10.1128/IAI.67.7.3512-3517.1999.

81. Drevets, D.A., Jelinek, T.A., and Freitag, N.E. (2001). Listeria monocytogenes-Infected Phagocytes Can Initiate Central Nervous System Infection in Mice. Infect Immun *69*, 1344–1350.

82. Drevets, D.A., Dillon, M.J., Schawang, J.S., van Rooijen, N., Ehrchen, J., Sunderkötter, C., and Leenen, P.J.M. (2004). The Ly-6C ^{high} Monocyte Subpopulation Transports *Listeria monocytogenes* into the Brain during Systemic Infection of Mice. J Immunol *172*, 4418–4424. 10.4049/jimmunol.172.7.4418.

83. Join-Lambert, O.F., Ezine, S., Le Monnier, A., Jaubert, F., Okabe, M., Berche, P., and Kayal, S. (2005). Listeria monocytogenes-infected bone marrow myeloid cells promote bacterial invasion of the central nervous system. Cell Microbiol *7*, 167–180. 10.1111/j.1462-5822.2004.00444.x.

84. Pamer, E.G. (2004). Immune responses to Listeria monocytogenes. Nat Rev Immunol *4*, 812–823. 10.1038/nri1461.

85. Unanue, E.R. (1997). Inter-relationship among macrophages, natural killer cells and neutrophils in early stages of Listeria resistance. Curr Opin Microbiol *9*, 35–43. 10.1016/S0952-7915(97)80156-2.

86. Buchmeier, N.A., and Schreiber, R.D. (1985). Requirement of endogenous interferon-gamma production for resolution of Listeria monocytogenes infection. Proc Natl Acad Sci *82*, 7404–7408. 10.1073/pnas.82.21.7404.

87. Dai, W.J., Bartens, W., Köhler, G., Hufnagel, M., Kopf, M., and Brombacher, F. (1997). Impaired macrophage listericidal and cytokine activities are responsible for the rapid death of Listeria monocytogenes-infected IFN-gamma receptor-deficient mice. J Immunol *158*, 5297–5304.

88. Portnoy, D.A., Schreiber, R.D., Connelly, P., and Tilney, L.G. (1989). Gamma interferon limits access of Listeria monocytogenes to the macrophage cytoplasm. J Exp Med *170*, 2141–2146. 10.1084/jem.170.6.2141.

89. Blow, J.J., and Laskey, R.A. (2016). Xenopus cell-free extracts and their contribution to the study of DNA replication and other complex biological processes. Int J Dev Biol *60*, 201–207. 10.1387/ijdb.160142jb.

90. Hang, B.I., Thorne, C.A., Robbins, D.J., Huppert, S.S., Lee, L.A., and Lee, E. (2012). Screening for small molecule inhibitors of embryonic pathways: sometimes you gotta crack a few eggs. Bioorg Med Chem *20*, 1869–1877. 10.1016/j.bmc.2011.12.044.

91. Cheng, L.W., and Portnoy, D.A. (2003). Drosophila S2 cells: an alternative infection model for Listeria monocytogenes. Cell Microbiol *5*, 875–885. 10.1046/j.1462-5822.2003.00327.x.

92. Levraud, J.-P., Disson, O., Kissa, K., Bonne, I., Cossart, P., Herbomel, P., and Lecuit, M. (2009). Real-time observation of listeria monocytogenes-phagocyte interactions in living zebrafish larvae. Infect Immun *77*, 3651–3660. 10.1128/IAI.00408-09.

93. Rosenblatt, J., Agnew, B.J., Abe, H., Bamburg, J.R., and Mitchison, T.J. (1997). Xenopus actin depolymerizing factor/cofilin (XAC) is responsible for the turnover of actin filaments in Listeria monocytogenes tails. J Cell Biol *136*, 1323–1332. 10.1083/jcb.136.6.1323.

94. Theriot, J.A., Rosenblatt, J., Portnoy, D.A., Goldschmidt-Clermont, P.J., and Mitchison, T.J. (1994). Involvement of profilin in the actin-based motility of L. monocytogenes in cells and in cell-free extracts. Cell *76*, 505–517. 10.1016/0092-8674(94)90114-7.

95. Marchand, J.B., Moreau, P., Paoletti, A., Cossart, P., Carlier, M.F., and Pantaloni, D. (1995). Actin-based movement of Listeria monocytogenes: actin assembly results from the local maintenance of uncapped filament barbed ends at the bacterium surface. J Cell Biol *130*, 331–343. 10.1083/jcb.130.2.331.

96. Gründling, A., Gonzalez, M.D., and Higgins, D.E. (2003). Requirement of the Listeria monocytogenes Broad-Range Phospholipase PC-PLC during Infection of Human Epithelial Cells. J Bacteriol *185*, 6295–6307. 10.1128/JB.185.21.6295-6307.2003.

97. Hanson, W.G., Benanti, E.L., Lemmens, E.E., Liu, W., Skoble, J., Leong, M.L., Rae, C.S., Fassò, M., Brockstedt, D.G., Chen, C., et al. (2019). A Potent and Effective Suicidal Listeria Vaccine Platform. Infect Immun *87*, e00144-19. 10.1128/IAI.00144-19.

98. Haber, A., Friedman, S., Lobel, L., Burg-Golani, T., Sigal, N., Rose, J., Livnat-Levanon, N., Lewinson, O., and Herskovits, A.A. (2017). L-glutamine Induces Expression of Listeria monocytogenes Virulence Genes. PLoS Pathog *13*, e1006161. 10.1371/journal.ppat.1006161.

99. Li, W., Xu, H., Xiao, T., Cong, L., Love, M.I., Zhang, F., Irizarry, R.A., Liu, J.S., Brown, M., and Liu, X.S. (2014). MAGeCK enables robust identification of essential genes from genome-scale CRISPR/Cas9 knockout screens. Genome Biol *15*, 554. 10.1186/s13059-014-0554-4.

100. Zhou, Y., Zhou, B., Pache, L., Chang, M., Khodabakhshi, A.H., Tanaseichuk, O., Benner, C., and Chanda, S.K. (2019). Metascape provides a biologist-oriented resource for the analysis of systems-level datasets. Nat Commun *10*, 1523. 10.1038/s41467-019-09234-6.

101. Hsiau, T., Conant, D., Rossi, N., Maures, T., Waite, K., Yang, J., Joshi, S., Kelso, R., Holden, K., Enzmann, B.L., et al. (2019). Inference of CRISPR Edits from Sanger Trace Data. bioRxiv, 251082. 10.1101/251082.

102. McCaffrey, R.L., Fawcett, P., O'Riordan, M., Lee, K.-D., Havell, E.A., Brown, P.O., and Portnoy, D.A. (2004). A specific gene expression program triggered by Gram-positive bacteria in the cytosol. Proc Natl Acad Sci *101*, 11386–11391. 10.1073/pnas.0403215101.

103. Suzuki, E., and Umezawa, K. (2006). Inhibition of macrophage activation and phagocytosis by a novel NF-κB inhibitor, dehydroxymethylepoxyquinomicin. Biomed Pharmacother *60*, 578–586. 10.1016/j.biopha.2006.07.089.

104. Zhu, F., Yue, W., and Wang, Y. (2014). The nuclear factor kappa B (NF-κB) activation is required for phagocytosis of staphylococcus aureus by RAW 264.7 cells. Exp Cell Res *327*, 256–263. 10.1016/j.yexcr.2014.04.018.

105. Keniry, M., and Parsons, R. (2008). The role of PTEN signaling perturbations in cancer and in targeted therapy. Oncogene *27*, 5477–5485. 10.1038/onc.2008.248.

106. Maehama, T., and Dixon, J.E. (1998). The Tumor Suppressor, PTEN/MMAC1, Dephosphorylates the Lipid Second Messenger, Phosphatidylinositol 3,4,5-Trisphosphate. J Biol Chem *273*, 13375–13378. 10.1074/jbc.273.22.13375.

107. Stambolic, V., Suzuki, A., de la Pompa, J.L., Brothers, G.M., Mirtsos, C., Sasaki, T., Ruland, J., Penninger, J.M., Siderovski, D.P., and Mak, T.W. (1998). Negative Regulation of PKB/Akt-Dependent Cell Survival by the Tumor Suppressor PTEN. Cell *95*, 29–39. 10.1016/S0092-8674(00)81780-8.

108. Tibarewal, P., Zilidis, G., Spinelli, L., Schurch, N., Maccario, H., Gray, A., Perera, N.M., Davidson, L., Barton, G.J., and Leslie, N.R. (2012). PTEN protein phosphatase activity correlates with control of gene expression and invasion, a tumor-suppressing phenotype, but not with AKT activity. Sci Signal *5*, ra18. 10.1126/scisignal.2002138.

109. Dey, N., Crosswell, H.E., De, P., Parsons, R., Peng, Q., Su, J.D., and Durden, D.L. (2008). The Protein Phosphatase Activity of PTEN Regulates Src Family Kinases and Controls Glioma Migration. Cancer Res *68*, 1862–1871. 10.1158/0008-5472.CAN-07-1182.

110. Wozniak, D.J., Kajdacsy-Balla, A., Macias, V., Ball-Kell, S., Zenner, M.L., Bie, W., and Tyner, A.L. (2017). PTEN is a protein phosphatase that targets active PTK6 and inhibits PTK6 oncogenic signaling in prostate cancer. Nat Commun *8*, 1508. 10.1038/s41467-017-01574-5.

111. Freeman, S.A., and Grinstein, S. (2014). Phagocytosis: receptors, signal integration, and the cytoskeleton. Immunol Rev *262*, 193–215. 10.1111/imr.12212.

112. Han, J., Luby-Phelps, K., Das, B., Shu, X., Xia, Y., Mosteller, R.D., Krishna, U.M., Falck, J.R., White, M.A., and Broek, D. (1998). Role of Substrates and Products of PI 3-kinase in Regulating Activation of Rac-Related Guanosine Triphosphatases by Vav. Science *279*, 558–560. 10.1126/science.279.5350.558.

113. Lv, Y., Fang, L., Ding, P., and Liu, R. (2019). PI3K/Akt-Beclin1 signaling pathway positively regulates phagocytosis and negatively mediates NF-κB-dependent inflammation in Staphylococcus aureus-infected macrophages. Biochem Biophys Res Commun *510*, 284–289. 10.1016/j.bbrc.2019.01.091.

114. Tachado, S.D., Samrakandi, M.M., and Cirillo, J.D. (2008). Non-Opsonic Phagocytosis of Legionella pneumophila by Macrophages Is Mediated by Phosphatidylinositol 3-Kinase. PLoS ONE *3*, e3324. 10.1371/journal.pone.0003324.

115. Lovewell, R.R., Hayes, S.M., O'Toole, G.A., and Berwin, B. (2014). Pseudomonas aeruginosa flagellar motility activates the phagocyte PI3K/Akt pathway to induce phagocytic engulfment. Am J Physiol Lung Cell Mol Physiol *306*, L698–L707. 10.1152/ajplung.00319.2013.

116. Shin, O.S., Miller, L.S., Modlin, R.L., Akira, S., Uematsu, S., and Hu, L.T. (2009). Downstream Signals for MyD88-Mediated Phagocytosis of *Borrelia burgdorferi* Can Be

Initiated by TRIF and Are Dependent on PI3K. J Immunol *183*, 491–498. 10.4049/jimmunol.0900724.

117. Gessain, G., Tsai, Y.-H., Travier, L., Bonazzi, M., Grayo, S., Cossart, P., Charlier, C., Disson, O., and Lecuit, M. (2015). PI3-kinase activation is critical for host barrier permissiveness to Listeria monocytogenes. J Exp Med *212*, 165–183. 10.1084/jem.20141406.

118. Hubbard, L.L.N., Wilke, C.A., White, E.S., and Moore, B.B. (2011). PTEN Limits Alveolar Macrophage Function against Pseudomonas aeruginosa after Bone Marrow Transplantation. Am J Respir Cell Mol Biol *45*, 1050–1058. 10.1165/rcmb.2011-0079OC.

119. Schabbauer, G., Matt, U., Günzl, P., Warszawska, J., Furtner, T., Hainzl, E., Elbau, I., Mesteri, I., Doninger, B., Binder, B.R., et al. (2010). Myeloid PTEN Promotes Inflammation but Impairs Bactericidal Activities during Murine Pneumococcal Pneumonia. J Immunol *185*, 468–476. 10.4049/jimmunol.0902221.

120. Serezani, C.H., Kane, S., Medeiros, A.I., Cornett, A.M., Kim, S.-H., Marques, M.M., Lee, S.-P., Lewis, C., Bourdonnay, E., Ballinger, M.N., et al. (2012). PTEN Directly Activates the Actin Depolymerization Factor Cofilin-1 During PGE2-Mediated Inhibition of Phagocytosis of Fungi. Sci Signal *5*, ra12–ra12. 10.1126/scisignal.2002448.

121. Mondal, S., Ghosh-Roy, S., Loison, F., Li, Y., Jia, Y., Harris, C., Williams, D.A., and Luo, H.R. (2011). PTEN Negatively Regulates Engulfment of Apoptotic Cells by Modulating Activation of Rac GTPase. J Immunol *187*, 5783–5794. 10.4049/jimmunol.1100484.

122. Schmid, A.C., Byrne, R.D., Vilar, R., and Woscholski, R. (2004). Bisperoxovanadium compounds are potent PTEN inhibitors. FEBS Lett *566*, 35–38. 10.1016/j.febslet.2004.03.102.

123. Ireton, K. (2007). Entry of the bacterial pathogen Listeria monocytogenes into mammalian cells. Cell Microbiol *9*, 1365–1375. https://doi.org/10.1111/j.1462-5822.2007.00933.x.

124. Myers, M.P., Pass, I., Batty, I.H., Van der Kaay, J., Stolarov, J.P., Hemmings, B.A., Wigler, M.H., Downes, C.P., and Tonks, N.K. (1998). The lipid phosphatase activity of PTEN is critical for its tumor supressor function. Proc Natl Acad Sci *95*, 13513–13518. 10.1073/pnas.95.23.13513.

125. Currie, R.A., Walker, K.S., Gray, A., Deak, M., Casamayor, A., Downes, C.P., Cohen, P., Alessi, D.R., and Lucocq, J. (1999). Role of phosphatidylinositol 3,4,5-trisphosphate in regulating the activity and localization of 3-phosphoinositide-dependent protein kinase-1. Biochem J *337*, 575–583. 10.1042/bj3370575.

126. Bilanges, B., Posor, Y., and Vanhaesebroeck, B. (2019). PI3K isoforms in cell signalling and vesicle trafficking. Nat Rev Mol Cell Biol *20*, 515–534. 10.1038/s41580-019-0129-z.

127. Arbibe, L., Mira, J.-P., Teusch, N., Kline, L., Guha, M., Mackman, N., Godowski, P.J., Ulevitch, R.J., and Knaus, U.G. (2000). Toll-like receptor 2–mediated NF-κB activation requires a Rac1-dependent pathway. Nat Immunol *1*, 533–540. 10.1038/82797.

128. Rhee, S.H., Kim, H., Moyer, M.P., and Pothoulakis, C. (2006). Role of MyD88 in Phosphatidylinositol 3-Kinase Activation by Flagellin/Toll-like Receptor 5 Engagement in Colonic Epithelial Cells. J Biol Chem *281*, 18560–18568. 10.1074/jbc.M513861200.

129. Hayashi, F., Smith, K.D., Ozinsky, A., Hawn, T.R., Yi, E.C., Goodlett, D.R., Eng, J.K., Akira, S., Underhill, D.M., and Aderem, A. (2001). The innate immune response to bacterial flagellin is mediated by Toll-like receptor 5. Nature *410*, 1099–1103. 10.1038/35074106.

130. Torres, D., Barrier, M., Bihl, F., Quesniaux, V.J.F., Maillet, I., Akira, S., Ryffel, B., and Erard, F. (2004). Toll-Like Receptor 2 Is Required for Optimal Control of Listeria monocytogenes Infection. Infect Immun *72*, 2131–2139. 10.1128/IAI.72.4.2131-2139.2004.

131. Cesinger, M.R., Daramola, O.I., Kwiatkowski, L.M., and Reniere, M.L. (2022). The Transcriptional Regulator SpxA1 Influences the Morphology and Virulence of Listeria monocytogenes. Infect Immun *90*, e00211-22. 10.1128/iai.00211-22.

132. Gründling, A., Burrack, L.S., Bouwer, H.G.A., and Higgins, D.E. (2004). Listeria monocytogenes regulates flagellar motility gene expression through MogR, a transcriptional repressor required for virulence. Proc Natl Acad Sci *101*, 12318–12323. 10.1073/pnas.0404924101.

133. Kim, S.H., Park, M.K., Kim, J.Y., Chuong, P.D., Lee, Y.S., Yoon, B.S., Hwang, K.K., and Lim, Y.K. (2019). Development of a sandwich ELISA for the detection of Listeria spp. using specific flagella antibodies. J Vet Sci *6*, 41–46. 10.4142/jvs.2005.6.1.41.

134. Becattini, S., Littmann, E.R., Carter, R.A., Kim, S.G., Morjaria, S.M., Ling, L., Gyaltshen, Y., Fontana, E., Taur, Y., Leiner, I.M., et al. (2017). Commensal microbes provide first line defense against Listeria monocytogenes infection. J Exp Med *214*, 1973–1989. 10.1084/jem.20170495.

135. Gillooly, D.J., Simonsen, A., and Stenmark, H. (2001). Phosphoinositides and phagocytosis. J Cell Biol *155*, 15–18. 10.1083/jcb.200109001.

136. Czech, M.P. (2000). PIP2 and PIP3: Complex Roles at the Cell Surface. Cell *100*, 603–606. 10.1016/S0092-8674(00)80696-0.

137. Mandal, K. (2020). Review of PIP2 in Cellular Signaling, Functions and Diseases. Int J Mol Sci *21*, 8342. 10.3390/ijms21218342.

138. Sumrall, E.T., Keller, A.P., Shen, Y., and Loessner, M.J. (2020). Structure and function of Listeria teichoic acids and their implications. Mol Microbiol *113*, 627–637. 10.1111/mmi.14472.

139. Vázquez-Boland, J.A., Kuhn, M., Berche, P., Chakraborty, T., Domínguez-Bernal, G., Goebel, W., González-Zorn, B., Wehland, J., and Kreft, J. (2001). Listeria Pathogenesis and Molecular Virulence Determinants. Clin Microbiol Rev *14*, 584–640. 10.1128/CMR.14.3.584-640.2001.

140. Sumrall, E.T., Shen, Y., Keller, A.P., Rismondo, J., Pavlou, M., Eugster, M.R., Boulos, S., Disson, O., Thouvenot, P., Kilcher, S., et al. (2019). Phage resistance at the cost of virulence: Listeria monocytogenes serovar 4b requires galactosylated teichoic acids for InlB-mediated invasion. PLoS Pathog *15*, e1008032. 10.1371/journal.ppat.1008032.

141. Disson, O., Blériot, C., Jacob, J.-M., Serafini, N., Dulauroy, S., Jouvion, G., Fevre, C., Gessain, G., Thouvenot, P., Eberl, G., et al. (2018). Peyer's patch myeloid cells infection by Listeria signals through gp38+ stromal cells and locks intestinal villus invasion. J Exp Med *215*, 2936–2954. 10.1084/jem.20181210.

142. McElroy, D.S., Ashley, T.J., and D'Orazio, S.E.F. (2009). Lymphocytes serve as a reservoir for Listeria monocytogenes growth during infection of mice. Microb Pathog *46*, 214–221. 10.1016/j.micpath.2009.01.003.

143. Broadley, S.P., Plaumann, A., Coletti, R., Lehmann, C., Wanisch, A., Seidlmeier, A., Esser, K., Luo, S., Rämer, P.C., Massberg, S., et al. (2016). Dual-Track Clearance of Circulating Bacteria Balances Rapid Restoration of Blood Sterility with Induction of Adaptive Immunity. Cell Host Microbe *20*, 36–48. 10.1016/j.chom.2016.05.023.

144. Uribe-Querol, E., and Rosales, C. (2020). Phagocytosis: Our Current Understanding of a Universal Biological Process. Front Immunol *11*, 1066. 10.3389/fimmu.2020.01066.

145. Lim, J.J., Grinstein, S., and Roth, Z. (2017). Diversity and Versatility of Phagocytosis: Roles in Innate Immunity, Tissue Remodeling, and Homeostasis. Front Cell Infect Microbiol *7*. https://doi.org/10.3389/fcimb.2017.00191.

146. D'Orazio, S.E.F. (2019). Innate and Adaptive Immune Responses during Listeria monocytogenes Infection. Microbiol Spectr *7*. 10.1128/microbiolspec.GPP3-0065-2019.

147. Pitts, M.G., and D'Orazio, S.E.F. (2018). A Comparison of Oral and Intravenous Mouse Models of Listeriosis. Pathogens *7*, 13. 10.3390/pathogens7010013.

148. Lobel, L., Sigal, N., Borovok, I., Ruppin, E., and Herskovits, A.A. (2012). Integrative Genomic Analysis Identifies Isoleucine and CodY as Regulators of Listeria monocytogenes Virulence. PLoS Genet *8*, e1002887. 10.1371/journal.pgen.1002887.

149. Loh, A., Brennan, R., Lang, W., Hickey, R., Malkas, L., and Sandoval, J. (2013). Dissecting the PI3K Signaling Axis in Pediatric Solid Tumors: Novel Targets for Clinical Integration. Front Oncol *3*. 10.3389/fonc.2013.00093.

150. Ozaki, S., DeWald, D.B., Shope, J.C., Chen, J., and Prestwich, G.D. (2000). Intracellular delivery of phosphoinositides and inositol phosphates using polyamine carriers. Proc Natl Acad Sci *97*, 11286–11291. 10.1073/pnas.210197897.

151. Gozzelino, L., De Santis, M.C., Gulluni, F., Hirsch, E., and Martini, M. (2020). PI(3,4)P2 Signaling in Cancer and Metabolism. Front Oncol *10*. 10.3389/fonc.2020.00360.

152. Pombinho, R., Pinheiro, J., Resende, M., Meireles, D., Jalkanen, S., Sousa, S., and Cabanes, D. (2021). Stabilin-1 plays a protective role against Listeria monocytogenes infection through the regulation of cytokine and chemokine production and immune cell recruitment. Virulence *12*, 2088–2103. 10.1080/21505594.2021.1958606.

153. Zhang, L.F., Lepenies, B., Nakamae, S., Young, B.M., Santos, R.L., Raffatellu, M., Cobb, B.A., Hiyoshi, H., and Bäumler, A.J. (2022). The Vi Capsular Polysaccharide of Salmonella Typhi Promotes Macrophage Phagocytosis by Binding the Human C-Type Lectin DC-SIGN. mBio *13*, e02733-22. 10.1128/mbio.02733-22.

154. Schulert, G.S., and Allen, L.-A.H. (2006). Differential infection of mononuclear phagocytes by Francisella tularensis: role of the macrophage mannose receptor. J Leukoc Biol *80*, 563–571. 10.1189/jlb.0306219.

155. Schlesinger, L. (1993). Macrophage phagocytosis of virulent but not attenuated strains of Mycobacterium tuberculosis is mediated by mannose receptors in addition to complement receptors. J Immunol *150*, 2920–2930.

156. Khan, H.S., Nair, V.R., Ruhl, C.R., Alvarez-Arguedas, S., Galvan Rendiz, J.L., Franco, L.H., Huang, L., Shaul, P.W., Kim, J., Xie, Y., et al. Identification of scavenger receptor B1 as the airway microfold cell receptor for Mycobacterium tuberculosis. eLife *9*, e52551. 10.7554/eLife.52551.

157. Hardy, J., Francis, K.P., DeBoer, M., Chu, P., Gibbs, K., and Contag, C.H. (2004). Extracellular Replication of Listeria monocytogenes in the Murine Gall Bladder. Science *303*, 851–853. 10.1126/science.1092712.

158. Nakane, A., Minagawa, T., Kohanawa, M., Chen, Y., Sato, H., Moriyama, M., and Tsuruoka, N. (1989). Interactions between endogenous gamma interferon and tumor necrosis factor in host resistance against primary and secondary Listeria monocytogenes infections. Infect Immun *57*, 3331–3337. 10.1128/iai.57.11.3331-3337.1989.

159. Bécavin, C., Bouchier, C., Lechat, P., Archambaud, C., Creno, S., Gouin, E., Wu, Z., Kühbacher, A., Brisse, S., Pucciarelli, M.G., et al. (2014). Comparison of Widely Used Listeria monocytogenes Strains EGD, 10403S, and EGD-e Highlights Genomic Differences Underlying Variations in Pathogenicity. mBio *5*, e00969-14. 10.1128/mBio.00969-14.

160. Bishop, D.K., and Hinrichs, D.J. (1987). Adoptive transfer of immunity to Listeria monocytogenes. The influence of in vitro stimulation on lymphocyte subset requirements. J Immunol *139*, 2005–2009.

161. Vincent, W.J.B., Freisinger, C.M., Lam, P., Huttenlocher, A., and Sauer, J.-D. (2016). Macrophages mediate flagellin induced inflammasome activation and host defense in zebrafish. Cell Microbiol *18*, 591–604. 10.1111/cmi.12536.

162. Jones, S., and Portnoy, D.A. (1994). Characterization of Listeria monocytogenes pathogenesis in a strain expressing perfringolysin O in place of listeriolysin O. Infect Immun *62*, 5608–5613. 10.1128/iai.62.12.5608-5613.1994.

163. Kind gift from Dr. Alex Meeske (University of Washington).

164. Glaser, P., Frangeul, L., Buchrieser, C., Rusniok, C., Amend, A., Baquero, F., Berche, P., Bloecker, H., Brandt, P., Chakraborty, T., et al. (2001). Comparative Genomics of Listeria Species. Science *294*, 849–852. 10.1126/science.1063447.

165. Meeske, A.J., Jia, N., Cassel, A.K., Kozlova, A., Liao, J., Wiedmann, M., Patel, D.J., and Marraffini, L.A. (2020). A phage-encoded anti-CRISPR enables complete evasion of type VI-A CRISPR-Cas immunity. Science *369*, 54–59. 10.1126/science.abb6151.

166. Portnoy, D.A., Tweten, R.K., Kehoe, M., and Bielecki, J. (1992). Capacity of listeriolysin O, streptolysin O, and perfringolysin O to mediate growth of Bacillus subtilis within mammalian cells. Infect Immun *60*, 2710–2717. 10.1128/iai.60.7.2710-2717.1992.

167. Kiritsy, M.C., Ankley, L.M., Trombley, J., Huizinga, G.P., Lord, A.E., Orning, P., Elling, R., Fitzgerald, K.A., and Olive, A.J. (2021). A genetic screen in macrophages identifies new regulators of IFNγ-inducible MHCII that contribute to T cell activation. eLife *10*, e65110. 10.7554/eLife.65110.

168. McFarland, A.P., Burke, T.P., Carletti, A.A., Glover, R.C., Tabakh, H., Welch, M.D., and Woodward, J.J. (2018). RECON-Dependent Inflammation in Hepatocytes Enhances Listeria monocytogenes Cell-to-Cell Spread. mBio *9*, e00526-18. 10.1128/mBio.00526-18.

169. Young, L., Sung, J., Stacey, G., and Masters, J.R. (2010). Detection of Mycoplasma in cell cultures. Nat Protoc *5*, 929–934. 10.1038/nprot.2010.43.

170. Lauer, P., Chow, M.Y.N., Loessner, M.J., Portnoy, D.A., and Calendar, R. (2002). Construction, Characterization, and Use of Two Listeria monocytogenes Site-Specific Phage Integration Vectors. J Bacteriol *184*, 4177–4186. 10.1128/JB.184.15.4177-4186.2002.

171. Whiteley, A.T., Pollock, A.J., and Portnoy, D.A. (2015). The PAMP c-di-AMP Is Essential for Listeria monocytogenes Growth in Rich but Not Minimal Media due to a Toxic Increase in (p)ppGpp. Cell Host Microbe *17*, 788–798. 10.1016/j.chom.2015.05.006.

172. Skoble, J., Portnoy, D.A., and Welch, M.D. (2000). Three Regions within Acta Promote Arp2/3 Complex-Mediated Actin Nucleation and Listeria monocytogenes Motility. J Cell Biol *150*, 527–538. 10.1083/jcb.150.3.527.

173. Khokha, M.K., Chung, C., Bustamante, E.L., Gaw, L.W.K., Trott, K.A., Yeh, J., Lim, N., Lin, J.C.Y., Taverner, N., Amaya, E., et al. (2002). Techniques and probes for the study of Xenopus tropicalis development. Dev Dyn *225*, 499–510. 10.1002/dvdy.10184.

174. Fulco, C.P., Munschauer, M., Anyoha, R., Munson, G., Grossman, S.R., Perez, E.M., Kane, M., Cleary, B., Lander, E.S., and Engreitz, J.M. (2016). Systematic mapping of functional enhancer-promoter connections with CRISPR interference. Science *354*, 769–773. 10.1126/science.aag2445.

175. Sanjana, N.E., Shalem, O., and Zhang, F. (2014). Improved vectors and genome-wide libraries for CRISPR screening. Nat Methods *11*, 783–784. 10.1038/nmeth.3047.

176. Stringer, B.W., Day, B.W., D'Souza, R.C.J., Jamieson, P.R., Ensbey, K.S., Bruce, Z.C., Lim, Y.C., Goasdoué, K., Offenhäuser, C., Akgül, S., et al. (2019). A reference collection of patient-derived cell line and xenograft models of proneural, classical and mesenchymal glioblastoma. Sci Rep *9*, 4902. 10.1038/s41598-019-41277-z.

177. Doench, J.G., Fusi, N., Sullender, M., Hegde, M., Vaimberg, E.W., Donovan, K.F., Smith, I., Tothova, Z., Wilen, C., Orchard, R., et al. (2016). Optimized sgRNA design to maximize activity and minimize off-target effects of CRISPR-Cas9. Nat Biotechnol *34*, 184–191. 10.1038/nbt.3437.

178. Chen, S., Sanjana, N.E., Zheng, K., Shalem, O., Lee, K., Shi, X., Scott, D.A., Song, J., Pan, J.Q., Weissleder, R., et al. (2015). Genome-wide CRISPR Screen in a Mouse Model of Tumor Growth and Metastasis. Cell *160*, 1246–1260. 10.1016/j.cell.2015.02.038.

179. Hayer, A., Shao, L., Chung, M., Joubert, L.-M., Yang, H.W., Tsai, F.-C., Bisaria, A., Betzig, E., and Meyer, T. (2016). Engulfed cadherin fingers are polarized junctional structures between collectively migrating endothelial cells. Nat Cell Biol *18*, 1311–1323. 10.1038/ncb3438.

180. Halsey, C.R., Glover, R.C., Thomason, M.K., and Reniere, M.L. (2021). The redox-responsive transcriptional regulator Rex represses fermentative metabolism and is required for Listeria monocytogenes pathogenesis. PLoS Pathog *17*, e1009379. 10.1371/journal.ppat.1009379.

181. Bou Ghanem, E.N., Myers-Morales, T., and D'Orazio, S.E.F. (2013). A mouse model of food borne Listeria monocytogenes infection. Curr Protoc Microbiol *31*, 9B.3.1-9B.3.16. 10.1002/9780471729259.mc09b03s31.